Characterisation of cultured airway basal cells to understand their role in human lung disease

Robert E. Hynds

Lungs for Living Research Centre

UCL Respiratory

University College London

A thesis presented for the degree of Doctor of Philosophy

2016

Declaration

I, Robert Hynds, confirm that the work presented in this thesis is my own. Where information has been derived from other sources, I confirm that this has been indicated and acknowledged.

Acknowledgements

I would like to thank my supervisory team – Professor Sam Janes, Dr. Adam Giangreco, Professor Rachel Chambers, Dr. Brett Cochrane and Dr. Paul Fowler – for the opportunity to pursue my PhD at UCL and their help, support and ideas throughout.

Thanks to the 'epithelial team' - Colin, Jim, Kate, Nick and Laura – for establishing coffee shop science and to Adam P, Bernie, Beth, Chris, Fraser, Krish, Leticia, Lizzie, Manu, Neelu, Noura, Paul, Qiang, Ricky, Sab, Sofia, Tammy, Tanvi and Vitor, for tolerating us. Together you have made Lungs for Living a great place to do research for the last four years. Thanks too to our collaborators - Dr. Cecilia Prêle (University of Western Australia), Dr. Helen Booth (University College London Hospitals), Professor Chris O'Callaghan (Institute of Child Health, UCL) and Professor Paolo De Coppi (Institute of Child Health, UCL) – and members of their laboratories who made this work possible.

Finally, I am grateful to the British Biotechnology and Research Council (BBSRC) and Unilever who funded this research through a BBSRC-CASE PhD studentship.

Abstract

Many studies in murine models have demonstrated the stem/progenitor cell potential of basal epithelial cells in the tracheal epithelium. However, significant differences exist between the respiratory epithelium in rodents and in man. As such, novel methodologies to study respiratory epithelial cells *in vitro* are in demand.

Here, methods to expand primary human airway epithelial cells from living patients were explored. The field's 'gold standard' medium for the expansion of these cells was poorly suited to initiating cultures from small endobronchial biopsy samples as proliferation of these cells was time-limited and after a short period of time in culture the cells became senescent and were unable to regenerate a mucociliary epithelium in organotypic models. As such, an alternative epithelial culture strategy involving the co-culture of human airway epithelial cells with 3T3-J2 fibroblast feeder cells in medium containing a small molecule Rho-associated protein kinase (ROCK) inhibitor was assessed. This method greatly improved both the yield and the longevity of human basal cell cultures and allowed multipotent airway differentiation in organotypic assays after longer culture periods than conventional techniques. Finally, the epithelial-stromal cell crosstalk between epithelial cells and feeder cells in co-culture was investigated, revealing a novel signalling pathway involving phosphorylation of the transcription factor signal transducer and activator of transcription 6 (STAT6) by hepatocyte growth factor (HGF) signalling.

Table of Contents

1 . Introduction

1.1 The human airway epithelium

Epithelia constitute the surfaces (epidermis and cornea) and linings (respiratory, digestive and uro-genital) of the body that are exposed to the outside world. Formed of cells tightly connected by cell-cell and cell-matrix adhesions, epithelia form a protective barrier and regulate the important processes of water transport, nutrient uptake and secretion [1].

Epithelial cells can be derived from any of the three germ layers and have diverse structural organisations [2]. Stratified epithelia, which have multiple cell layers, can be keratinised, as is the case for epidermis, or non-keratinised, as in the oral mucosa. Simple epithelia are only a single cell layer and are found in the alveolus of the lungs and in the kidney tubules. In the lungs, the proximal airway epithelium is an endoderm-derived, pseudostratified epithelium where all cells in the tall epithelium make some contact with the basement membrane [3]. Despite these structural differences, all epithelia share common characteristics, with intercellular communication among cells within an epithelium mediated by tight junctions, adherens junctions and desmosomes, which enables coordination of their function [4]. Further, cells express integrins that bind to basement membrane extracellular matrix (ECM) proteins in focal adhesions and hemi-desmosomes and that initiate outside-in signalling processes through connection with the cytoskeleton [5].

1.1.1 Function of the airway epithelium

The respiratory system consists of a branched airway tree connecting a single trachea proximally to millions of well-vascularised gas exchange units, the alveoli, in the distal lungs (Figure 1.1). The conducting airways are far more than a conduit to pass air to the alveoli and represent a specialised interface with the outside world [6]. The epithelium that lines

the conducting airways must form a barrier to protect against bacterial and viral pathogens and inhaled particulate matter and to eliminate these via the mucociliary escalator. Epithelial cells secrete mucus to form a 10 µm layer of airway surface liquid formed of two layers: a low-viscosity periciliary sol permissive of ciliary beat and an overlying viscous mucus gel that inhibits bacterial adherence and traps particles [7]. The airway surface liquid is moved at a rate of approximately 3 mm per minute towards the mouth, where it is swallowed [7]. In addition, the secretory functions of epithelial cells assist in the prevention of microbial colonisation through the production of antimicrobial peptides and proteins, such as lysozyme and lactoferrin [8]. As the first line of defence against inhaled pollutants, the respiratory epithelium is also responsible for the metabolism of these particles to form less toxic by-products. Finally, it is increasingly recognised that the epithelium is an important regulator of the innate and adaptive immune response during airway infection and injury [9, 10].

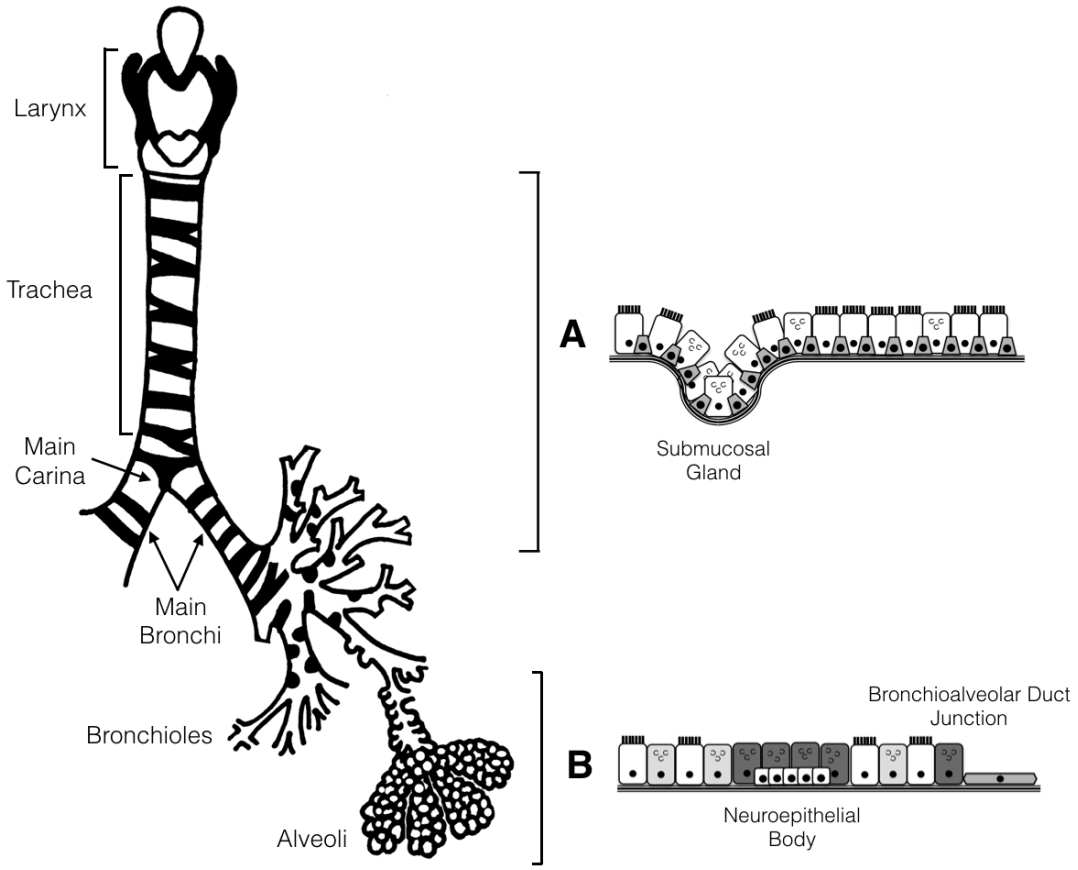

Figure 1.1: Proximal-distal anatomical variation in the bronchial tree. A) The airway epithelium in the proximal airways consists of a pseudostratified epithelium composed of basal progenitor cells and ciliated and mucosecretory cells. B) The distal bronchiolar epithelium is columnar and represents a transition zone between the conducting airway and alveolar respiratory epithelium.

1.1.2 Adult cell types

The respiratory epithelium is a continuous lining that arises from the foregut endoderm during embryonic development [11-13]. The work that follows will focus on the pseudostratified epithelium of the human proximal airways. In healthy individuals, this consists of cell types that can be broadly divided into basal cells and non-basal, or luminal, cells. The basal population lines the basement membrane and is not significantly exposed to the airway lumen during homeostasis, whereas the luminal cells perform differentiated airway functions.

1.1.2.1 Basal cells

Basal cells line the upper airway basement membrane and have a distinctive cuboidal morphology with a high nuclear-cytoplasmic volume ratio [3]. These cells form a range of cellular attachments, including intra-epithelial attachments mediated by desmosomes and attachment to the basement membrane via hemi-desmosomes. These cells express abundant cytokeratins, notably cytokeratin 5 (CK5) and in some circumstances cytokeratin 14 (CK14), p63, nerve growth factor receptor (NGFR), TROP2, integrin α6 and aquaporin 3 [14], but also show a great deal of heterogeneity in their protein expression [15, 16]. Studies in both murine and human airways suggest that basal cells are the proliferative population of airway epithelial cells during homeostasis and following tissue injury.

While basal cells have traditionally been considered to be relatively undifferentiated, there is emerging evidence that they are active contributors to the airway microenvironment independently of their differentiated progeny [17]. Recently, expansion of an interleukin-33 (IL-33)-producing subpopulation of basal cells was identified in the airways of patients with

chronic obstructive pulmonary disease (COPD) [18]. This finding suggests that basal cells can have an innate immune function because IL-33 acts on T-cells, innate lymphoid cells and natural killer T cells in the lung to increase pro-inflammatory IL-13 production [18]. Further support for this comes from an *in vitro* study in which basal cells but not differentiated airway cell types produced the anti-microbial protein RNase 7 in response to cigarette smoke [19]. The large surface area of basal cells in contact with the airway basement membrane makes this cell type well equipped to mediate epithelial cell interaction with stromal and immune cells.

1.1.2.2 Goblet cells

Goblet cells are responsible for the production of many secreted proteins in the airways. These cells contain abundant mucosubstances including mucins that exist in either a membrane-tethered or a secreted form, as is found in the gel-like layer of airway surface liquid. The transcription factor SPDEF is associated with goblet cell differentiation and the regulation of mucus production [20, 21]. The prominent mucins produced in human airway goblet cells are mucin 5AC (MUC5AC) and MUC5B, although a broad range of large structurally related gel-forming mucin glycoproteins are expressed [22]. In addition to these markers, cells can also be detected by positive histochemical staining with periodic acid-Schiff (PAS). While goblet cells are considered to be post-mitotic in the human lungs, their abundance increases dramatically in certain airway diseases, including asthma, COPD and cystic fibrosis but the mechanisms leading to goblet cell metaplasia are incompletely understood.

1.1.2.3 Ciliated cells

Ciliated cells line the luminal surface of the airways and produce motile force to move airway surface liquid. Ciliated cells are the most abundant airway epithelial cell type, accounting for between 30-50% of cells [3]. Early ciliated cell differentiation is marked by the expression of the transcription factor forkhead box protein J1 (FOXJ1) [23], which is expressed before the appearance of cilia at the apical surface. These cilia are microtubule-based projections containing acetylated α-tubulin. Mature ciliated cells are also distinguished by the polarised concentration of basal bodies in the luminal cytoplasm and mitochondria in the apical cytoplasm [24].

Each ciliated cell contains around 100-200 cilia (5-7 μm in length) and each cilium consists of nine peripheral doublets and two central microtubules in a '9+2' arrangement [25]. Peripheral doublets are connected by nexin links, each doublet is connected to the central microtubule pair by a radial spoke and each doublet has an inner and an outer dynein arm. The outer arm controls the frequency of ciliary beat while the inner arm controls bending of the cilium. Cilia beat with a simple backwards-forwards motion [26] through the ATPase activity of the dynein arms. ATP hydrolysis causes sliding of adjacent microtubules and bending of the cilium. Notably, it is known that genetic mutations in an increasing number of genes cause primary ciliary dyskinesia (PCD), a rare autosomal recessive disease in which motile cilia function is compromised [27].

1.1.2.4 Club cells

Club cells were first described by Max Clara in 1937 [28] and were known as 'Clara cells' until the discovery that the anatomist was an "outspoken Nazi" who studied tissue derived from

executed prisoners [29]. Club cells are found in the bronchiolar epithelium and are so named because of their rounded, club-like appearance. Club cells are non-ciliated, luminal epithelial cells characterised by agranular endoplasmic reticulum and electron-dense granules in their apical cytoplasm and by granular endoplasmic reticulum basally. Club cells have an important secretory function and produce proteins such as inflammatory secretoglobins, including the club cell secretory protein (CCSP; SCGB1A1), which is commonly used as a molecular marker of club cells, surfactant proteins and uteroglobin gene-related protein [30]. Further, the cells act to detoxify airway pollutants by their expression of cytochrome P450 monooxygenases; this family of metabolic enzymes acts to oxidise potentially damaging exogenous compounds rendering them more water-soluble [31].

1.1.2.5 Neuroendocrine cells

Pulmonary neuroendocrine cells (PNECs) are rare epithelial cells that occur either as individual cells or in clusters known as neuroepithelial bodies (NEBs) that are particularly associated with airway branch points [32, 33]. Despite their integration with other cell types derived from foregut endoderm, there has been some controversy about the developmental origin of neuroendocrine cells, which have been proposed to be independently derived from the neural crest [34]. However, recent evidence using lineage tracing in mice revealed that these cells shared a common developmental precursor with alveolar epithelial cells [35]. PNECs are small epithelial cells and are located in the basal epithelium. These cells contain secretory dense-core granules, which comprise signalling molecules such as serotonin (5-hydroxytryptamine) and neuropeptides such as calcitonin and calcitonin gene-related peptide (CGRP). Functionally, PNECs are activated by a range of stimuli and act as biosensors for changes in airway oxygen levels and chemical stimuli [36]. Indeed, recently it was shown that human PNECs are chemosensory through their expression of olfactory receptors, at

least *in vitro* [37]. While PNECs are not proliferative during homeostasis, it is believed that they can act to replenish club and ciliated cells following severe lung injury. Their rare appearance within the epithelium means that the PNEC contribution to airway regeneration is minor [38] but a more significant contribution might come through their role as a niche for other airway epithelial cell subtypes that survive injury.

1.1.3 Species differences

It is important to note that anatomical differences exist between the lungs of mammalian species. The diameter of the largest mouse airway is just 1.5 mm compared with a tracheal diameter of 1.75 cm in adult humans [39], meaning it is more comparable to the much smaller peripheral human bronchioles. In mice, extrapulmonary airways have cartilage rings but human airways are cartilaginous for many generations within the lungs. Similarly, submucosal glands are only found in the upper half of the mouse trachea, but extend for many bronchial generations in humans.

The cellular composition of the airways also varies between species. Human airways exhibit a pseudostratified, keratinised epithelium with abundant basal cells throughout the trachea, bronchi and bronchioles: only the respiratory bronchioles with <0.5 mm diameter contain a simple cuboidal epithelium lacking basal cells [40]. However, only the trachea and mainstem bronchi of murine airways contain basal cells under homeostatic conditions [41]. In contrast to humans, club cells are the predominant airway cell type in the rodent lungs, making up 50% of the proximal epithelium and 70% of the distal epithelium. However, in humans club cells vary in their abundance through the distal bronchial tree and are really only abundant in terminal bronchioles. In this respect, only the tracheal epithelium of mice is composed similarly to the majority of the human airway epithelium. Additionally, goblet cells are

abundant in human airways but in mice, presumably because of the relative sterility of laboratory conditions, these cells are rare.

These inter-species distinctions most probably result from differences in the respiratory demands placed upon human and murine lungs [42] and contribute significantly to the need for *in vitro* models representative of human airway epithelium.

1.1.4 The conducting airway epithelium in lung disease

1.1.4.1 Cancer

Lung cancer affects 34,000 patients per year in the UK and is the most common cause of cancer death worldwide [43]. The three most frequent histopathological subtypes of lung cancer are adenocarcinomas, small cell and squamous cell carcinomas (SCCs). Importantly, there appears to be a correlation between the location at which these tumours occur within the bronchial tree and the cell types present in those regions [44]. Adenocarcinomas arise in the distal lung and express markers of distal lung epithelial cells such as surfactant protein C (SPC), which is normally expressed by alveolar type II cells, and CCSP, which is normally expressed in club cells [45]. Small cell lung cancers arise in bronchioles and express CGRP, a protein that is normally expressed by neuroendocrine cells. SSCs are found in the proximal airways and result from step-wise changes in the epithelium that include basal cell hyperplasia, metaplasia, dysplasia, carcinoma-*in-situ* and ultimately invasive cancer [46]. The expansion of basal cells in pre-invasive lesions and the expression of basal cell proteins, such as CK5, led to the hypothesis that SSCs originate from basal epithelial cells. While 86% of lung cancers are caused by smoking [47], little is known about the molecular mechanisms that initiate the formation of neoplastic lesions from a healthy epithelium, primarily because

lung cancer diagnoses are made late in tumour progression compared with diagnoses in other organs [48].

1.1.4.2 Inflammatory lung diseases

Inflammation is a key hallmark in a range of respiratory conditions including adult respiratory distress syndrome [49], asthma, COPD and idiopathic pulmonary fibrosis (IPF). Epithelial disruption is central to the pathogenesis of these airway mucosecretory diseases, where goblet cell abundance increases and excessive mucus is secreted into narrowed, inflamed airways [50]. While the site and the nature of inflammation differs according to the pathophysiology of specific diseases, all involve immune and inflammatory cell types being recruited to the lungs, being activated and producing inflammatory cytokines. This environment causes the remodelling of the airway epithelium to favour goblet cell metaplasia and excessive secretion of mucus into the airways. The underlying molecular mechanisms that lead to the inflammatory and mucosecretory components of these diseases — and in particular the communication between stromal cells, immune cells and the overlying basal epithelial cells — are not well understood [51-53].

Airway epithelial cells initiate the process of airway inflammation by producing cytokines such as thymic stromal lymphopoietin (TSLP), IL-1, IL-25 and IL-33 [9]. These cytokines activate dendritic cells, mast cells and other cells to recruit haematopoietic cells and to induce the release of T helper type 2 (T_H2) cytokines such as IL-4, IL-5 and IL-13 [54]. IL-4 and IL-13 cause airway hyperresponsiveness and mucus overproduction in asthma. Through binding to the type II IL-4 receptor complex (IL-13Rα1 and IL-4Rα), these cytokines activate Janus kinases [55], which associate with interleukin receptor cytoplasmic domains [56, 57]. Downstream signalling pathways are then activated by these kinases. Specifically, IL-13 can

promote cell survival and growth via phosphoinositide 3-kinase (PI3K) signalling and can promote transcription of a wide variety of genes associated with airway inflammation, mucus production and hyperreactivity via signal transducer and activator of transcription 6 (STAT6) [58, 59]. STAT6 is expressed in normal and asthmatic human airway epithelium *in vivo* [60] and the cytokine secretion profile of human airway epithelial cells is altered in response to IL-4 and IL-13 in a STAT6-dependent manner. Epithelial cells upregulate cytokines such as granulocyte/macrophage colony-stimulating factor (GM-CSF) and eotaxin (CCL11), the promoter sequences of which contain STAT6-binding sites [61], and IL-8, which act to recruit neutrophils, eosinophils and monocytes to sites of inflammation [62]. Interestingly, mice lacking STAT6 are protected from IL-13-mediated airway hyperreactivity, mucus hypersecretion and eosinophilic inflammation [63], suggesting that it is a key driver of the epithelial response to inflammation. Although IL-4 and IL-13 are primary activators of STAT6, studies have suggested that STAT6 can be activated via a number of alternative pathways including angiotensin II in cardiomyocytes [64], CD28 engagement in naïve T cells [65] and platelet-derived growth factor (PDGF) signalling in NIH3T3 cells [66]. However, the physiological role of STAT6 that is activated by these alternative pathways is not clear.

1.1.5 Airway epithelial tissue engineering

Patients with end-stage tracheal disease have a poor quality of life and often prognosis due to the limited reconstruction options available. While in some patients it is possible to remove the region of affected airway and to re-join the surrounding healthy airways by end-to-end anastomosis, this option is only available for smaller airway defects; less than 30% and 50% of the tracheal length in children and adults, respectively [67]. While organ transplantation has dramatically reduced patient mortality and morbidity, demand for donor organs outstrips supply and life-long immunosuppression is required [68]. Tissue engineering

aims to bioengineer cell-scaffold technologies as an alternative strategy [69]. The first bioengineered tracheal transplant took place in 2008 and more have followed [70-72], making upper airway reconstruction among the first in the field to see clinical translation of advanced tissue-engineering methods [73]. While the clinical need for these transplants is established, many aspects of this nascent therapy remain to be investigated in detail [74], including the use of decellularised versus synthetic scaffolds [75], the value of graft pre-vascularisation or enhanced angiogenesis [76], and the optimal combination of growth factors and cultured cells to stimulate regeneration [77, 78].

Following tracheal transplantation, compromised mucociliary clearance represents an important challenge because secretions are retained at the distal anastomosis site, promoting infection and airway obstruction [79, 80]. Therefore, inclusion of a functional epithelium in tracheal transplants is desirable and some of the first tracheal transplants have included autologous epithelial cells with a view to expediting mucosal recovery [70, 71]. However, there is limited time available to culture cells owing to the urgent nature of some interventions and the inability to study cell fate in humans means that little is known about the contribution of these cells to the tracheal transplant. Clinical observations show that patients were slow to regenerate healthy mucosa in the cases in which tissue-engineered tracheal transplants were used [70, 71, 80, 81].

In general, bioengineering applications require high cell seeding densities and, given the large surface area of clinical tracheal grafts, obtaining sufficient numbers of autologous epithelial cells and finding methods to successfully apply these cells to scaffolds are challenges for the field.

In previous clinical cases, epithelial cells were obtained from endobronchial biopsies and cultured in serum-free bronchial epithelial growth medium (BEGM) for multiple passages [70]. This is a useful tool to generate basal cells for *in vitro* investigations [82] but the suitability of cells grown in this way for transplantation has not been shown. Similarly, efforts are underway to obtain autologous airway epithelial cells through the step-wise differentiation of induced pluripotent stem cells [83], but it has not been defined how useful or safe these cells will be for use in regenerative medicine because of doubts about their genetic stability during culture [84] and the added time-burden of iPS-based therapy; current techniques would require several months between cell isolation and delivery [85], unless 'off-the-shelf' allogeneic applications prove successful.

For clinical transplantation, there are three criteria that the ideal epithelial expansion system must meet: (i) the cells must not cause an adverse immune response (for example, be of autologous origin); (ii) they must be rapidly expandable to respond to challenging clinical scenarios; and (iii) they must be of high quality in terms of their karyotype, their expression of tissue-specific markers, their differentiation and their functional capacity. To date, no airway epithelial cell culture system has been described that convincingly meets all of these criteria.

1.2 Epithelial stem cells

1.2.1 Properties of adult stem cells

The nature of epithelial tissues means that there is a continuous physiological need to replace damaged or dead cells to maintain organ homeostasis and to respond to tissue injury [1]. This process is mediated by the presence of stem cells. By traditional definition, an

adult stem cell must be capable of self-renewal through asymmetric division and multilineage differentiation — that is, a cell must be able to give rise to multiple cell types of the organ from which it originates [86]. However, there are some circumstances in which epithelial stem cells from one organ display plasticity and are able to repopulate the epithelial compartment of another organ [87]. No universal markers exist to easily identify stem cells from different organs but in general they lack tissue-specific lineage-committed markers.

The best understood adult stem cell is the haematopoietic stem cell (HSC) and much stem cell theory has been applied to epithelial tissues from this system [88]. Following the first use of atomic bombs, radiation research showed that mice whose spleens or femurs were shielded with lead were protected from the lethal effects of ionising radiation on white blood cell counts [89]. Further experiments demonstrated that the mice could also be protected by intravenous injection of bone marrow [90] and this lead to the realisation that the entire haematopoietic system of the mouse could be reconstituted by transplanted stem cells residing in the bone marrow and spleen and that it was this population of stem cells that conferred radiation protection [91]. Till and McCulloch described the generation of multilineage myeloerythroid colonies in the spleen from cells [92] that subsequently emerged as a progenitor cell rather than the HSC itself. Nevertheless, the development of further *in vitro* and colony-forming assays for HSCs and their lineage-restricted progeny followed.

The HSC paradigm of step-wise generation of increasingly lineage-restricted progenitor cells that together can give rise to all blood cells has been hugely influential in other organs; organs contain true stem cells and progenitor cells (or transit-amplifying (TA) cells) that are committed to terminal differentiation but will first undergo a limited number of further cell

divisions [93]. In this way, the pool of progenitor cells greatly amplifies the number of differentiated cells that are produced. Slow cycling of stem cells is believed to reduce the chances of genetic mutation in stem cells by increasing the time available for DNA repair processes to proceed and thus preventing extensive progeny from sharing mutations that arise as a result of rapid division [94]. This model can be used to explain label retention experiments in which all cells in a tissue are labelled by incorporation of thymidine analogues, such as tritiated thymidine or BrdU, into dividing cells. Over time cells proliferate and at each cell division the label is diluted. As such, the 'label-retaining cells' (LRCs) are the slowest cycling population and are considered candidate stem cells.

The HSC paradigm promoted a view in which differentiation of cells is a unidirectional cascade away from the true stem cell. Of note, the discovery that, in adult bone marrow, multipotent and unipotent progenitor cells dominate, with few oligopotent intermediates, now threatens to overturn this influential dogma [95]. In other organs too, it has become clear that differentiation does not occur in this regimented fashion. Differences between organs are perhaps unsurprising given that the adult human haematopoietic system produces billions of cells per day whereas turnover is much slower in other organs such as the skin (4 weeks) or the lungs (6 months). Firstly, the epidermis is maintained by an abundant proliferative population located in the basal layer but no slow-cycling 'epidermal stem cell' has ever been identified. In fact, it appears, based on clonal labelling of epidermal basal cells *in vivo*, that a single stem/progenitor cell is sufficient to maintain the epidermis [96] and homeostasis can be maintained by a balance of symmetric (stem cell-stem cell or differentiated cell-differentiated cell) and asymmetric (stem cell-differentiated cell) divisions within this widespread progenitor cell population [97, 98]. Secondly, the definition of 'stemness' is now largely defined as a function rather than a cell type as progenitor cells can revert to stem cells despite having begun the differentiation process [99]. Evidence in a

variety of organs suggests that, under the right conditions, particularly following severe injury, more differentiated cell types can de-differentiate to perform stem cell functions [100, 101], leading to a much more flexible, bidirectional definition of stem cell function. However, the capability of cells to de-differentiate is likely to decline as mature differentiation status is achieved [102].

1.2.2 Multilineage airway stem cells

Adult organs are thought to be maintained by multiple populations of distinct stem/progenitor cells with distinct anatomical niches that respect the boundaries of the germ layer from which those cell populations are derived [103]. The existence of multipotent stem cells that can contribute to regeneration of multiple lung compartments would therefore be of considerable interest. Kajstura and co-workers reported that such a population of cells could be isolated from human lungs based on their expression of the receptor tyrosine kinase c-kit, that these cells could be cultured and that they retain their capacity to contribute to bronchiolar, alveolar, smooth muscle and endothelial cell lineages in a murine lung cryoinjury model [104]. However, the presence of an endogenous multipotent lung stem cell has not been supported in subsequent studies as c-kit+ cells in the human airway epithelium co-stain with the leukocyte marker CD45 [105] but not with the basal epithelial cell marker CK5 and, while c-kit is expressed in the majority of vascular endothelial cells in the murine lungs, careful *in vivo* lineage-tracing studies demonstrate that these cells do not contribute to epithelial repair after cryoinjury [106].

1.2.3 Airway epithelial stem cells

As a consequence of continuous pathogen and particulate exposure within the lungs, all conducting airways undergo a slow but continuous renewal [107]. This process of constant regeneration results in the complete turnover of the human bronchiolar epithelium every 100-300 days.

1.2.3.1 Proximal airway epithelial stem cells

Pulse-chase labelling experiments in rodents demonstrate that basal cells proliferate during airway homeostasis [108] and following injury [109], making these a probable candidate stem cell population. *In vitro*, the basal cell fraction of the rat airway epithelium has a higher colony-forming capacity that the non-basal cell fraction, although both are able to reconstitute a well-differentiated epithelium in tracheal xenografts [110], which could be explained by minor basal cell contamination of the non-basal cell population. Subsequent lineage-tracing studies from the CK5 [15] and CK14 promoter [111, 112] confirmed that basal cells are also multipotent *in vivo*, giving rise to all of the cell types of the differentiated airway epithelium.

It is increasingly recognised that basal cells are not a homogeneous cell population. This was initially suggested by variation in their *in vitro* colony-forming efficiency [113]. Long-term clonal analysis of the murine trachea demonstrated that the basal cell population (as marked by CK5 expression) contains approximately equal numbers of basal stem cells and basal luminal progenitor cells that are marked by expression of CK5 and the luminal marker CK8 [114] . Given that these CK5+/CK8+ cells do not divide at a greater rate than basal stem cells,

they do not meet the criteria of a TA population and support a model of stochastic homeostasis similar to that in the interfollicular epidermis [96, 115].

Following SO_2 injury, CCSP+ club cells in the mouse trachea give rise to basal cells with very low efficiency, suggesting that luminal cells might be able to regenerate basal stem cells under some conditions [116]. Recently, a genetic method was developed to ablate CK5+ basal cells using inhaled doxycycline to activate expression of the active subunit of diphtheria toxin in these cells [102]. Following basal cell ablation, CCSP+ tracheal club cells proliferate and de-differentiate to regenerate the basal cell compartment. These basal cells persist for at least 2 months and are able to regenerate a fully differentiated airway epithelium when the airway is injured [102].

Studies of human airway epithelial cells are largely consistent with these murine studies. Human airway basal cells are proliferative in culture and can differentiate into mucosecretory and ciliated cells both *in vitro* [117] and in tracheal xenograft models [118, 119], suggesting that they can act as a stem/progenitor cell population. Securing direct evidence of a homeostatic stem/progenitor cell role *in situ* is experimentally challenging. Nevertheless, using naturally occurring somatic mutations in mitochondrial DNA, it has been possible to trace clonal lineages and to demonstrate that maintenance of human airways relies on a multipotent epithelial stem cell that resides within the basal cell population [105]. Human basal cells display heterogeneous expression of cell surface markers such as epidermal growth factor receptor (EGFR) [16, 120], so it is likely that the human basal cell population is a mix of cells with different potentials and that subsets that represent true basal stem cells and those that represent more committed progenitor cells will be defined in the future. Similarly, no direct evidence of de-differentiation of luminal cells back to cells

capable of basal stem cell functions has been described in humans so if, and in what circumstances, this might occur in humans is currently unknown.

1.2.3.2 Distal airway epithelial stem cells

In the 1970s, secretory club cells were identified as the predominant mitotic cell population in the distal bronchiolar airways [121]. In rodents, oxidant exposure caused club cell de-differentiation to morphologically variant 'type A' cells that accounted for more than 70% of cell proliferation within the damaged bronchioles [121]. Pulse-chase experiments involving tritiated thymidine nucleoside incorporation subsequently established that 'type A' club cells were capable of multipotent differentiation into both club and ciliated cell types [121, 122].

In recent years, genetically modified mouse models have demonstrated that CCSP-expressing club cells are indeed a progenitor cell population that maintains distal bronchiolar homeostasis in murine lungs. Specifically, aggregation chimera and *Scgb1a1* lineage-tracing models demonstrated that large numbers of clonal CCSP cell-derived cell patches exhibiting multipotent differentiation to both club and ciliated cell lineages were present in distal bronchioles in the absence of epithelial injury [116, 123]. Overall, the results of these studies suggest that in the murine airways an abundant population of club cells functions as stem cells that maintain distal bronchiolar homeostasis.

Under normal conditions, less than 0.5% of bronchiolar epithelial cells undergo proliferation in any given day [124]. Therefore, most studies of distal bronchiolar stem cells have involved rodent models of airway injury that increase lung cell proliferation [125-127]. In addition to a contribution to airway homeostasis, previous severe injury and repair studies also identified subpopulations of club cells that contribute to lung regeneration. The most

frequently used severe bronchiolar injury model involves intraperitoneal or aerosolised delivery of naphthalene [128-130], a derivative of coal tar that causes significant club cell-specific toxicity in murine airways [131] due to their expression of cytochrome P-450 isozyme 2F2 (CYP2F2), which produces the toxic metabolite 1R,2S-naphthalene oxide upon naphthalene exposure [132]. Following naphthalene-mediated club cell ablation, a small number of naphthalene-resistant club cells (termed variant CCSP-expressing cells; vCE cells) survive by virtue of their low expression of CYP2F2 [133].

In addition to normal and variant club cells, a multipotent population of cells, termed bronchioalveolar stem cells (BASCs), are reported to reside in murine bronchiolar airways and to be capable of differentiation towards both bronchiolar club cell and alveolar cell lineages [134]. Further, recent studies identified a population of p63-expressing basal-like cells that contribute to distal lung repair following influenza infection [135]. At the peak of influenza infection the number of these p63+ basal cells increased dramatically and these cells were essential for restoration of a phenotypically normal epithelium with abundant club cells [136]. These studies, along with recent complementary evidence of de-differentiation of CCSP+ cells into upper airway basal stem cells, suggest previously unappreciated lineage plasticity among cells that survive lung epithelial injury [102].

Importantly, it is unclear how applicable these findings in rodent models are to human airway homeostasis, particularly as CCSP-expressing club cells are significantly less abundant in human airways [137] than in murine airways and a combination of both club and basal cells are present in human distal bronchioles [105]. This suggests that either club cells or basal cells might function as stem cells in human bronchioles. *In vitro* studies using human cells support the hypothesis that CK5- and/or CK14-expressing basal cells might function as bronchiolar stem cells in human lungs [135]. These results suggest that basal cells are

abundant and widely distributed human airway stem cells. It is as yet unclear whether these basal stem cells responsible for human airway homeostasis and regeneration are equivalent to the CK5- and CK14-expressing p63+ cells associated with post-influenza lung regeneration in mice [135, 136].

Recently, expression of Wnt-responsive genes such as leucine-rich repeat-containing G protein-coupled receptor 5 (LGR5) and LGR6 have been found in rare stem cells in a broad range of epithelial organs [138], including the lungs [55]. Following these discoveries, a discrete population of E-Cadherin+/LGR6+ cells was isolated from human small bronchioles [139]. Reminiscent of murine BASCs, single cells were capable of significant expansion *in vitro* and generated differentiated bronchioalveolar cell types when injected under the kidney capsule of immune-deficient mice [139]. The relationship of these cells to other known stem cell populations in either mouse or human lungs and their relative importance to *in vivo* homeostasis and repair is unknown.

1.2.4 Airway stem cell niches

The term 'niche' was first used to describe the idea that HSCs are dependent upon the complex three-dimensional (3D) environment created by neighbouring non-HSCs [140] and this concept has now been adopted across a wide range of stem cell types [141-144]. Studies have determined that the regulation of stem cells within their niche is coordinated through both intrinsic and extrinsic mechanisms (Figure 1.2). Specific components of niche-stem cell interactions include cell-cell interactions, stem cell-basement membrane interactions (governed by physical parameters such as extracellular matrix stiffness, composition and shear forces), regulation via local and systemic secreted factors, inflammation and environmental factors such as hypoxia and pathogenic stimuli [145]. Under normal

conditions, the niche is finely tuned to provide signals that balance stem/progenitor cell self-renewal and differentiation but this is disrupted in disease. It is hoped that future therapies may manipulate the niche environment to better preserve, mobilise or enhance endogenous stem cell potential [146]. Given the importance of airway epithelial cells in disease and the role of stem cells in maintaining and repairing the epithelium, there is great research interest in understanding the airway stem cell niche.

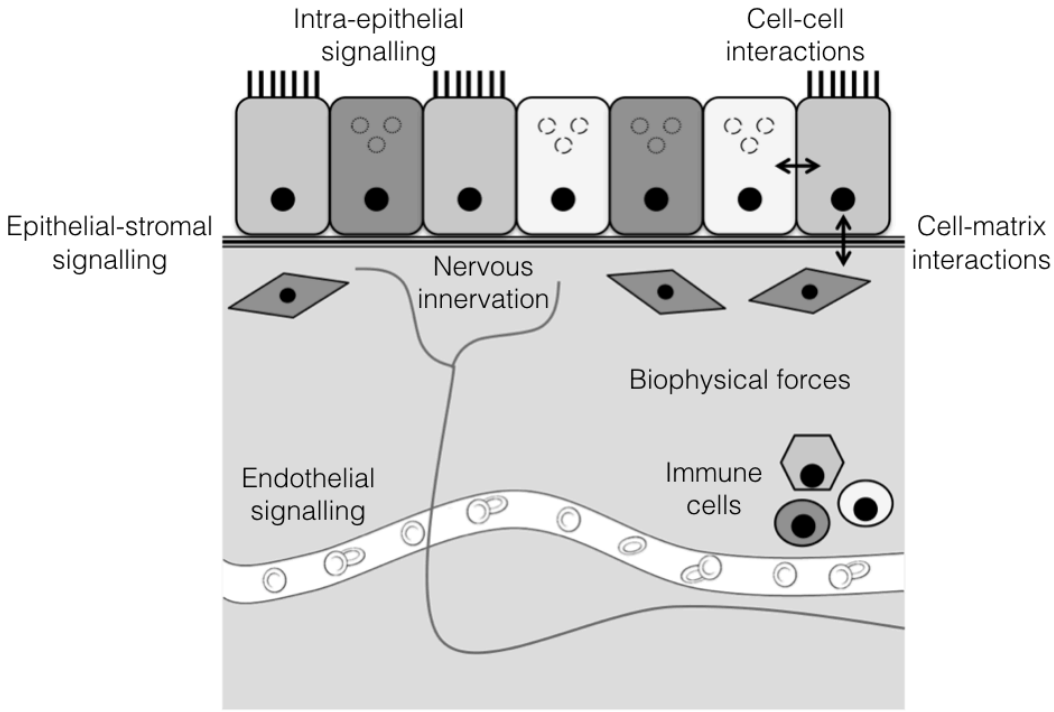

Figure 1.1: Components of an epithelial stem cell niche. The niche, or local microenvironment where stem cells reside, functions as a dynamic system that integrates local, systemic and cell-intrinsic signals to determine cellular fate and phenotype. Local signals include interactions among and between cells and their extracellular matrix as well as intra-epithelial and bidirectional epithelial-stromal signalling cascades. In turn, these signals both influence and respond to biophysical components of the niche including matrix stiffness, composition, local tension and microenvironment shape. In addition, signals from nearby inflammatory and immune cells, nervous innervation and the local circulation are known to influence stem cell phenotypes.

1.2.4.1 Anatomical location

The anatomical location of stem cells in an organ provides the first indication of the niche environment [147]. In the proximal airways, basal cells are a widespread stem cell population during homeostasis. However, following severe injury label-retaining cells with the capacity to regenerate surface epithelium are found in the submucosal glands of the upper murine trachea and cartilage-intercartilage junctions in the lower trachea [148]. Submucosal glands are specialised secretory structures that are continuous with the surface epithelium via ciliated ducts (Figure 1.1A); gland tubules within the submucosal glands produce mucus and the acini themselves are serous-producing [149, 150]. It is unclear whether submucosal gland basal cells are intrinsically different to surface epithelial basal cells or whether their protection stems from the physical protection from assault afforded by glands.

In murine distal airways, vCE cells located adjacent to NEBs and bronchioalveolar duct junctions (BADJs; Figure 1.1B) regenerate the airways following injury making these anatomical locations putative airway stem cell niches [134, 151, 152]. In support of this, epithelial cells in close proximity to pulmonary neuroendocrine cells and NEBs are more proliferative [153, 154]. Similarly, in adult mice exposed to naphthalene, surviving vCE cells co-localise with neuroendocrine cells located at airway branch points [152, 155]. Separately, the BADJ represents a second stem cell niche identified in distal bronchiolar airways [134, 151]. Here, neuroendocrine cells are largely absent, suggesting that other cell populations regulate BASC activation. It is as yet unclear whether NEBs or terminal bronchioles serve a similar role in maintaining populations of injury-resilient stem cells in human conducting airways.

1.2.4.2 The airway niche in murine models

The cellular basis of niche maintenance of airway stem cells is only beginning to be unravelled. Cells within the epithelium are an essential component of the stem cell niche. For example, following injury luminal cells signal to surviving basal stem cells and reactivate proliferation programmes, notably via EGFR signalling [156]. In intact airways, EGF family ligands produced apically are physically separated from their receptors, the human epidermal growth factor receptor (HER) family, which are expressed basolaterally. When the epithelium is compromised, this close cell-cell contact is disturbed and ligands interact with normally inaccessible receptors on the basolateral membrane of airway basal cells [120, 157]. The subsequent activation of HER family receptors engages signalling pathways that ensure proliferation occurs and barrier integrity is rapidly restored.

As well as secreted factors, direct cell-cell contact with neighbouring epithelial cells is an important regulator of stem cell behaviour. A low level of Notch signalling is present in the intact epithelium but following injury this is greatly upregulated and the amount of Notch ligand that cells are exposed to during repair appears to influence basal cell fate, but not proliferation, with high levels of Notch favouring secretory differentiation over ciliated differentiation [158]. This is consistent with previous data that Notch signalling favours goblet cell differentiation during development [159, 160] and data showing that deletion of the mouse *Pofut1* gene, which encodes an enzyme responsible for the Notch receptor fucosylation that is required for optimal ligand binding, leads to an airway devoid of goblet cells and lined by a completely ciliated epithelium [161]. Notch appears to be particularly important in defining early progenitor cells — that is, cells that express markers of both basal and luminal cell types [158]. Recent work shows that during airway differentiation active Notch 3 signals are found in CK5+/CK8+ parabasal cells and limit the abundance of

basal cells [115]. Further, subsets of basal cells can be identified that are committed to either mucosecretory or ciliated lineages. The populations are marked by intracellular Notch 2 activation and c-MYB expression, respectively [162]. The involvement of Notch signals in goblet cell differentiation may also represent a therapeutic target as antibodies against the Notch ligand Jagged have showed therapeutic effect in a murine asthma model [163]. While it is probable, based on our understanding of the Notch pathway in binary fate choices by lateral inhibition [164], that the expression of Notch components is determined by intra-epithelial signals, it remains possible that immune or stromal cells that are recruited following injury could contribute to epithelial Notch activity. Recently, it was discovered that stem cells themselves contribute to the niche of these lineage-restricted progenitor cells in the murine airway epithelium. Undifferentiated basal epithelial cells signal to secretory progenitor cells through expression of Jagged 2, thereby preventing their differentiation to the ciliated lineage [165]. Overall, there is strong evidence of epithelial-epithelial interactions acting to influence the fate of basal stem cells and their progeny, particularly by Notch signalling.

There is strong evidence that lung mesenchymal cells are key to the airway epithelial stem cell niche. Fibroblast growth factor 10 (FGF10)-expressing mesenchymal cells act as progenitor cells during lung development [166, 167] and become more abundant following naphthalene-mediated lung injury in mice [168], suggesting that this population contributes to the niche following acute epithelial injury. Following a range of epithelial injury types, surviving epithelial cells secrete Wnt 7b into the stroma, stimulating FGF10 secretion from mesenchymal cells [168] in a c-MYC-dependent manner [169]. FGF10 signals then feed back to epithelial cells to promote epithelial repair. Mesenchymal cells also provide essential trophic support to isolated epithelial cells in an *ex vivo* culture system [170] and their support capacity correlates with FGF10 expression [171]. Further evidence of the

importance of mesenchymal cells comes from a recent study that revealed that IL-6-induced STAT3 signalling in basal cells encourages the regeneration of a ciliated epithelium following SO_2 injury [172]. Importantly, the increase in STAT3 activation correlated with augmented IL-6 production in PDGF receptor-α (PDGFRα)-positive mesenchymal cells. The relationship between this population and those described by others [168, 170] remains to be determined as mesenchymal populations remain poorly characterised in the lungs, particularly following injury, as is the case in other organ systems [173]. Additionally, multiple mesenchymal populations may be capable of contributing to the niche through similar mechanisms.

Another contributor to the epithelial stem cell niche is the vasculature. In murine models, vascular endothelial cells participate in signalling pathways that control lung regeneration. In a unilateral pneumonectomy model, matrix metalloproteinase 14 (MMP14) produced by endothelial cells releases EGF protein family ectodomains to stimulate epithelial regeneration [174]. Recently, a novel endothelial cell-derived signalling axis was found to influence the fate of distal airway BASCs [175]. Primary murine lung endothelial cells were able to support multiple passages of BASCs with bronchiolar and alveolar differentiation capacity in 3D *ex vivo* culture [175]. Thrombospondin 1 (TSP1)-deficient endothelial cells tip the balance of BASC differentiation in favour of bronchiolar cell types, suggesting that TSP1 is an endothelial-derived factor that promotes alveolar differentiation of BASCs. Addition of recombinant bone morphogenetic protein 4 (BMP4) to BASC cultures produced the reverse effect in a TSP1-dependent manner, favouring alveolar differentiation [175]. Thus BMP4, probably produced by epithelial cells [176], induces TSP1 expression in endothelial cells via the calcineurin-nuclear factor of activated T cells (NFAT) pathway, which in turn promotes alveolar differentiation of murine distal lung stem cells.

In the bone marrow, neuronal cells are an essential component of the HSC niche [177] and, given that the airways are highly innervated by autonomic nerves [178], nerves are also likely to be important modulators of airway stem cell behaviour. Parasympathetic and most sensory airway nerve fibres stem from the vagus nerves while some sensory fibres originate in the dorsal root ganglia and run alongside spinal sympathetic nerves [179]. The wide range of physiological functions of acetylcholine in the airways, including as a bronchoconstrictor, stimulator of secretion and regulator of epithelial proliferation/cytokine production and fibroblast differentiation [83], imply that parasympathetic nerve fibres are likely to contribute to the niche environment. Indirect evidence for neural niche function comes from the observation that the neuropeptide CGRP activates cystic fibrosis transmembrane conductance regulator (CFTR) in the airway epithelium and is upregulated in the submucosal glands of patients with cystic fibrosis, presumably due to aberrant negative feedback. This leads to altered submucosal gland niche function and proliferation of normally slow-cycling glandular stem cells [180].

1.2.4.3 The human airway stem cell niche

Unfortunately, the signalling pathways and factors that regulate stem cell activity in human, rather than mouse, airways remain only partially characterised as a result of the inaccessibility of native human airways and a lack of human model systems. However, the data that we do have indicate that many of the same factors implicated in murine airway niches act similarly in human airway cells. For example, all four Notch receptors are expressed in cultured human airway basal cells and Notch activation is required for differentiation of human airway epithelial cells *in vitro* [181]. Furthermore, consistent with a Notch 2-active subset of basal progenitor cells destined to be become mucosecretory cells [162], Notch 2 is also required for the induction of goblet cell metaplasia in human airway

epithelial cells in culture and antibody-mediated inhibition of Notch 2 reduces goblet cell number in both human *in vitro* and murine *in vivo* models [49]. Interestingly, lentiviral-mediated sustained expression of the active Notch intracellular domains revealed that Notch 1 and Notch 3 induced human basal cells to differentiate towards mucosecretory lineages whereas Notch 2 and Notch 4 had minimal effects [181]. This suggests that Notch 2 activation might be necessary but not sufficient to induce goblet cell metaplasia.

In vitro studies also implicate endothelial signalling in the human basal cell niche as secretion of vascular endothelial growth factor (VEGF) [182] and FGF ligands [183] from basal epithelial cells alters the expression of factors, including MMP14, in human umbilical vein endothelial cells (HUVECS) that increase basal cell proliferation in co-culture.

Finally, studies of prospectively isolated LGR6+ human lung stem cells injected under the murine kidney capsule have identified putative endogenous cells and factors that are involved in lung stem cell growth and differentiation [139]. Expression of the cytokine stromal cell-derived factor 1 (SDF1; CXCL12) in transplanted stem cells activates and recruits stromal fibroblasts [184]. These fibroblasts secrete tumour necrosis factor-α (TNFα), which provides an activating signal for lung stem cells to produce more transforming growth factor-β (TGFβ) and consequently more SDF1. Further, endothelial cells are recruited in a process dependent on secretion of IL-8 and VEGF by activated fibroblasts [184]. Whilst the relevance of these *ex vivo* findings to the native human lung stem cell niche remains unclear, these data support the human relevance of the aforementioned studies, indicating the importance of mesenchymal and endothelial-derived signals in the stem cell niche.

1.3 Epithelial cell culture

Cell culture is a method for the expansion of cells under laboratory conditions. The temperature, gas composition, media composition and substrate of cells are controlled to allow replicable experiments in single or multiple cell types. The most common form of cell culture is on plastic surfaces to which cells adhere and multiply. Immortalised and cancer cell lines have allowed the detailed characterisation of fundamental biological processes but lack relevance to the tissue from which they were derived as a result of genetic changes. Primary cell culture has the advantage of improved tissue relevance but cultures are often limited in their scalability *in vitro* because of senescence [185], probably as a result of suboptimal culture conditions [186].

1.3.1 Human epithelial cell culture and cell therapy

A major breakthrough in epidermal keratinocyte culture came with the observation that in co-culture with lethally irradiated fibroblasts isolated from disaggregated mouse embryos [187], epithelial cells from mouse teratomas could be serially sub-cultured [188]. These cells shared characteristics of epidermal keratinocytes so human epidermal cells were cultured in the same system [189]. Over the years that followed the cell culture conditions allowed the derivation of enough epithelial cells from a small biopsy to cover the human body [190], suggesting that previous unsuccessful attempts to culture epidermal keratinocytes long-term were limited by the culture media composition — that is, the defined factors in Green's medium along with factors derived from 3T3 cells are permissive of long-term expansion in culture.

3T3-J2 co-culture of epidermal cells has had huge implications for cell therapy, particularly in burns patients for whom epidermal loss is a cause of mortality. Sheets of epidermis, cultured epithelial autografts, could be prepared by detaching confluent sheets of cells using the enzyme dispase and, when grafted onto wounds in immune-compromised mice, these sheets regenerated human epidermis [191]. Grafts prepared from the remaining healthy epidermis in severe burns patients engrafted successfully [192] and proved life-saving in two patients who had third-degree burns to 80-90% of their body surface [193]. Subsequently, keratinocyte co-cultures have been used in combined cell and gene therapy for junctional epidermolysis bullosa [194]. Regenerated, fully functional epidermis was maintained for more than 6 years after transplantation and was dependent on transduced epidermal stem cells present in the engrafted sheets [195]. Cultured epithelial autografts (Epicel; Genzyme Biosurgery) have been FDA-approved in the United States of America under the humanitarian device exemption since 2007 and are technically classified as a xenotransplantation product by virtue of the use of inactivated murine feeder cells. Similar products have been used clinically worldwide, including in the United Kingdom [196].

Beyond the epidermis, this culture protocol allows the expansion of a variety of stratified squamous epithelia, including oral and oesophageal epithelia. Limbal stem cells maintain the corneal epithelium [197] and limbal stem cells can also be grown on 3T3-J2 feeder cells. Chemical burns of the eye lead to vision loss but vision can be restored by transfer of material from the limbus of the healthy eye to the affected eye. In cases of bilateral limbal stem cell deficiency in which only a small area containing limbal stem cells is preserved, cells have been expanded from tiny biopsies of the healthy limbus and transplanted into the damaged eye in a procedure that has relieved symptoms in 80% of patients in a sample of more than 100 people [198, 199]. In 2015, commercial limbal stem cell therapy using this

technique (Holoclar; Chiesi Farmaceutici S.p.A.) was approved for medical use by the European Commission [200].

1.3.2 2D versus 3D cell culture

Cellular interactions are difficult to study *in situ* so 2D monolayer cultures were established to facilitate their study in many organ systems (Figure 1.3). However, *in vivo* cells exist in a complex milieu of neighbouring cells and ECM and interactions with both provide biochemical and mechanical signals that maintain tissue-specific gene expression programmes [201]. Traditional 2D cell culture models often bear little physical, molecular or physiological similarity to their tissue of origin so recent work has aimed to establish 3D cell cultures — or 'organoids' — that closely resemble the *in vivo* tissue from which they were derived [202]. Ideally, the physical, cellular and molecular characteristics of organoids mean that they share more morphological and physiological characteristics with *in vivo* differentiated epithelium [203].

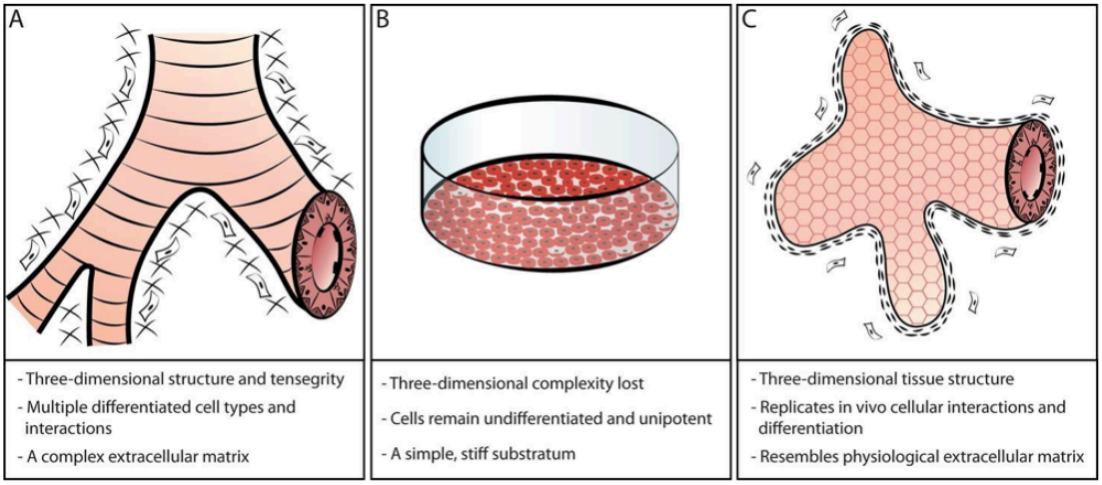

Figure 1.3: Three-dimensional (3D) tissue culture models attempt to recapitulate *in vivo* tissue complexity. A) *In vivo*, epithelial cells inhabit complex organ microenvironments that are composed of epithelial cells, stromal cells and the surrounding extracellular matrix. B) 2D culture models do not resemble normal *in vivo* tissues. C) Stem cell-derived organoid models recapitulate *in vivo* cellular interactions, multipotent differentiation and *in vivo* tissue architecture.

Work in mammary epithelial cells demonstrates that cells lose their characteristic architecture and molecular signature when grown on plastic substrates [204]; however, growth in a 3D, laminin-rich extracellular matrix, such as Matrigel, restores cellular architecture and mammary cells continue to respond to lactogenic stimuli [205], suggesting that tissue-specific function can also be maintained in 3D culture. Further, under the correct culture conditions, the ability of adult tissue-specific stem cells to maintain functional epithelium can also be maintained *ex vivo*. Despite high demand for pre-clinical models of the human intestines, cells were refractory to primary culture until a methodology for the expansion of mouse intestinal organoids from either whole intestinal crypts or single LGR5+ adult stem cells was reported [206]. Matrigel-embedded organoids derived from single stem cells are indistinguishable from those derived from whole crypts, with all four mature intestinal cell types present and a growth rate comparable to that expected *in vivo* [206]. Modification of these protocols led to their translation to the long-term culture of human small intestine and colon organoids through optimisation of the signalling molecules included in the medium [207].

Overall, 3D organoid cultures offer an opportunity to study a more physiologically relevant cell population as they contain not only the cells that proliferate upon contact with plastic substrates but a wider range of differentiated cells that are maintained by contact with a reconstituted basement membrane.

1.3.3 Airway epithelial cell culture systems

1.3.3.1 Generation of human airway epithelium from pluripotent cells

The requirement for rapidly expandable, high-quality human airway epithelial cell cultures spans many fields including basic lung science, toxicity testing and regenerative medicine. Towards this goal, several groups have investigated the possibility of generating airway cells from pluripotent human embryonic (ES) or induced pluripotent stem [83] cells. Early attempts suggested that this approach would be fruitful, generating cells that expressed a range of mature lung epithelial markers [208] and, by modified culture conditions, pure populations of type II alveolar cells characteristic of the distal airway epithelium [209].

Given the ethical problems that surround the use of ES cells, the derivation of lung progenitor cells from iPS cells was another important breakthrough [210]. Importantly, this work suggested that the step-wise application of developmentally important signalling molecules to pluripotent cells encouraged *in vivo*-like differentiation. These studies demonstrated the capacity to generate lung stem/progenitor cells but recent advances show that mature, differentiated epithelia can also be derived from human ES and iPS cells [211, 212]. Using similarly developmental approaches, cells are exposed to cocktails of growth factors that first induce endodermal differentiation, then promote anterior foregut identity as demonstrated by increased SRY-box 2 (SOX2) and NK2 homeobox 1 (NKX2.1) expression, before airway epithelial lineages can be specified using factors such as FGF7, FGF10 and BMP4. Finally, specific epithelial cell populations can be obtained by further modification of the growth factor pool; for example, proximal airway differentiation is encouraged by the addition of FGF18, the overexpression of which during development leads to airway proximalisation [212, 213]. Culture of these cells at an air-liquid interface confirms their potential to form a polarised, well-differentiated epithelium [214]. Subsequently, protocols

that allow the generation of 3D lung organoids containing both basal and mature cell lineages have been developed [215]. Consistent with an important role for low Notch signalling in ciliated cell differentiation, including a Notch inhibitor, DAPT, in culture medium favours formation of highly ciliated organoids [216].

Presently, there are concerns over the similarities between endogenous airway epithelium and ES/iPS cell-derived tissue due to our incomplete understanding of the differences in gene expression [84] and DNA methylation [217]. Further, researchers must contend with ethical concerns over the use of embryonic tissue, in the case of ES-derived cells, and the added time-burden of ES and iPS cell differentiation; current techniques require several months between cell isolation and stable differentiation [85].

1.3.3.2 Primary human airway basal epithelial cell culture

Primary airway cell cultures have been generated from human tissue for more than 30 years [218]. Culture of human airway epithelium has been reported from both endobronchial brushings [219] and endobronchial biopsies, either as explants [82, 220] or digested to obtain a cell suspension [221], and many *in vitro* studies have relied on cadaveric samples to generate large cell numbers [222, 223]. Cells are traditionally cultured in serum-free media formulated to allow the expansion of only epithelial cells [218]. Cells with a basal epithelial cell phenotype are expanded on plastic. At early passages (≤2), these methods produce cells suitable for a wide range of *in vitro* applications [117, 224].

Unfortunately, cell cultures expanded using these techniques degenerate over time: cultured basal cells become senescent, lose the capacity for airway differentiation and cease to proliferate, indicating a failure to maintain the stem/progenitor cell population in culture

[49]. These problems of limited differentiation capacity and growth arrest in culture are worsened if samples are derived from patient biopsies because only small tissue samples can be obtained, limiting the number of cells that can be isolated and the utility of these cultures. This is a severe limitation of existing basal cell expansion techniques because large numbers of cells are required for airway tissue-engineering applications and there is an increasing demand for personalised medicine, both of which require autologous epithelial cell cultures from living patients.

1.3.3.3 *Differentiation of primary human airway epithelial cells* in vitro

Models of airway disease frequently require a model of the differentiated epithelium that more closely mimics the *in vivo* epithelium than basal cells alone. For this, the field relies on air-liquid interface methods, in which confluent layers of human basal cells are exposed to an air-liquid interface for culture periods of several weeks on a transwell membrane, allowing their maturation into a mucosecretory, ciliated epithelium [225, 226]. Retinoic acid in the culture medium is essential to prevent a squamous epithelial cell phenotype in these cultures [227, 228]. These cultures have barrier properties, mucus secretion and ciliary beat that are similar to those of the endogenous airway epithelium. Despite the suitability of air-liquid interface cultures for aerosol exposure experiments [229], they are generally inconsistent due to variation between donor cultures. Further, air-liquid interface assays are poorly suited to high-throughput applications, for which there is increasing demand, because expansion of basal cells using existing technologies leads to decreasing differentiation potential.

As discussed in Section 1.3.2, there is evidence from a wide range of organ systems suggesting that 3D culture more closely resembles *in vivo* physiology and that primary adult

tissue-specific stem cells are able to re-initiate morphogenesis if isolated and cultured in 3D assays *in vitro*. While such models exist in other epithelia, the unlimited expansion of human airway epithelial cells in 3D organoid culture has yet to be reported. However, human airway basal cells proliferate and undergo lumen formation to form 'tracheospheres' in 3D culture, a characteristic that distinguishes them from malignant cells [230]. In initial studies, these structures displayed evidence of early ciliated differentiation but no markers of mature goblet cells could be detected [15], while the formation of mucus-secreting glandular acini from human basal cells was also reported in the absence of ciliated differentiation [231, 232]. Well-differentiated tracheospheres are of interest to the field because they would allow a platform more suited to high-throughput compound screening than traditional air-liquid interface cultures, in which transwell inserts are used.

1.4 Hypothesis

I hypothesise that co-culture with mitotically inactivated 3T3-J2 feeder cells and Rho-kinase inhibition (3T3+Y) will increase the rate of proliferation of human airway basal cells and maintain the multipotent differentiation capacity of these cells towards multiciliated and mucosecretory cell lineages when compared to traditional culture in bronchial epithelial growth medium (BEGM).

1.5 Aims

- To isolate and characterise primary human airway basal epithelial cells *in vitro*.
- To compare conventional cell culture methods with a recently described protocol involving the co-culture of basal cells with 3T3-J2 fibroblast feeder cells in the presence of a Rho-associated protein kinase (ROCK) inhibitor (3T3+Y).
- To investigate methods to improve the applicability of 3T3+Y co-culture to clinical translation
- To investigate the signalling mechanisms involved in basal cell expansion in 3T3+Y.

2 . Materials and Methods

2.1 Chemicals, solvents and plasticware

All chemicals were of analytical grade or above and were purchased from Sigma Aldrich, unless otherwise stated. Distilled and deionised water (ddH_2O) from a Millipore Q Plus water purification system was used to prepare all buffers. Laboratory plasticware was purchased from BD Biosciences.

2.2 Human airway epithelial cell isolation

2.2.1 Isolation from whole airways

Primary human bronchial epithelial cells (HBECs) were obtained from regions of normal airway from cadaveric donors or patients undergoing lobectomy procedures according to a previously described protocol [222, 223]. Ethical approval was obtained through the National Research Ethics Committee (REC reference 06/Q0505/12). Airways were cut under sterile conditions into approximately 5 mm^3 pieces in sterile conditions and incubated in a solution of 0.15% (w/v) pronase [66] in Dulbecco's modified Eagle's medium (DMEM, Gibco 41966) at 4°C overnight on a roller. Pronase solution was neutralised using 20% fetal bovine serum (FBS; v/v; Life Technologies). Cells were centrifuged at 300 x *g* for 5 minutes and resuspended in bronchial epithelial growth medium (BEGM; Lonza) at a seeding density of 1 x 10^6 cells/25 cm^2. Cells were maintained in 37°C incubators with 5% CO_2. Medium changes were performed three times per week and after initial expansion cells were frozen using Profreeze medium (Lonza) according to manufacturer's instructions for use in future experiments.

2.2.2 Isolation from endobronchial biopsy and brushing samples

Human bronchial epithelial cell cultures were derived from biopsies taken during tracheobronchoscopy procedures with patient consent. Ethical approval was obtained through the National Research Ethics Committee (REC references 06/Q0505/12 and 11/LO/1522). Biopsies were obtained from healthy regions of airways and received on ice in transport medium (αMEM supplemented with penicillin/streptomycin and amphotericin B) in 15 ml falcon tubes. Explant cultures were plated directly onto T25 flasks and enough BEGM applied to cover the flask.

Where indicated, endobronchial biopsies were digested using 16 U/ml dispase in RPMI for 20 minutes at room temperature. Epithelium was dissected away, DMEM containing 10% FBS was added to the dispase solution. After washing with PBS once, both epithelial and non-epithelial components were then digested in 0.1% trypsin/EDTA at 37°C for 30 minutes with agitation by pipetting every 10 minutes. Digests were neutralised with DMEM containing 10% FBS and combined with the neutralised dispase solution. Cells were centrifuged and resuspended in culture medium for counting and plating.

Endobronchial brushing samples were collected in the same transport medium in 15 ml falcon tubes. Cells were dissociated from the brush by vigorous pipetting and collected by centrifugation (with the brush *in situ*).

2.3 Human airway epithelial cell culture

All sterile culture media, sterile tissue culture grade trypsin/EDTA, tissue culture antibiotics and FBS were purchased from Invitrogen (now Thermo Fisher) unless otherwise stated. Sterile tissue culture flasks and plates were purchased from Nunc.

2.3.1 Human airway epithelial cell culture in BEGM

Human airway epithelial cells were thawed from frozen stocks into pre-warmed BEGM and medium was changed after 8 hours to remove residual dimethyl sulfoxide (DMSO). When cells were 80-90% confluent, cells were trypsinised using 0.05% trypsin/EDTA. This reaction was quenched using 10% serum-containing medium, cells were pelleted by centrifugation for 5 minutes at 300 x *g* and resuspended in BEGM for further passage or use in experiments. For BEGM cultures, a seeding density of 3,500 cells per cm^2 was used.

2.3.2 Feeder cell culture

3T3-J2 mouse embryonic fibroblasts were cultured in DMEM (Gibco; 41966) supplemented with 100 U/ml penicillin, 100 µg/ml streptomycin (Gibco; 15070) and 9% bovine serum (Gibco; 26170). Cells were cultured at 37°C in 5% CO_2 with three changes of medium per week. To generate feeder layers, confluent flasks of 3T3-J2 cells were mitotically inactivated by treatment with 4 µg/ml mitomycin C (Sigma; M4287) in culture medium for 2 hours (this can also be achieved using 40 Gy irradiation). Cells were trypsinised and plated at a density

of 20,000 cells/cm^2 in growth medium (approximately 1/3 confluent). Epithelial cells were added the following day [233].

2.3.3 Human airway epithelial cell culture in 3T3-J2 co-culture with ROCK inhibition (3T3+Y)

For co-cultures, feeder cells were prepared as described above. Epithelial culture medium consisted of DMEM (Gibco; 41966) and F12 (Gibco; 21765) in a 3:1 ratio with penicillin/streptomycin (Gibco; 15070) and 7.5% FBS (Gibco; 10270) supplemented with 5 µM Y-27632 (Cambridge Bioscience; Y1000), 25 ng/ml hydrocortisone (Sigma; H0888), 0.125 ng/ml epidermal growth factor (EGF; Sino Biological; 10605), 5 µg/ml insulin (Sigma; I6634), 0.1 nM cholera toxin (Sigma; C8052), 250 ng/ml amphotericin B (Fisher Scientific; 10746254) and 10 µg/ml gentamycin (Gibco; 15710). Epithelial cells were cultured at 37°C and 5% CO_2 with three changes of medium per week. When experiments required isolation of a pure epithelial cell population from co-cultures, differential trypsinisation was performed taking advantage of the greater trypsin sensitivity of feeder cells in comparison to strongly adherent epithelial cells. Briefly, co-cultures were trypsinised once for 1-2 minutes to remove the 3T3-J2s, before being washed in PBS and more trypsin added for a further 5 minutes to detach epithelial cells. Where indicated, feeder cells and epithelial cells were pre-stained with Vybrant DiI or DiO Cell-Labeling Solution (Thermo Fisher Scientific) according to manufacturer's instructions. Trypsinisation was performed using either 0.05% Trypsin/EDTA or TrypLE (Life Technologies), a recombinant enzyme, avoiding the use of porcine trypsin. Population doublings (PD) were calculated as PD = 3.32 * (log (cells harvested / cells seeded), 10).

For experiments comparing matched donor cells under different culture conditions, cells were thawed in BEGM for one passage and then divided into experimental culture conditions.

2.3.4 Lentiviral vector production and transduction of primary airway epithelial cells in 3T3+Y

A lentiviral vector that constitutively expresses ZS-Green green fluorescent protein (GFP) and luciferase (ZS-Green-Luc) was generated as previously described [234]. The backbone plasmid, pHIV-Luc-ZS Green, was a gift from Bryan Welm (Addgene plasmid #39196) [235]. The envelope plasmid, pMD2.G, was a gift from Didier Trono (Addgene plasmid #12259). The packaging plasmids, pRSV-Rev and pMDLg/pRRE, were also a gift from Didier Trono (Addgene plasmid #12253, #12251) [236]. Briefly, viral supernatants were created by co-transfecting 293T HEK cells with the above plasmids using JetPEI (Polyplus Transfection). Supernatants were concentrated by ultracentrifugation. Viral titres were determined with 293T HEK cells plated at 5 x 10^4 cells per well in a 12-well plate overnight. Virus was added to each well at serial dilutions and analysed by flow cytometry after 72 hours to determine transduction efficacy.

Primary human bronchial epithelial cells were transduced using ZS-Green-Luc lentivirus (generated from plasmids as described above). Following initial expansion from biopsies, 5 x 10^4 primary epithelial cells were plated onto 3T3-J2 feeders in T25 flasks. Cells were allowed to adhere overnight prior to transduction. Lentivirus was prepared in epithelial culture medium with 4 μg/ml polybrene (Sigma) and cells were incubated with the lentivirus for 16 hours. Following transduction, cells were grown as per standard 3T3+Y conditions for a

further 8 days and FACS sorted (FACS Aria II) to generate a 100% positive population. Sorted cells were maintained in 3T3+Y conditions over multiple passages and retained their ability to differentiate in air-liquid interface cultures.

2.3.5 Colony-forming assays

To analyse colony-forming capacity, primary human bronchial epithelial cells were seeded onto 6-well plates pre-coated with collagen I (rat tail collagen I; BD 354236) at 1000 cells per well. 3T3-J2 feeder cells were seeded at 2 x 10^4 cells/cm^2 the day prior to epithelial cell seeding. Plates were fixed and stained after 10 days using 1% crystal violet solution (Sigma). Plates were washed extensively in water and allowed to dry at room temperature overnight. Colonies were counted manually using a brightfield microscope.

2.3.6 Air-liquid interface cultures

Air-liquid interface cultures for airway epithelial cells expanded in 3T3+Y were adapted from a previously published protocol [237]. Basal cells were seeded on collagen-coated, semi-permeable membrane supports (Transwell-Col, 0.4 µm pore size; Corning) in submerged culture in BEGM + 5 µM Y-27632. For 12-well transwells, 1 x 10^6 cells were seeded per membrane in 250 µl medium, while for 24-well transwells, 5 x 10^5 cells were seeded in 125 µl. After two days (that is, at confluence), cells were fed only from the basolateral side with air-liquid interface medium (50% BEGM and 50% hi-glucose DMEM containing 100 nM retinoic acid; Gibco 41966). Medium was exchanged 3 times per week and mucus produced on the apical surface was removed by gentle washing with PBS.

Transepithelial electrical resistance (TEER), an indicator of epithelial integrity, was measured in established air-liquid interface cultures by Prof. Chris O'Callaghan's laboratory (Institute of Child Health, UCL) using an EVOM2 resistance meter and Endohm chamber (World Precision Instruments) with cup size appropriate for the size of culture insert (6 mm culture cup for 24-well transwells and 12 mm culture cup for 12-well transwells). Resistance is measured using one probe in the upper chamber (culture insert) and one in the lower chamber. Each probe can measure voltage and contains an electrode to pass current. Using a control insert without cultured cells, the resistance of the cell layer can be measured as R(cell layer) = R(total) – R(control). For 24-well transwells, 1 ml (0.5 ml for 12-well) BEGM was loaded into the culture cup and 200 µl (100 µl for 12-well) onto the apical side of cultures. Transwells were placed into the culture cup and readings were taken after the TEER value had stabilised (typically 5-10 seconds). Readings were taken from three independent transwells to obtain an average TEER value for each culture.

Ciliary beat frequency and pattern were determined by Prof. Chris O'Callaghan's laboratory (Institute of Child Health, UCL). Airway epithelial cells were expanded in 3T3+Y, differentiated as air-liquid interface cultures and observed using an inverted microscope system (Nikon TU1000). Beating cilia were recorded using a Troubleshooter digital high-speed video camera (Lake Image Systems) at a rate of 250 frames/second using a 40x objective. The number of multiciliated cells in each area was counted and half were used to determine the average ciliary beat frequency (CBF). The CBF of individual ciliated cells was determined by counting the number of frames required for 5 full sweeps of a clearly visible ciliary tip. This was converted to CBF where CBF = 250 / (number frames for 5 beats) x 5. The dyskinesia index presented is the percentage of dyskinetic ciliated cells relative to the total number of motile ciliated cells.

For contact inhibition studies, primary human airway epithelial cells grown in 3T3+Y were seeded submerged in tracheosphere medium for either two or eight days. Cells were fixed with 4% PFA before immunocytochemistry.

2.3.7 3D tracheosphere cultures

To generate differentiated 3D airway tracheosphere, or spheroid, cultures, basal epithelial cells were trypsinised from either BEGM or 3T3+Y cultures and counted. Tracheosphere medium consisted of 50% BEBM (Lonza) and 50% DMEM (Gibco; 41966) supplemented with BEGM supplements (minus triiodothyronine, gentamycin, amphotericin and retinoic acid). 100 nM retinoic acid (Sigma) was added immediately before each use. Ultra-low attachment 96-well plates (Corning; clear, flat bottom) were coated with 30 µl 25% Matrigel (growth factor reduced; BD Biosciences; in tracheosphere medium) and allowed to gel at 37^{o}C for 20 minutes. 2,500 basal cells per well were then seeded in 65 µl 5% Matrigel (growth factor reduced; in tracheosphere medium). Cells were fed by addition of 70 µl tracheosphere medium on day 3, day 8 and day 14. On day 18, tracheospheres were collected in cold PBS and centrifuged at 200 x *g* for 3 minutes. Tracheospheres were then fixed by resuspension in 4% PFA for 30 minutes, washed with PBS and resuspended in Histogel specimen-processing gel (Thermo Fisher) for processing and paraffin embedding. Tracheosphere size was quantified by measuring the diameter of the 30 largest tracheospheres per well. Triplicate wells were analysed in three matched donor cultures per passage using Volocity software (PerkinElmer).

2.3.8 3D airway epithelial aggregate cultures

For differentiation as airway epithelial aggregates, we modified a protocol previously described by Jorissen and colleagues [238-241]. Primary human basal cells were cultured in 3T3+Y for two passages, trypsinised and 50,000 were seeded per well of a 96-well ultra-low adhesion plate (Corning) in 150 µl tracheosphere medium (see above) plus 5 µM Y-27632. The plate was shaken continuously at 100 rpm for 5 days of culture using a rotating shaker and then remained static for a further 18 days. Aggregates were fed by addition of 50 µl medium on day 3, day 8, day 14 and day 18 of culture.

2.4 Other cell culture

2.4.1 Mycoplasma testing

All cultured cells were routinely tested for the absence of mycoplasma contamination using published PCR-based techniques [242] or a MycoAlert mycoplasma testing kit (Lonza).

2.4.2 Cell lines

A431 (epidermoid carcinoma) and A549 (lung adenocarcinoma) cancer cell lines were authenticated using STR profiling and cultured in DMEM (Gibco; 41966) plus 100 U/ml penicillin, 100 µg/ml streptomycin (Gibco; #15070) and 10% FBS at 37°C with 5% CO_2 with three changes of medium per week.

2.4.3 Human MSCs and lung fibroblasts

Primary human lung fibroblasts derived from healthy donor lungs were a kind gift from Professor Robin McAnulty (University College London, UK) and were cultured in DMEM with 100 U/ml penicillin, 100 μg/ml streptomycin (Gibco; #15070) and 10% fetal bovine serum [243]. Human mesenchymal stromal cells (MSCs) were purchased from Texas A&M Health Science Center and were cultured in α-minimum essential medium (αMEM) containing 17% fetal bovine serum [244]. Cells were cultured at 37°C with 5% CO_2 with three changes of medium per week. The generation of feeder cells from these was performed as described above for 3T3-J2 cells.

2.4.4 Small molecule inhibitors

The MET inhibitor PF-0421903 was purchased from Sigma, resuspended in DMSO as a 10 mM stock solution and stored in aliquots at -20°C until use. In experiments using PF-0421903, cells were pre-treated with the inhibitor at the relevant concentration for 20 minutes prior to stimulation. The STAT6 inhibitor AS-1517499 was purchased from Axon Medchem, resuspended in DMSO as a 10 mM stock solution and stored in aliquots at -80°C until use. In experiments using AS-1517499, cells were pre-treated with the inhibitor at the relevant concentration for 30 minutes prior to stimulation.

2.5 Histology and immunofluorescence staining

2.5.1 Immunohistochemistry

Haematoxylin and eosin (H&E) and periodic acid-Schiff (PAS) staining were performed on 5 µm sections using an automated staining system (Tissue-Tek). For immunofluorescence, slides were dewaxed using an automated protocol and antigen retrieval was performed using citrate buffer. Slides were blocked using 10% FBS for 1 hour at room temperature. Primary antibodies were diluted in block buffer as indicated in Table 2.1 and applied overnight at 4°C. Species-appropriate secondary antibodies conjugated to AlexaFluor dyes (Molecular Probes) were applied at a 1:500 dilution in block buffer for 2 hours at room temperature. Images were acquired using a Zeiss LSM700 confocal microscope.

2.5.2 Immunocytochemistry

Cells were grown in 4-well or 8-well chamber slide (Millipore), washed once with PBS and fixed at room temperature for 20 minutes using 4% PFA (Sigma). Samples were stored in PBS at 4°C until the time of staining. Cells were blocked for 1 hour at room temperature in block solution consisting of 10% FBS in PBS. Where necessary, cells were permeabilised in block solution containing 0.1% Triton X-100 (Sigma). Cells were stained overnight at 4°C in block buffer (without Triton X-100) containing primary antibody at the concentration indicated in Table 2.1. Cells were washed three times with PBS and incubated with species-appropriate AlexaFluor-conjugated secondary antibodies (Molecular Probes) at a 1:500 dilution in block buffer for 2 hours at room temperature. Images were acquired using a Zeiss LSM700 confocal microscope.

Antibody	Species	Isotype	Supplier	Product Code	Dilution Factor
Pan-cytokeratin (Epithelial cells)	Rabbit	IgG	Abcam	ab9377	1/400
E-cadherin (Epithelial cells)	Mouse	IgG1	Abcam	ab1416	1/200
CD31 (Endothelial cells)	Mouse	IgG1	Abcam	ab9498	1/200
CD45 (Haematopoetic cells)	Rabbit	IgG	Abcam	ab10558	1/200
Cytokeratin 5 (Airway basal cells)	Rabbit	IgG	Abcam	ab24647	1/400
Cytokeratin 8 (Airway luminal cells)	Mouse	IgG1	Abcam	ab9023	1/400
Cytokeratin 14 (Airway basal cells)	Mouse	IgG3	Novus	NB600-1190	1/400
Cytokeratin 14 (Airway basal cells)	Rabbit	IgG	Covance	PRB-155P	1/400
MUC5AC (Airway mucous and mucosecretory cells)	Mouse	IgG1	Sigma	M5293	1/500
MUC5B (Airway mucous and mucosecretory cells)	Rabbit	IgG	Sigma	HPA008246	1/500
CCSP (Club cell secretory protein)	Rabbit	IgG	Abcam	ab40273	1/200
ACT (Airway ciliated cells)	Mouse	IgG2b	Sigma	T6793	1/500
FOXJ1 (Airway ciliated cells)	Mouse	IgG1	Abcam	ab40869	1/200
p63 (Airway basal cells)	Rabbit	IgG	Abcam	ab53039	1/200
NGFR (Airway basal cells)	Goat	IgG	Abcam	ab87472	1/200
TROP2 (Airway basal cells)	Rabbit	IgG	Abcam	ab65005	1/200
ITGA6 (Airway basal cells)	Mouse	IgG2b	Abcam	ab20142	1/200
Ki67 (Proliferating Cells)	Mouse	IgG1	Dako	M7240	1/400

Table 2.1: Antibodies used for immunofluorescence staining.

2.6 Flow cytometry

2.6.1 EdU Uptake

For experiments comparing proliferation in BEGM and 3T3+Y, matched donor airway epithelial cells (P2) were seeded in these conditions for 3 days. Feeder cells were removed by differential trypsinisation. Single cell suspensions were obtained by trypsinisation of epithelial cell cultures treated with 10 μM EdU (Life Technologies Click-iT EdU Alexa Fluor 488; C10633) for 2 hours prior to the experiment. Cells were stained according to manufacturer's instructions and co-stained with DAPI. Flow cytometry was performed using an LSRFortessa (BD Biosciences) and analysed using FlowJo 10.0.6 (Tree Star).

2.6.2 Basal cell marker expression

Matched donor airway epithelial cells (P3) were seeded in BEGM or 3T3+Y for 4 days. Feeder cells were removed by differential trypsinisation and single cell suspensions were obtained by subsequent trypsinisation of epithelial cells. All staining was performed in FACS buffer (PBS containing 1% bovine serum albumin (BSA) and 0.1% sodium azide) at 4°C. Cells were blocked in FACS buffer + 10% FBS for 20 minutes and stained with NGFR PerCP-Cy5.5 (Biolegend; 1:100), integrin α6 PE (BD Biosciences; 1:20),TROP2 AF610-PE (Abcam; 1:50) or CK5 AF647 (Abcam; 1:50) for a further 20 minutes. For intracellular staining, cells were fixed in BD Cytofix Fixation Buffer (BD Biosciences) for 15 minutes at 4°C. Cells were then incubated with intracellular antibodies in permeabilisation buffer (eBiosience) for 20 minutes at 4°C. A Live/Dead fixable violet dead cell stain (Invitrogen) was included to ensure that only living cells were analysed.

2.7 Chromosome analyses

2.7.1 Karyotype analysis

Cells for karyotype analysis were cultured for 5-7 passages in 3T3+Y. After 5 days in culture (to ensure log phase cells), T25 flasks of cells were incubated in 5 ml growth medium containing 10 µg/ml KaryoMAX colcemid solution (Gibco) at 37°C for 3 hours. Cells were differentially trypsinised to remove feeder cells and then epithelial cells were removed using TrypLE (1x; Life Technologies) until a single cell suspension was obtained. TrypLE was neutralised using the growth medium + colcemid solution. Epithelial cells were centrifuged at 1000 rpm for 8 minutes in 15 ml falcon tubes. Supernatant was discarded and 4 ml 0.075 M KCl (Ambion) was added drop-by-drop and tubes incubated at 37°C for 25 minutes. 10 drops of fixative (3:1 methanol/acetic acid; warmed to 37°C) were added and tubes were mixed by inversion and incubated at room temperature for 10 minutes. Tubes were centrifuged at 1000 rpm for 8 minutes, supernatant removed, pellets resuspended in 4 ml fixative, inverted to mix and incubated for 30 minutes at room temperature. Tubes were centrifuged in the same way a second time and pellets resuspended in 2 ml fixative. The cell suspension was stored at 4°C overnight before shipping to Cell Guidance Systems (Cambridge, UK) for karyotype analysis. 20 cells were analysed per donor cell culture.

2.7.2 Multiplex ligation-dependent probe amplification (MLPA)

Matched donor biopsy tissue and cultured cells were transported to the cytogenetics laboratory within the North East Thames Regional Genetics Service Laboratories (London, UK) in αMEM supplemented with 100 U/ml penicillin, 100 µg/ml streptomycin and 0.25

µg/ml amphotericin B. DNA was extracted using the iGENatal kit (Igen Biotech) and MLPA analysis performed using the SALSA P036 Subtelomeres Mix 1 Probemix (MRC-Holland) to investigate copy number changes at the ends of each chromosome. Data were processed and analysed using Genemarker (Softgenetics). Balanced rearrangements would not be detected using this technique.

2.8 Microarrays

2.8.1 Microarrays

Human airway epithelial cells (P1) from four donors were grown in either BEGM or 3T3+Y for one passage (7 days). Cells grown in 3T3+Y were differentially trypsinised to remove murine feeder cells. Cells in all conditions were trypsinised and resuspended in 500 µl TRIzol reagent for RNA extraction. RNA extraction was performed using a Direct-zol RNA MiniPrep Kit (Zymogen) according to manufacturer's instructions. Total RNA yield was determined using a Nanodrop spectrophotometer. RNA integrity was analysed using a Bioanalyzer 2100 (Agilent) and only RNAs with an RNA integrity number higher than 8.5 were used for the microarrays experiment. RNA was supplied to Source Biosciences (UK). RNA was synthesised, amplified and purified using the Illumina TotalPrep RNA Amplification Kit (Life Technologies) following manufacturer's recommendations. Briefly, 500 ng of RNA was reverse transcribed. After second strand synthesis, the cDNA was transcribed *in vitro* and cRNA labelled with biotin-16-UTP. Labelled probe hybridisation to Illumina Human HT-12 v4 Expression BeadChip (~48,000 probes) was carried out using Illumina's protocol. Beadchips were scanned on the Illumina BeadArray 500GX Reader using Illumina BeadScan image data acquisition software. RNA control samples were analysed with each run. Expression data

underwent quality control analysis and normalisation using the BeadStudio data analysis software v2009.1 (Illumina). Briefly, quality control assessed the Direct Hyb control plots within the BeadStudio software. All control plots displayed expected values as per the Illumina specifications. Control measures included hybridisation controls, negative and background controls, biotin-, low- and high-stringency controls, housekeeping gene intensities and average gene intensities.

Data are expressed as log2 ratios of fluorescence intensities of the experimental and the common reference sample. The Illumina data were then normalised using the 'normalise quantiles' function in the BeadStudio Software. Differential expression analysis was performed using the significance analysis of microarrays [71] v2.23 [245]. The raw p-values were adjusted by the Benjamini-Hochberg procedure [246], which controls the false discovery rate (FDR). A gene was considered differentially expressed if the Benjamini-Hochberg-corrected p-value was less than 0.05. Genes that were expressed at significantly different levels between two different groups were analysed by supervised hierarchical clustering (uncentered correlation, complete linkage) [247] to visualise the correlation of co-expressed genes in Treeview (available at http://rana.lbl.gov/EisenSoftware.htm).

All microarray data reported in this thesis are analysed in accordance with MIAME guidelines and have been deposited in the National Center for Biotechnology Information Gene Expression Omnibus (GEO, http://www.ncbi.nlm.nih.gov/geo/) public repository and they are accessible through GEO accession number GSE69005.

2.8.2 Validation of microarrays by qPCR

For quantitative real-time polymerase chain reaction (qPCR) validation, we confirmed the expression of two upregulated genes (FOXA1 and SERPIN B4) and four downregulated genes (TRIB3, EGFR, RNASE7 and HSD17B2) in donor cell lines cultured in 3T3+Y. Gene-specific primers (Table 2.2) were designed inside or nearby the microarray sequence targeted using Primer Express Software (Applied Biosystems). Total RNA was reverse transcribed using qScriptTM cDNA Super-Mix (Quanta Biosciences) according to the manufacturer's protocol. qPCR was carried out using the Power SYBR Green RT-PCR Master Mix (Life Technologies) in an Eppendorf real-time PCR machine following cycling conditions: 10 min at 95°C, 40 cycles of 95°C for 15 s and 60°C for 60 s, followed by melting curve analysis.

Relative gene expression was quantified using the threshold cycle [248] method and normalised to the amount of ACTB, which meets the criteria of minimal variation between samples and compatible expression level with the studied genes. Absence of cross contamination and primer dimer was checked on genomic DNA and water. Each sample was tested in triplicate and a sample without template was included in each run as a negative control. From microarray and qPCR data, we calculated the BEGM/3T3+Y ratio for each gene. Correlations between microarrays and qPCR data were measured using the Pearson coefficient.

Gene	Direction	Primer Sequence
FOXA1	Forward	GGGAGCTGGATTTCAAAACGT
	Reverse	CCGTCTGGCTATACTAACACCA
SERPINB4	Forward	TTCAATGGGGATGCAGACCT
	Reverse	ACTCCCTCCTCAGTGACCTC
TRIB3	Forward	GTCCAGGCCTGTCAACCAT
	Reverse	CCCAGAAGAGTCCCACCTG
EGFR	Forward	CAGGTGCGAATGACAGTAGC
	Reverse	AGTCAGGTTACAGGGCACAC
RNASE7	Forward	CATTGCACATGTCTCCCCTG
	Reverse	TTCAGGTCACCTCACTGCC
HSD17B2	Forward	TCAACTCGTTAGCCAGCAAG
	Reverse	CAGATCCACAAGTAAGCGCC
ACTB	Forward	CATGCCATCCTGCGTCTG
	Reverse	TGGCCATCTCTTGCTCGAA

Table 2.2: Primer sequences used for qPCR microarray validation.

2.9 Antibody arrays

Proteome profiler human phospho-RTK antibody arrays (R&D Systems; ARY001B) were performed according to the manufacturer's instructions. 500 µg fresh protein lysates from cells grown in BEGM and treated with 3T3-J2-conditioned medium for 30 minutes were incubated with pre-blocked nitrocellulose membranes overnight at 4°C on a rocking platform. Activated receptors were detected using Luminata Crescendo HRP substrate (Merck Millipore) and imaged by X-ray film exposure.

Human cytokine arrays (R&D Systems; #ARY005) were performed according to the manufacturer's instructions. 3T3-J2 feeder cells were removed from human basal cell co-cultures using differential trypsinisation and cells were serum-starved overnight in

DMEM/F12. Cells were stimulated as described for 24 hours before cell culture medium was collected for array analysis. 700 µl of cell culture supernatant was incubated with membranes overnight at 4°C on a rocking platform. Cytokines were detected using Luminata Crescendo HRP substrate (Merck Millipore) and imaged using an ImageQuant LAS 4000 system (GE Healthcare).

2.10 Western blotting and co-immunoprecipitation

Cell lysis was performed using RIPA buffer containing Halt protease and phosphatase inhibitor cocktail (Thermo Fisher). After scraping, cell lysates were transferred to microfuge tubes, incubated at 4°C on a rotating wheel for 30 minutes, centrifuged at 14, 000 x *g* for 10 minutes and supernatant transferred to a clean microfuge tube. After quantification by BCA assay, proteins were denatured by heating at 95°C for 10 minutes in Laemmli sample buffer, separated on 4-12% Bis-Tris gels (Invitrogen) and transferred onto nitrocellulose membranes using the iBlot system (Invitrogen). Blots were blocked with tris-buffered saline containing 0.1% Tween-20 (TBST; Sigma) and 5% skimmed milk powder (Sigma) for 1 hour at room temperature. Blots were incubated with primary antibodies (Table 2.3) in either TBST containing 5% BSA or TBST containing 5% skimmed milk powder at 4°C overnight. After 3 washing steps with TBST, blots were incubated with species-appropriate HRP-conjugated secondary antibodies (Cell Signaling) for 1 hour at room temperature. After 3 washing steps with TBST, blots were developed using Luminata Crescendo HRP substrate (Merck Millipore) and imaged using an ImageQuant LAS 4000 system (GE Healthcare). For re-probing, blots were washed once with TBS and incubated with Restore PLUS western blot stripping buffer (Thermo Fisher) for 15 minutes at room temperature.

For experiments involving subcellular fractionation, fractions were isolated using a subcellular protein fractionation kit (Thermo Fisher) according to manufacturer's instructions. Resulting lysates were BCA assayed to normalise protein concentration and blotted as described above.

For co-immunoprecipitation (IP) experiments, cells were grown in two T75 flasks per condition, feeder cells were removed and epithelial cells were serum starved overnight. Cells were treated with either a vehicle control or 10 ng/ml recombinant human hepatocyte growth factor (HGF) for 30 minutes before lysis in Pierce IP Lysis Buffer (Thermo Fisher). Protein concentration was normalised to 2 mg/IP in 500 µl volume and lysates were incubated with 20 µl primary antibody overnight at 4°C on a rotating wheel. The next day, Dynabeads (Protein A; Thermo Fisher) were used to isolate antibody and bound protein from the lysates according to manufacturer's instructions. After washing, beads were resuspended in 20 µl Laemmli sample buffer and heated to 95°C for 10 minutes. Beads were removed by centrifugation and samples run on 4-12% Bis-Tris gels (Invitrogen). Transfer and western blotting was performed as described above.

Antibody	Species	Isotype	Supplier	Product Code	Dilution Factor
Y397 FAK	Rabbit	IgG	Cell Signaling	8556	1/1000
Y576/Y577 FAK	Rabbit	IgG	Cell Signaling	3281	1/1000
Y925 FAK	Rabbit	IgG	Cell Signaling	3284	1/1000
Total FAK	Rabbit	IgG	Cell Signaling	13009	1/1000
Y307 GAB1	Rabbit	IgG	Cell Signaling	3234	1/1000
Y1003 MET	Rabbit	IgG	Cell Signaling	3135	1/1000
Y1234/Y1235 MET	Rabbit	IgG	Cell Signaling	3077	1/1000
Y1349 MET	Rabbit	IgG	Cell Signaling	3133	1/1000
Total MET	Rabbit	IgG	Cell Signaling	8198	1/1000 WB 1/50 IP
Y452 GAB2	Rabbit	IgG	Cell Signaling	3881	1/1000
Total GAB2	Rabbit	IgG	Cell Signaling	3239	1/1000
Y641 STAT6	Rabbit	IgG	Cell Signaling	9361	1/1000
Total STAT6	Rabbit	IgG	Cell Signaling	9362	1/1000
MEK1/2	Rabbit	IgG	Cell Signaling	8727	1/1000
Histone H3	Rabbit	IgG	Cell Signaling	4499	1/1000
α-tubulin	Rabbit	IgG	Cell Signaling	9099	1/1000

Table 2.3: Antibodies used for western blot and co-immunoprecipitation experiments.

2.11 Quantitative real-time polymerase chain reaction (qPCR)

Total RNA was isolated from cultured human epithelial cells using a SV RNA Isolation Kit (Promega). Co-cultures containing 3T3-J2 fibroblasts were differentially trypsinised to remove feeder cells before RNA isolation. Taqman pre-designed, inventoried probes and 2x PCR Master Mix (Applied Biosciences) were used (Table 2.4). Quantitative PCR was performed under standard conditions using an Eppendorf Real-Time PCR machine in technical triplicates. Relative RNA quantitation was achieved based on deltaCT calculations and all samples were compared using β2-microglobulin (β2M) as a control.

Gene	Product Code
β2M	Hs00187842_m1
β2M	Mm00437762_m1
NGFR	Hs00609977_m1
ITGA6	Hs01041011_m1
TROP2	Hs01922976_s1
IL-8	Hs00174103_m1
GM-CSF	Hs00929873_m1
HGF	Mm01135184_m1

Table 2.4: Product codes for Taqman qPCR probes

2.12 ELISAs

2.12.1 HGF

Secretion of HGF by 3T3-J2 cells following mitotic inactivation was assessed using a mouse HGF DuoSet ELISA kit (R&D Systems; DY2207) performed according to manufacturer's instructions. 3T3-J2 medium consisting of DMEM (Gibco; 41966) supplemented with 100 U/ml penicillin, 100 µg/ml streptomycin (Gibco; 15070) and 9% bovine serum (Gibco; 26170) was changed immediately following 2 hours of inactivation with 0.4 µg/ml mitomycin C

(Sigma; M4287) and medium was collected for analysis and refreshed after 24 hours, 48 hours and 72 hours.

2.12.2 GM-CSF and IL-8

Secretion of granulocyte/macrophage colony-stimulating factor (GM-CSF) and interleukin-8 (IL-8) by human airway epithelial cells following stimulation with HGF was assessed using a human GM-CSF DuoSet ELISA kit (R&D Systems; DY215) and a human CXCL8/IL-8 DuoSet ELISA kit (R&D Systems; DY008) performed according to manufacturer's instructions.

Primary human airway epithelial cells were cultured in 3T3+Y in T25 flasks until they reached 80% confluence. Feeder cells were removed by differential trypsinisation and cells were serum starved in 2 ml DMEM/F12 overnight. The following day, cells were stimulated with 2 ml DMEM/F12 containing 10 ng/ml HGF, 10ng/ml HGF and 250 nM PF-0421903, or a vehicle control containing the appropriate amount of 0.1% BSA and DMSO. Media was collected for analysis after 24 hours.

2.13 Luciferase reporter assays

2.13.1 STAT6 consensus sequence reporter assay

A431 cells were plated in 96-well plates at a density of 20,000 cells per well. After two days, cells were transfected with signal transducer and activator of transcription 6 (STAT6) luciferase reporter (p4xSTAT6-Luc2P was a gift from Axel Nohturfft; Addgene plasmid #35554) and renilla luciferase control (pGL4.74 [hRluc/TK]; Promega) plasmids using jetPEI

according to manufacturer's instructions. 0.25 µg DNA was added to each well (0.225 µg STAT6 reporter and 0.025 µg renilla luciferase control). After 24 hours, cells were washed once with PBS and serum starved in serum-free DMEM overnight. The following day, cells were stimulated with vehicle control, human recombinant IL-13 or human recombinant HGF, as described in figure legends. To quantify luciferase activity, a dual luciferase reporter kit (Promega) was used according to manufacturer's instructions. Assay reagents were injected and bioluminescence was recorded using a TROPIX TR717 microplate luminometer (2 second delay, 10 second recording time).

2.13.2 IL-8 promoter reporter assay

IL-8 promoter luciferase plasmids were a kind gift from Dr. Joel Raingeaud (Inserm, France) and Dr. Marie Annick Buendia (Inserm, France) and have been previously described [249, 250]. A restriction digest was performed to verify the identity of the plasmids. 20 µl reactions containing 2 µl NEBuffer 3.1 (New England Biolabs), 1 µg DNA, 1 µl NotI restriction enzyme (New England Biolabs) and 1 µl XhoI restriction enzyme (New England Biolabs) were incubated at 37°C for 1 hour. 50 ng DNA in DNA loading dye (Thermo Fisher) was loaded onto 1% agarose gel containing gel red (Cambridge Bioscience) and visualised using an ImageQuant LAS 4000 system (GE Healthcare). Luciferase reporter experiments were performed as described for STAT6 reporter assays above.

3 . Characterisation and isolation of human airway basal cells

3.1 Background

In human airways, basal epithelial cells are considered a stem/progenitor cell population: cytokeratin 5 (CK5)+ basal cells are proliferative in culture and able to reconstitute pseudostratified epithelial layers containing both mucosecretory and ciliated cells *in vitro* [117] and in an *in vivo* xenograft [118]. Furthermore, mathematical modelling suggests that basal cells are equipotent progenitor cells in homeostatic human airways [105]. As such, *ex vivo* expansion of the airway stem/progenitor cell population is desirable in order to develop model systems that allow investigation of their functions in normal homeostasis and repair following airway damage, to investigate their potential in cell therapies and tissue-engineered airway transplantation and to study their role in human respiratory disease. Indeed, basal cells are increasingly recognised as key contributors to disease independently of their role as precursor cells for differentiated cell types. For example, the recent discovery of basal cell-specific responses to damage suggests that these cells can orchestrate lung innate immunity [18, 19].

While large tissue samples from either lobectomy procedures or cadaveric donor lungs deemed unsuitable for transplantation are occasionally available to our laboratory, we have regular access to human airway mucosal samples from bronchoscopy procedures [46]. The small bronchoscopic biopsies are also the laboratory's preferred route of cell acquisition because personalised medicine approaches and airway tissue engineering will require cell derivation from living patients. Previous airway basal cell culture strategies have largely focused on the larger tissue samples available from lobectomy or cadaveric sources [222, 223] but successful culture of airway epithelial cells from biopsy samples has also been demonstrated [82, 219-221].

An important end point of experiments involving the derivation of cultured human basal cells is that they retain as far as possible their resemblance to native basal cells. A key criterion in this regard is their retention of multipotent airway differentiation capacity; that is, the ability to form a pseudostratified epithelium containing airway mucosecretory cells, which produce the mucus lining of the airways, and multiciliated cells, which produce motile force to move mucus and inhaled pathogens and particulate matter trapped within it, out of the lungs. To gain a better understanding of the human airways, I characterised the cell types present in the airways and the markers that these cells express. In addition, I sought to optimise a method to isolate human airway epithelial cells from small endobronchial biopsy samples and to characterise the cells that grow in terms of phenotype and number. To ensure that isolated cells retain their differentiation potential, I also developed methods to induce epithelial cell differentiation *in vitro*.

3.2 Aims

- To develop immunofluorescence methods to characterise the cell types present in the human airways.
- To optimise a method to isolate and expand human basal cells from living patients.
- To develop cell culture methods to assess the differentiation of expanded human airway basal cells.

3.3 Results

Characterisation of human airway cell types

Sections of human trachea from surgical resections were fixed in 4% paraformaldehyde, embedded in paraffin and sectioned. Following antigen retrieval, sections were first stained with antibodies against proteins expected to be found in all epithelial cells (pan-cytokeratin (panCK) and E-cadherin; Figure 3.1) as well as those expected to be found in endothelial (CD31; Figure 3.1) and haematopoietic cells (CD45; Figure 3.1). As expected, panCK+ E-cadherin+ epithelial cells were found above the basement membrane at the luminal surface, while CD31 and CD45 expression was largely restricted to the tissue stroma.

To distinguish subpopulations of epithelial cells present within the human airway epithelium, antibodies against proteins expected to be expressed in unique populations of cells were optimised. CK5 is a basal epithelial cell marker [15] and was only seen among epithelial cells in close proximity to the basement membrane (Figure 3.2). On the other hand, luminal, differentiated epithelial cells but not basal stem/progenitor cells express CK8 (Figure 3.2), as has previously been described [251]. Mucosecretory epithelial cells were visualised using antibodies against mucin 5AC (MUC5AC; Figure 3.2). Club cell secretory protein (CCSP), a protein that is abundant in the club cells of murine airways [252], was rarely seen in the human surface epithelium but could occasionally be detected in the submucosal glands (Figure 3.2). Ciliated epithelial cells were visualised using the transcription factor forkhead box protein J1 (FOXJ1) [253] and acetylated α-tubulin (ACT) [214], a microtubule protein found in cilia themselves (Figure 3.2). As expected, the

differentiated luminal fraction of the epithelial layer comprises a mixture of mucosecretory and ciliated cells.

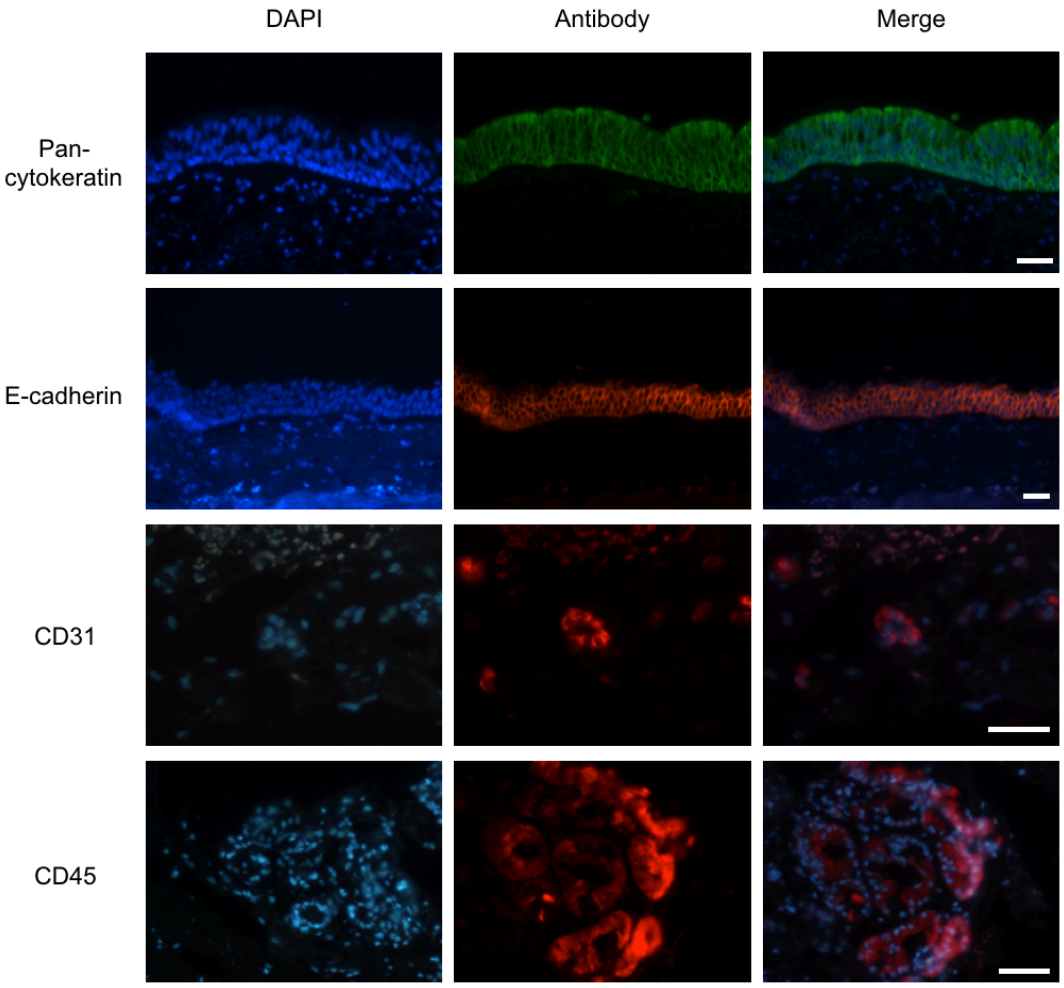

Figure 3.1: Characterisation of the cell types present in human airway epithelium. Paraformaldehyde-fixed human donor trachea stained using immunofluorescence demonstrated the presence of cytokeratin, a family of intermediate filament proteins characteristic of epithelial tissues. These cells also express E-Cadherin, a calcium-dependent adhesion protein and member of the cadherin superfamily that is important in cell-cell adhesion in epithelia. Below the epithelial basement membrane that separates the epithelial cells from the airway stroma, CD31-expressing endothelial cells and CD45-expressing cells are present, here in glandular structures. DAPI (blue) was used as a counterstain. Scale bars = 50 µm.

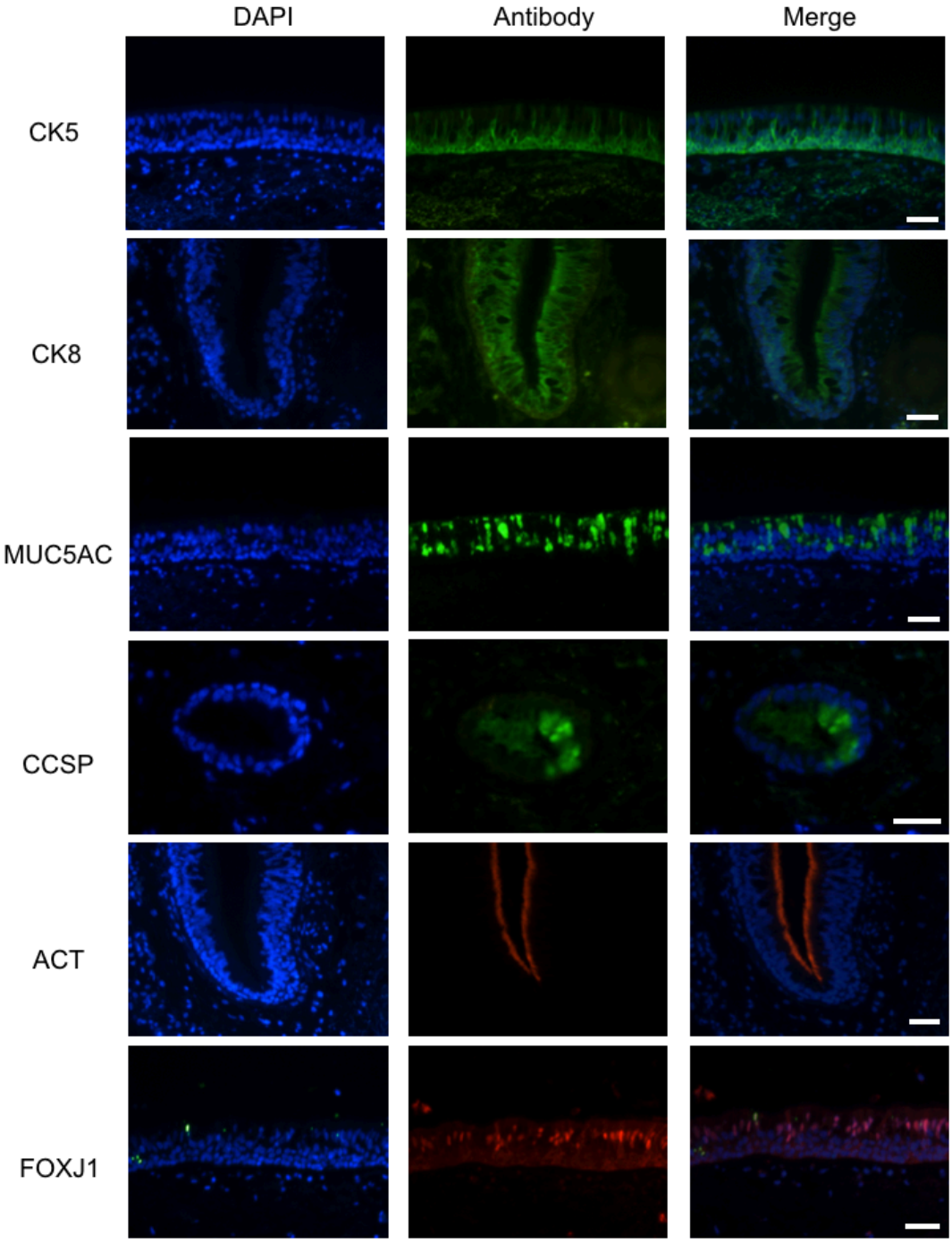

Figure 3.2: Characterisation of the main epithelial cell types within the human airway epithelium.
Paraformaldehyde-fixed human donor trachea stained using immunofluorescence demonstrated the presence of cytokeratin 5, a characteristic marker of undifferentiated basal epithelial cells in a number of epithelial tissues, including the airway. Cytokeratin 8 is also expressed in the airway epithelium but in non-basal, or luminal cells; these cells are considered the differentiated airway epithelial cell types and contain both ciliated and mucosecretory cells. Club cell secretory protein (CCSP) is expressed abundantly in murine airways in club cells but in the human trachea its expression was restricted to submucosal glands. Mucin 5AC (MUC5AC) positive cells are seen within the luminal population and is a marker of mucosecretory cells. Acetylated α-tubulin (ACT) is expressed in cilia, the microtubule-based projections that define ciliated cells. FOXJ1 is a transcription factor that regulates the multiciliated cell lineage and as such is also uniquely expressed in ciliated cells.

In human airways, basal cells are abundant stem cells during homeostasis and contribute to repair following injury [105, 254]. Given the focus on *in vitro* characterisation and expansion of human airway basal cells, expression *in situ* of proteins associated with basal cells was assessed. CK14 was expressed in a subset of human airway basal cells, as it is in murine airways [255], possibly reflecting a distinct progenitor cell phenotype or role in regeneration for these cells [256]. Expression of the transcription factor p63 is also uniquely found in airway basal cells [257] (Figure 3.3). Finally, the restriction of proliferation to the basal epithelial cell compartment *in vivo* was confirmed by Ki67 staining [258] (Figure 3.3).

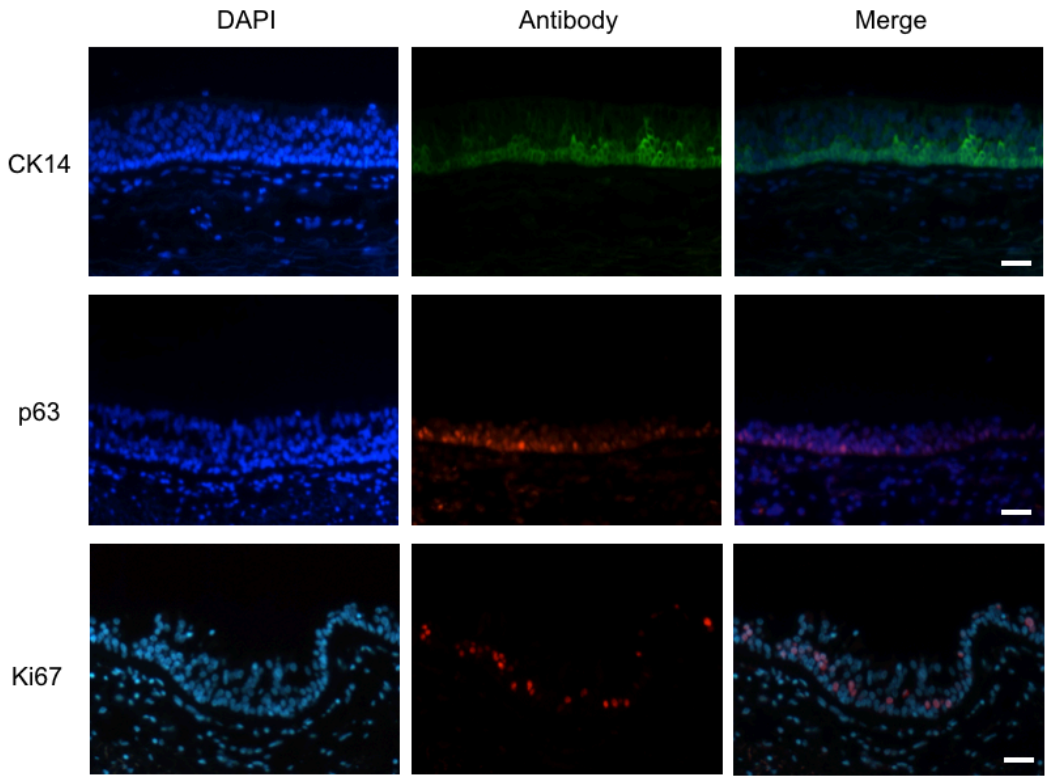

Figure 3.3: Further characterisation of protein expression in human airway basal cells. Paraformaldehyde-fixed human donor trachea stained using immunofluorescence demonstrated the presence of cytokeratin 14 in a subset of basal cells. CK14 expression has been associated with regeneration and repair of the tracheal epithelium in mice. P63 is a transcription factor expressed uniquely in human airway basal cells. Proliferation of a subset of basal cells *in vivo* was demonstrated by the presence of Ki67 protein, which is cell cycle regulated and only expressed during interphase. DAPI (blue) was used as a counterstain. Scale bars = 50 μm.

Isolation of human airway basal cells

Having examined the human airway epithelium *in situ*, I sought to isolate airway basal cells and expand them *in vitro* so that more detailed characterisation and functional studies could be performed. Protocols established in the laboratory were used to isolate epithelial cells from cadaveric airway samples (Figure 3.4A). Briefly, the trachea and bronchi were cut into small pieces and digested overnight in 0.15% pronase at 4°C. The resulting suspension was then vigorously agitated and plated. As expected, epithelial cells that proliferated in cell culture (Figure 3.4B) were universally cytokeratin 5- and cytokeratin 14-positive (Figure 3.4C), indicating their probable basal cell origin. After one passage to expand cells, cells were cryopreserved in liquid nitrogen to form a bank of cells suitable for use in future experiments.

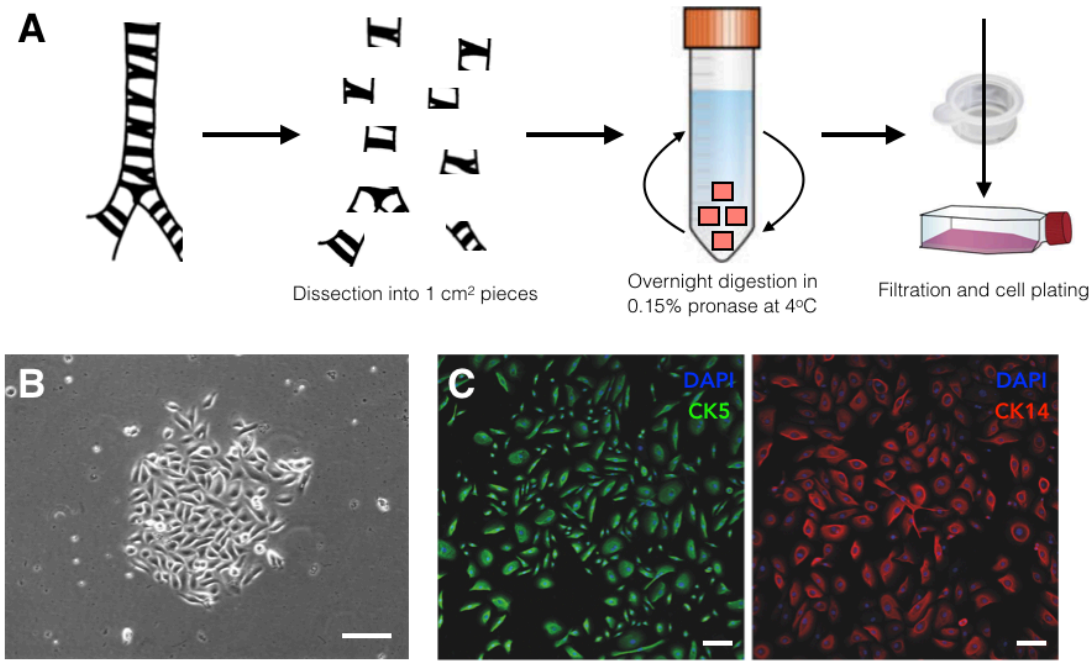

Figure 3.4: Pronase digestion of cadaveric human tracheae to initiate basal cell culture. A) Enzymatic digestion using pronase creates a cell suspension that can be plated in tissue culture plastic in bronchial epithelial growth medium (BEGM) to initiate basal cell cultures. Adapted from methods described by Fulcher and Randell [217]. B) Brightfield microscopy demonstrates the outgrowth of epithelial cells in these conditions. Scale bar = 50 µm. C) Immunofluorescence staining shows epithelial cells are cytokeratin 5 (CK5)+ (green) and CK14+ (red) basal cells. Scale bars = 20 µm.

Access to cadaveric airway tissue is infrequent so alternative methods to derive airway basal cells for *in vitro* characterisation were investigated. More regular access to endobronchial biopsy samples (Figure 3.5A) is available and these have previously been used to expand cells in culture for in vitro characterisation [219-221] and for use in airway tissue engineering [70]. Epithelial cells were isolated from endobronchial biopsy samples by plating them as explants in bronchial epithelial growth medium (BEGM). Over the course of two weeks in culture, epithelial cell expansion was apparent, with cells visibly growing out of the biopsy (Figure 3.5B). The basal cell status of these cells was confirmed by immunofluorescence staining for CK5, CK14 and p63 (Figure 3.5C). Rare p63-negative cells were also observed in explant cultures (although not in subsequent cultures), suggesting that migration as well as proliferation might contribute to the outgrowth of epithelial cells as has previously been described in explant epidermal keratinocyte cultures [259] (Figure 3.5C). The explant cells also express CK5, integrin α6, TROP2 and nerve growth factor receptor (NGFR) when analysed by flow cytometry, confirming that they are basal cells (Figure 3.5D).

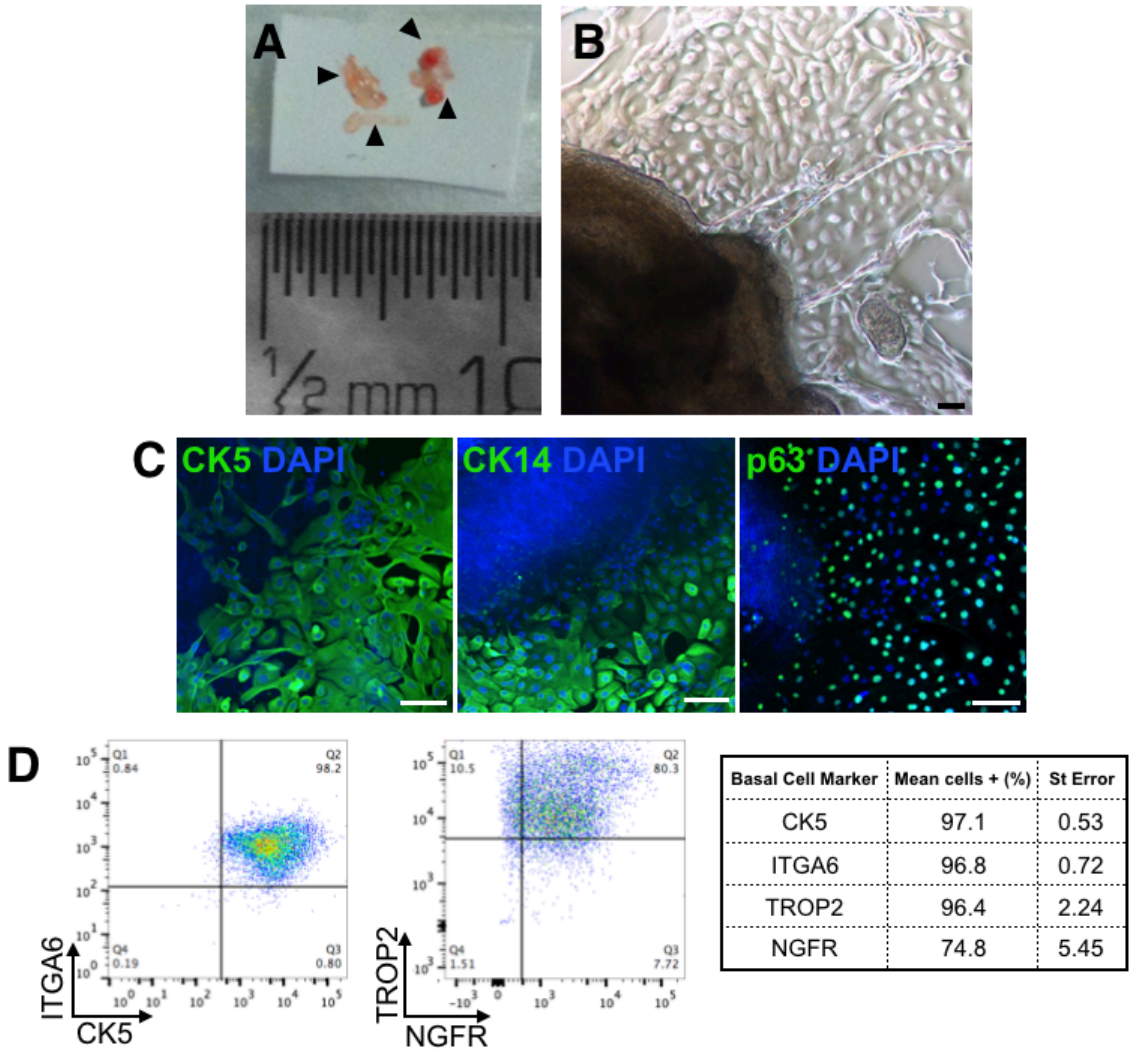

Basal Cell Marker	Mean cells + (%)	St Error
CK5	97.1	0.53
ITGA6	96.8	0.72
TROP2	96.4	2.24
NGFR	74.8	5.45

Figure 3.5: Isolation of airway epithelial cells from small endobronchial biopsy samples. A) Endobronchial biopsy samples are approximately 1 mm^3. Ruler shown for scale. B) Epithelial cell outgrowths were evident 3-5 days after plating as explants in bronchial epithelial growth medium (BEGM). Scale bar = 20 µm. C) Epithelial cells are cytokeratin 5 (CK5)+ (left) and CK14+ (centre), suggesting they are basal epithelial cells. The majority of cells are p63+ (right) but some p63- cells are seen, suggesting that some non-basal epithelial cells might also migrate from biopsy samples. Cells were counterstained with DAPI (blue). Scale bars = 100 µm. D) Flow cytometry confirms that outgrowths consist of CK5+, integrin α6+, TROP2+ basal cells. The majority of cells also express NGFR.

Approximately 1.5 x 10^5 of cells were obtained following two weeks of explant growth from biopsies so we passaged these cells to investigate whether larger numbers of cells could be obtained for downstream experiments (Figure 3.6A). Cells continued to proliferate after passage and around 2 x 10^6 cells could be obtained from a single biopsy by passage two (Figure 3.6B). However, the proliferation of basal cells grown in this way declined over passage when analysed by incorporation of EdU (Figure 3.6C).

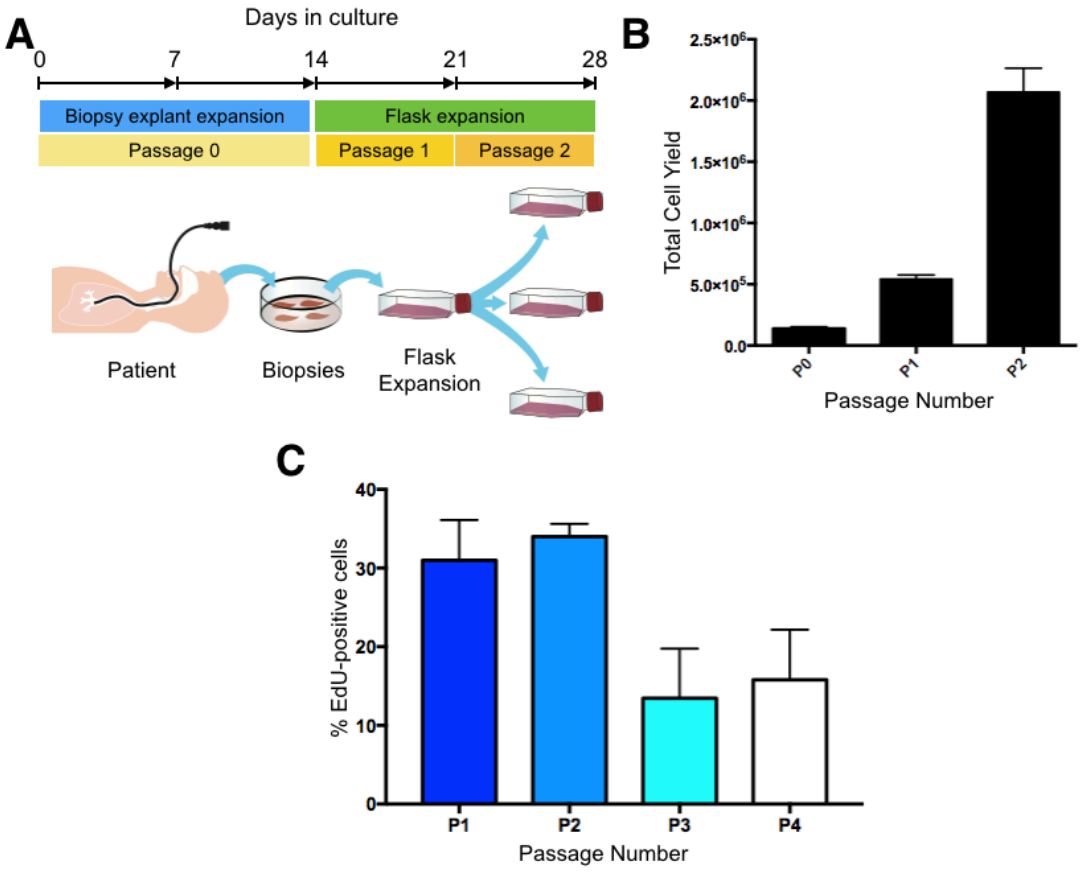

Figure 3.6: Expansion of human epithelial cells from endobronchial biopsy samples in BEGM. A) Schematic representation of isolation and expansion timeline for epithelial cells from endobronchial biopsies. B) Quantification of total epithelial cell number following one passage (14 days) of explant culture in bronchial epithelial growth medium (BEGM; n = 19 donors; mean +/- SEM). This experiment was performed by Dr. Colin Butler. C) Quantification of basal cell proliferation in cells grown in BEGM (n = 3 donors; mean +/- SEM).

Differentiation of cultured human airway basal cells

Next, methods to differentiate human airway basal cells were established. In the literature, this generally relies upon differentiation at air-liquid interface using a transwell membrane [222]. Basal cells are seeded at high density in transwell membranes and cultured in submerged conditions until confluency is achieved. After this, cells are fed basally through the transwell and apical medium is removed, exposing cells to air (Figure 3.7A). Over the course of several weeks of culture, basal cells differentiate to form a mucosecretory, ciliated epithelium [260, 261]. In these conditions we found that early passage basal cells (that is, P0 and P1 cells) differentiate to form both mucosecretory and ciliated cells (Figure 3.7B). However, beyond this passage we found that cultured basal cells declined in their capacity to form differentiated epithelium, with very few ciliated cells visible in P4-derived air-liquid interface cultures. Furthermore, by passage 4, cultured basal cells were unable to maintain confluency for the full length of culture (Figure 3.7C).

In addition to air-liquid interface cultures, there is also evidence that human airway basal cells are capable of differentiating in submerged culture conditions [238-241]. Air-liquid interface models are labour intensive and poorly suited to high-throughput applications so a three-dimensional (3D) tracheosphere model was developed (Figure 3.8). Here, cells are cultured in the basement membrane extract Matrigel in submerged culture. A suspension of single basal cells is seeded and over the course of 2-3 weeks of culture 3D spheroid structures form with a hollow lumen (Figure 3.8).

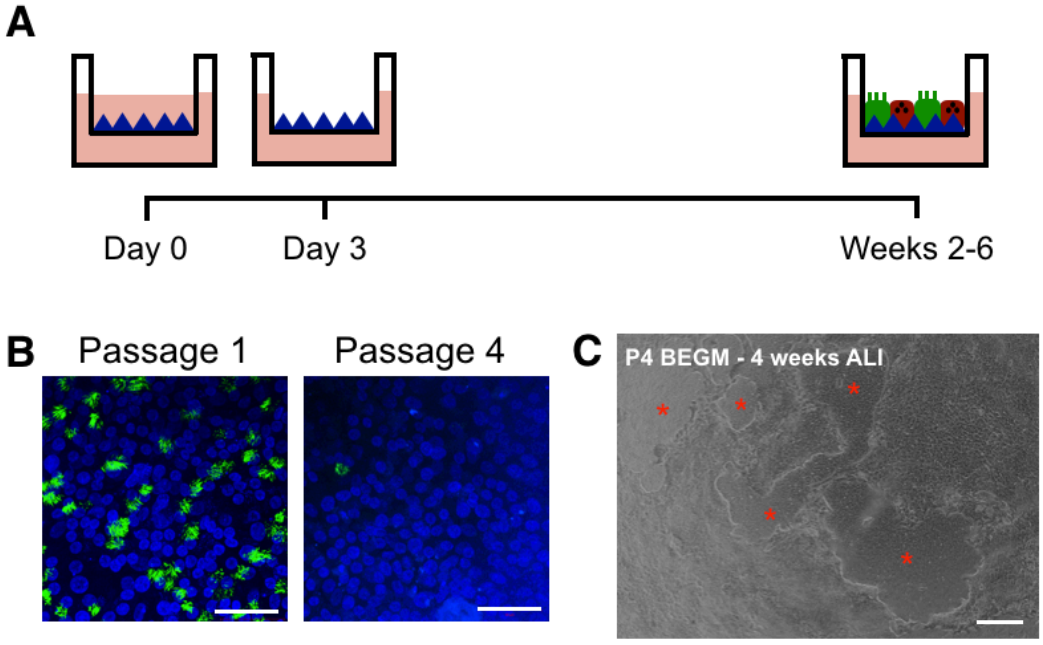

Figure 3.7: Establishment of an air-liquid interface differentiation protocol for human airway basal cells. A) In air-liquid interface cultures a high density of human basal cells are seeded in submerged culture until confluency is reached (2-3 days). At this stage, medium is removed from the apical surface and cells are fed only through the basal transwell membrane, exposing cells to air. Over the course of 2-3 weeks, a multiciliated, mucosecretory epithelium emerges. B) Immunofluorescence staining shows ciliated cells (acetylated α-tubulin (ACT)-positive; green) derived from early (passage 1) and late (passage 4) passage basal cells after culture at air-liquid interface. DAPI (blue) is used as a counterstain. Scale bars = 50 µm. C) Late passage basal cells did not form successful air-liquid interface cultures. Holes appeared in the epithelium and air-liquid interface was not maintained. Scale bar = 200 µm.

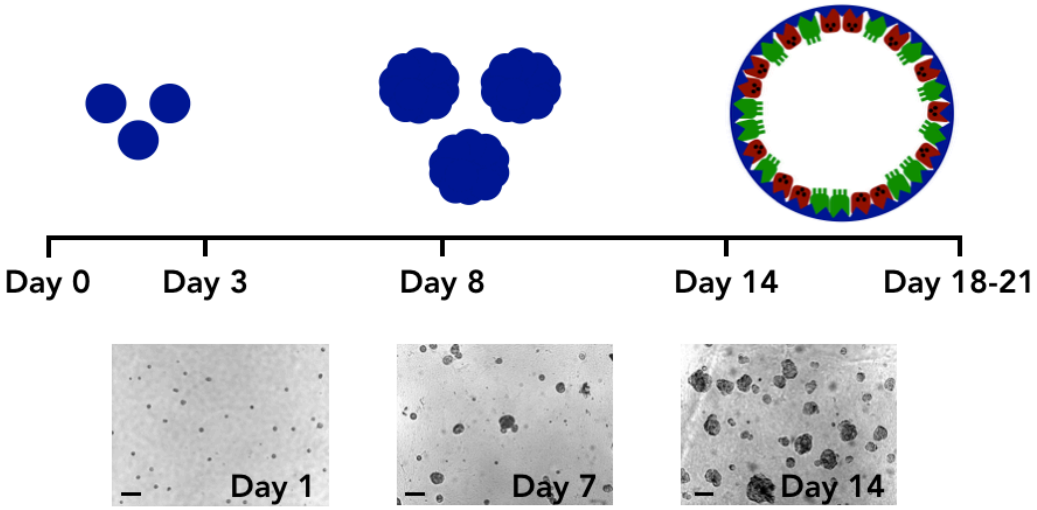

Figure 3.8: Three-dimensional (3D) tracheosphere differentiation of human airway basal cells. 3D culture of human basal cells was performed to generate tracheospheres, which may also be referred to as spheroids or organoids. A suspension of single basal epithelial cells are seeded in 5% Matrigel and proliferate to form spheroids. Over 2-3 weeks in culture these spheroids develop a central lumen and basal cells differentiate to form an epithelium containing both mucosecretory and ciliated epithelial cells. Scale bars = 100 µm.

Basal cells seeded in Matrigel proliferate to form spheroids; after 7 days, tracheospheres showed abundant BrdU uptake but the number of BrdU-positive cells decreased by day 14 of culture (Figure 3.9A). Separately, time-lapse microscopy data from our laboratory had indicated that at the seeding density used here (2,500 basal cell per well of a 96-well plate), tracheospheres were not clonal (that is, they were not derived from a single cell) but in fact basal cells were motile and able to form aggregates. This finding was also subsequently published by other another group [49]. Tracheosphere formation varied depending on the passage of basal cells seeded, with cells at early passage giving rise to larger spheroids than matched donor cells at late passage (Figure 3.9B). Consistent with a decrease in tracheosphere quality over basal cell culture time, differentiation was also affected by basal cell passage number. At very early passages, basal cells formed tracheospheres that contained a pseudostratified, differentiated epithelium (Figure 3.9C) containing both mucosecretory and ciliated cells oriented towards the sphere lumen (Figure 3.9D). At later passages, larger tracheospheres frequently contained few ciliated cells (Figure 3.9E) and more often did not undergo lumen formation at all (Figure 3.9F).

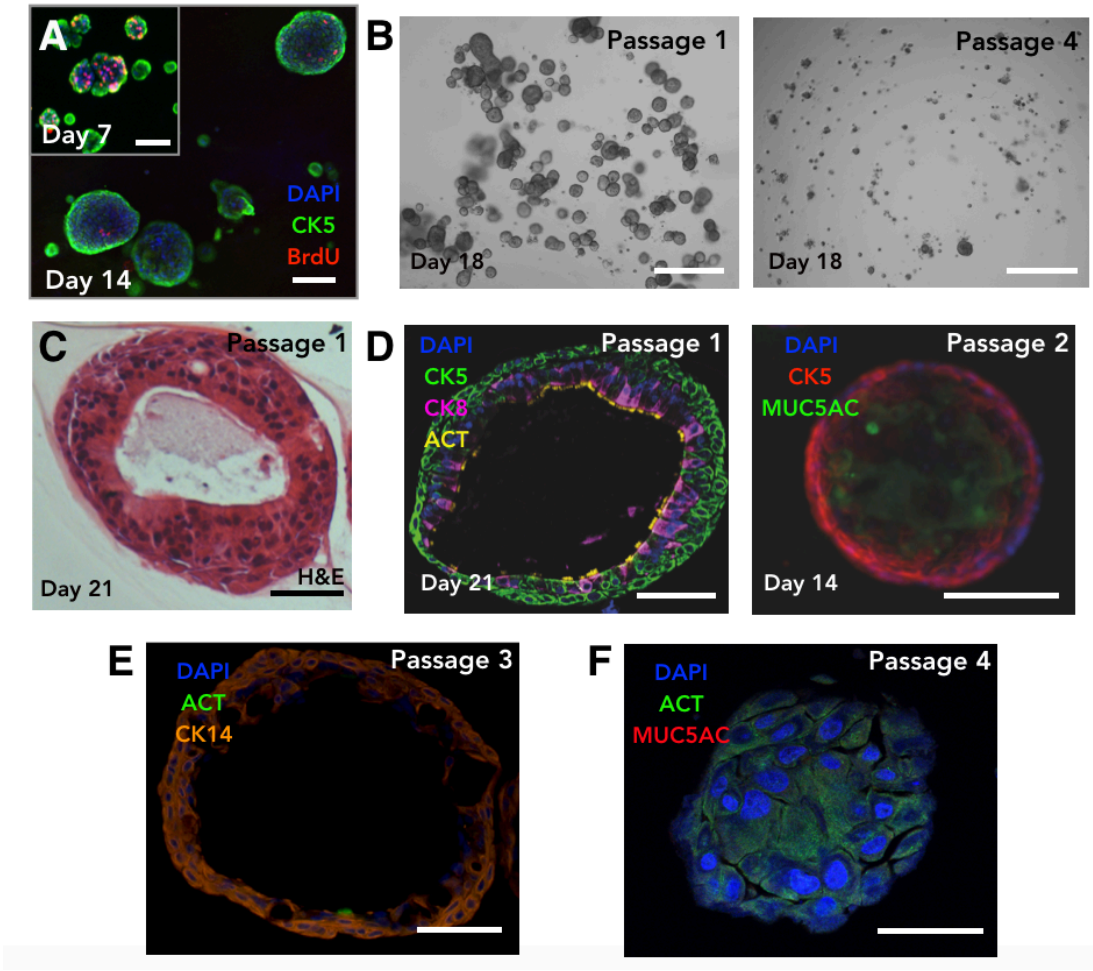

Figure 3.9: Establishment of a three-dimensional (3D) tracheosphere differentiation protocol for expanded human airway basal cells. A) Proliferation of tracheospheres was assessed by BrdU labelling and antibody staining (red). Tracheospheres contained more proliferating cells at day 7 than at day 14. Scale bar = 100 µm. B) Brightfield images of tracheosphere morphology after 18 days of culture. Tracheospheres were generated from donor matched passage 1 (left) or passage 4 (right) airway basal cells. Scale bar = 500 µm. C) Haemotoxylin and eosin staining reveal a pseudostratified epithelium in tracheospheres derived from passage 1 airway basal cells. Scale bar = 50 µm. D) Passage 1 basal cell-derived tracheospheres show distinct cytokeratin 5 (CK5)+ (green) basal cell and CK8+ (magenta) luminal cell populations as well as ciliated cells (acetylated α-tubulin (ACT; yellow; left)). Tracheospheres secreted the mucin 5AC (MUC5AC; red) into the lumen (right). Scale bars = 50 µm. E) Passage 3 basal cell-derived tracheospheres contained few ciliated cells (ACT; green) but were positive for CK14 (orange). Scale bar = 50 µm. F) Passage 4 basal cell-derived tracheospheres often did not undergo lumen formation and were often not positive for MUC5AC. Scale bars = 50 µm. DAPI (blue) was used as a counterstain for immunofluorescence staining. These experiments were performed with Dr. Colin Butler.

As such, the methods developed here allowed us to expand our pool of cryopreserved basal cells to include those from living donors by using cells derived from endobronchial biopsies. However, we found that basal cells cultured in BEGM lost both their proliferative potential and their capacity to differentiate over time in culture, suggesting that this culture method is suboptimal and fails to maintain the characteristics of airway basal stem cells. Early passage basal cells performed well in airway differentiation assays but the scarcity of cadaveric tissue and the small number of cells that can be obtained from endobronchial biopsies limits their utility in biological or pre-clinical tissue-engineering studies. Overall, these results suggest a need to improve the basal cell culture protocol to better maintain the potential of these cells.

3.4 Summary

- The cell types of the human airways were characterised *in situ* using an optimised immunofluorescence protocol.
- Protocols were optimised to isolate and expand human airway epithelial cells from cadaveric samples and endobronchial biopsies.
- Human airway epithelial cells expanded in BEGM from cadaveric samples and endobronchial biopsies express basal stem cell markers.
- Cultured basal cells at early passages differentiate to form pseudostratified epithelia containing both ciliated cells and mucosecretory cells.
- After passage 2, the differentiation capacity of cultured basal cells declines and fewer ciliated cells are seen in both air-liquid interface and tracheosphere cultures, limiting the utility of this expansion protocol.

4 . Rapid and sustained expansion of human airway basal cells using 3T3-J2 co-culture and ROCK inhibition

4.1 Background

Previously, primary human airway epithelial cells were obtained from either endobronchial biopsies, lobectomy tissue or from cadaveric tissue and cultured in serum-free bronchial epithelial growth medium (BEGM) for multiple passages. While this has historically been a useful tool to generate basal cells for *in vitro* investigations [222], it is likely to be inefficient for applications that require large numbers of cells such as airway bioengineering or high-throughput epithelial cell assays, particularly when the amount of starting tissue is limited. Indeed, as I have shown in Chapter 3, many cultures fail and those that grow are often unable to produce enough cells with complete differentiation capacity for downstream assays.

Consequently, alternative means to expand primary human airway epithelial cells were investigated. We sought to establish a method that would generate greater numbers of epithelial cells than is possible using BEGM and, importantly, that would maintain the differentiation capacity and normal karyotype of the isolated cells. Avoidance of senescence in cultured basal cells, which we hypothesised occurs during culture in BEGM, is important as these cells do not maintain their *in vivo* characteristics, particularly in terms of differentiation potential. Indeed, assays using cells in which their *in vivo* characteristics are not maintained are likely to be confounded by the effects of senescence and cell stress. To enable me to study cell behaviour and potential, it was important to overcome these cell culture obstacles. In addition, a main focus of the laboratory is to generate epithelial cell cultures that have the potential to be used in the future in human tracheal transplantation procedures: for this application, it is crucial that expanded epithelial cells maintain their differentiation potential to generate a functional epithelial barrier and are safe for transplantation [77].

Successful *ex vivo* long-term expansion of human epidermal stem cells is achieved by co-culture with mitotically inactive mouse embryonic fibroblast feeder cells [189]. Inhibition of Rho-associated protein kinases (ROCK) in these cultures increases proliferation and 'conditionally immortalises' cells, allowing indefinite propagation of stem cells with tissue-appropriate differentiation capacity [262, 263]. Airway epithelial cells grown in these conditions have been shown to maintain their differentiation potential at late passages but have not been characterised in detail [264]. Therefore, I investigated the growth of endobronchial biopsy-derived primary human airway epithelial cells on 3T3-J2 feeder cells in the presence of the ROCK inhibitor Y-27632 (3T3+Y) and their potential utility in differentiated airway epithelial cell models.

4.2 Aims

- To investigate an alternative epithelial cell culture protocol using 3T3-J2 fibroblast co-culture and ROCK inhibition (3T3+Y).
- To compare epithelial cells expanded in 3T3+Y and BEGM in terms of their expression of basal stem cells markers.
- To compare epithelial cells expanded in 3T3+Y and BEGM in terms of their differentiation potential.

4.3 Results

Expansion of airway epithelial cells in 3T3+Y

Following initial cell outgrowth in BEGM, the growth of matched donor epithelial cells was compared in BEGM and 3T3+Y, where a mitotically inactivated feeder layer of 3T3-J2 mouse embryonic fibroblasts was combined with growth medium containing 5 μM Y-27632, which is a small molecule inhibitor of the ROCK pathway. When cells were passaged sequentially in BEGM they displayed a cuboidal morphology with little cell-cell contact at early passages (Figure 4.1A). Over time, cells became larger and flatter, consistent with senescence-associated changes reported in the literature [49, 117, 265-267]. By contrast, serum-containing epithelial growth medium in combination with 3T3-J2 feeder cells and Y-27632 led to the formation of colonies of smaller epithelial cells that retained cell-cell contact, the morphology of which did not change with passage (Figure 4.1A). Consistent with studies in other epithelia [262, 264], we saw that a greater number of cells were stained by antibodies against the proliferation marker Ki67 after 4 days of culture in 3T3+Y than in BEGM (Figure 4.1B), suggesting that there was greater epithelial cell proliferation in 3T3+Y than in BEGM. This apparent growth advantage was sustained over passage (Figure 4.1C), whereas cells cultured in BEGM underwent a well-characterised deterioration in proliferation rate over time [49, 117, 265, 267]. Flow cytometric analysis of EdU uptake and DNA content using DAPI showed that 3T3+Y increased the number of cells in S-phase compared with BEGM, validating the increased proliferation rate seen by Ki67 staining (Figure 4.1D). Taken together, these results show that 3T3+Y conditions induce greater epithelial cell proliferation than BEGM and that this is maintained over passage.

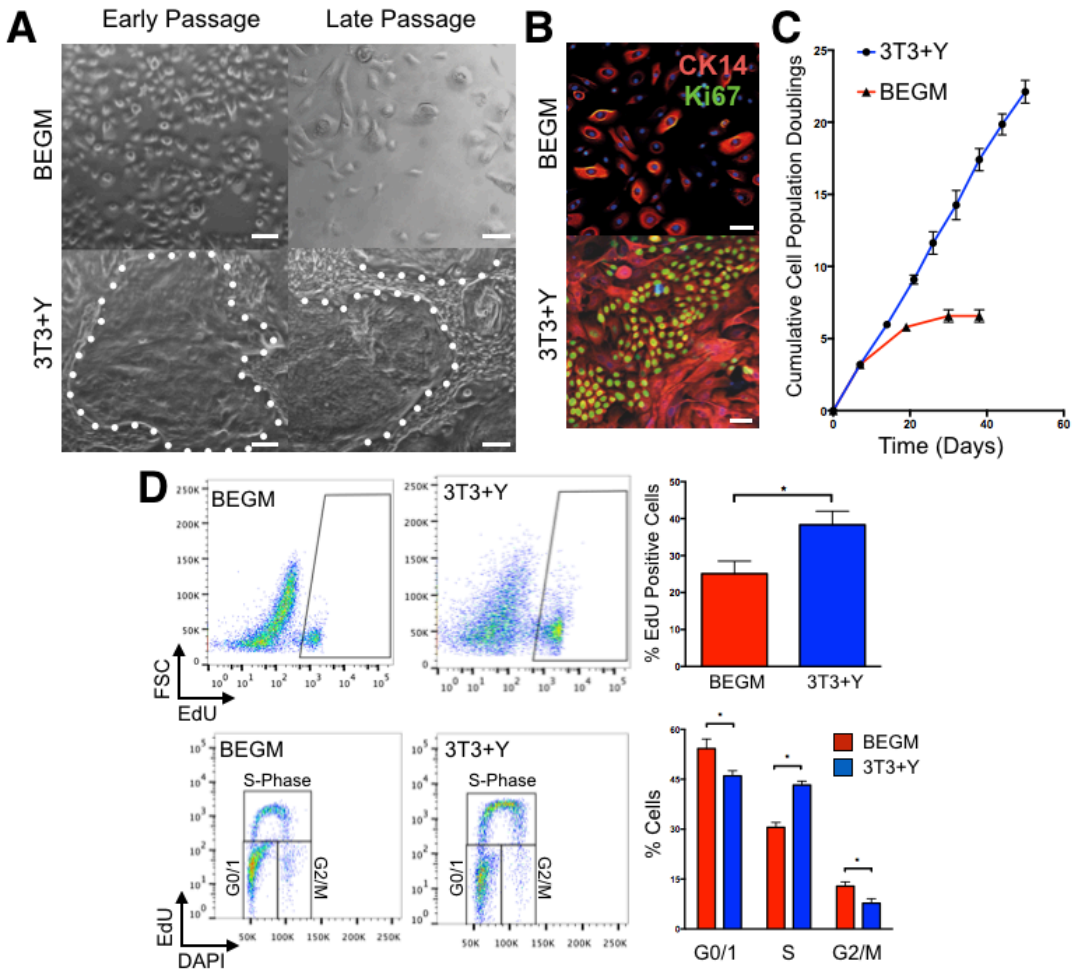

Figure 4.1: Expansion and increased proliferation of human airway basal cells with 3T3-J2 co-culture and ROCK inhibition. A) Brightfield images show the morphology of cells in bronchial epithelial growth medium (BEGM) and in 3T3-J2 co-culture and ROCK inhibition (3T3+Y) at both early (P1) and late (P4) passage. White dotted lines indicate epithelial colonies in 3T3+Y cultures. Scale bar = 20 µm. B) Airway epithelial cells stained by immunofluorescence with a marker of actively dividing cells (Ki67; green), cytokeratin 14 (CK14; red) and DAPI (blue) after 4 days of culture in BEGM or in 3T3+Y (scale bar = 50 µm). C) Population doublings for human airway epithelial cells grown in BEGM and 3T3+Y plotted over time. D) Representative plots showing EdU uptake in P2 cells grown in BEGM (top left) or in 3T3+Y (top centre) for 3 days. Summary data are shown for six donors (top right; mean ± SEM; experiment performed in technical triplicate for each donor and averaged). Cells were co-stained with DAPI to analyse cell cycle progression. Representative plots for cells grown in BEGM (bottom left) or in 3T3+Y (bottom centre) are shown. Summary data are shown for six donors (bottom right; mean ± SEM; experiment performed in technical triplicate for each donor and averaged). Differences between conditions were assessed using a Wilcoxon matched pairs signed ranked test (* indicates $p<0.05$).

To further investigate the characteristics and behaviour of airway epithelial cells expanded in 3T3+Y it was crucial to be able to easily separate the epithelial cells from the 3T3-J2s. Importantly, I was able to take advantage of differences in the trypsin sensitivity of the mitotically inactive feeder cells, which are weakly adherent, and the proliferating epithelial cells, which are strongly adherent, to effectively separate epithelial cells from 3T3-J2s at each passage. To demonstrate this, epithelial cells were stained with the lipophilic membrane stain DiO (green; Figure 4.2A) and 3T3-J2 feeder cells with DiI (red; Figure 4.2A) and were seeded in co-culture. Once epithelial colonies had formed, feeder cells were removed by 'differential trypsinisation' and cultures were imaged by fluorescence microscopy. In co-culture, colonies of epithelial cells (green) can clearly be seen surrounded by 3T3-J2 feeder cells (red; Figure 4.2A; top panel). After an initial round of trypsinisation, effective removal of feeder cells was apparent (Figure 4.2A; bottom panel). To validate these findings, primary airway epithelial cells grown in 3T3+Y were stably transduced with a lentivirus containing green fluorescent protein (GFP). In co-cultures that were fully trypsinised (that is, in which differential trypsinisation was not performed), both GFP+ epithelial cells and GFP- feeder cells were observed by flow cytometry. However, when differential trypsinisation was performed to eliminate 3T3-J2 feeder cells, more than 98% of the remaining cells were epithelial (Figure 4.2B), showing that epithelial cells can be effectively separated from feeder cells for further analysis.

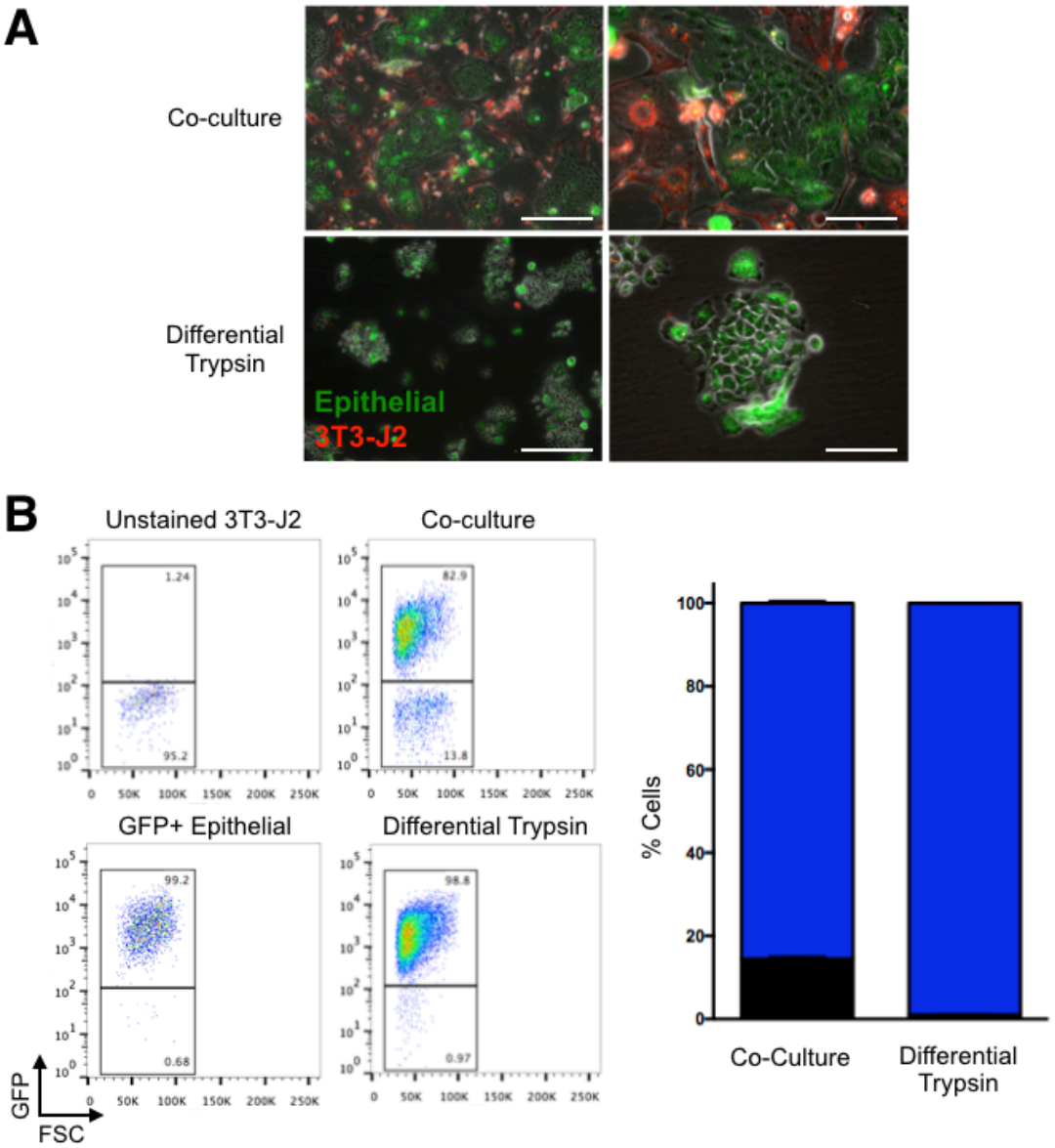

Figure 4.2: Trypsin sensitivity of mitotically inactivated 3T3-J2 feeder cells allows differential trypsinisation of epithelial cells. A) Immunofluorescence images showing co-cultures consisting of DiI-labelled 3T3-J2 feeder cells (red) and DiO-labelled primary human airway epithelial cells (green) before (top row) and after (bottom row) the first trysinisation step, which removes feeder cells. Scale bars = 200 µm. B) Flow cytometric analysis of differential trypsinisation. Primary human epithelial cells were transduced with a lentivirus containing green fluorescent protein (GFP). These were co-cultured with unlabelled 3T3-J2 cells for 5 days before analysis. Cultures in which a differential trypsinisation step was not performed contained both GFP+ epithelial cells and unlabelled 3T3-J2 feeder cells (top right; co-culture) whereas when a differential trypsinisation step was introduced ~99% of cells were GFP+ epithelial cells.

Epithelial cells expanded in 3T3+Y are basal stem cells

Based on previous observations that CK5+/p63+ basal cells are expanded during culture in BEGM, the expression of the basal cell markers (CK5, CK14 and p63) was investigated in 3T3+Y using immunofluorescence staining to establish whether basal cells are also expanded in these conditions. Additionally, the markers integrin α6 (ITGA6) [268], TROP2 [269] and nerve growth factor receptor (NGFR) [15] were included as previous literature indicates that basal cells with higher expression of these proteins behave as stem cells *in vitro*. The staining confirmed that airway epithelial cells expressing all of these markers are expanded in 3T3+Y culture, indicating that the cells are basal cells (Figure 4.3). Furthermore, higher levels of expression of all of these markers was observed in basal cells grown in 3T3+Y than in those grown in BEGM, further suggesting that basal cells grown in 3T3+Y may have greater stem cell potential.

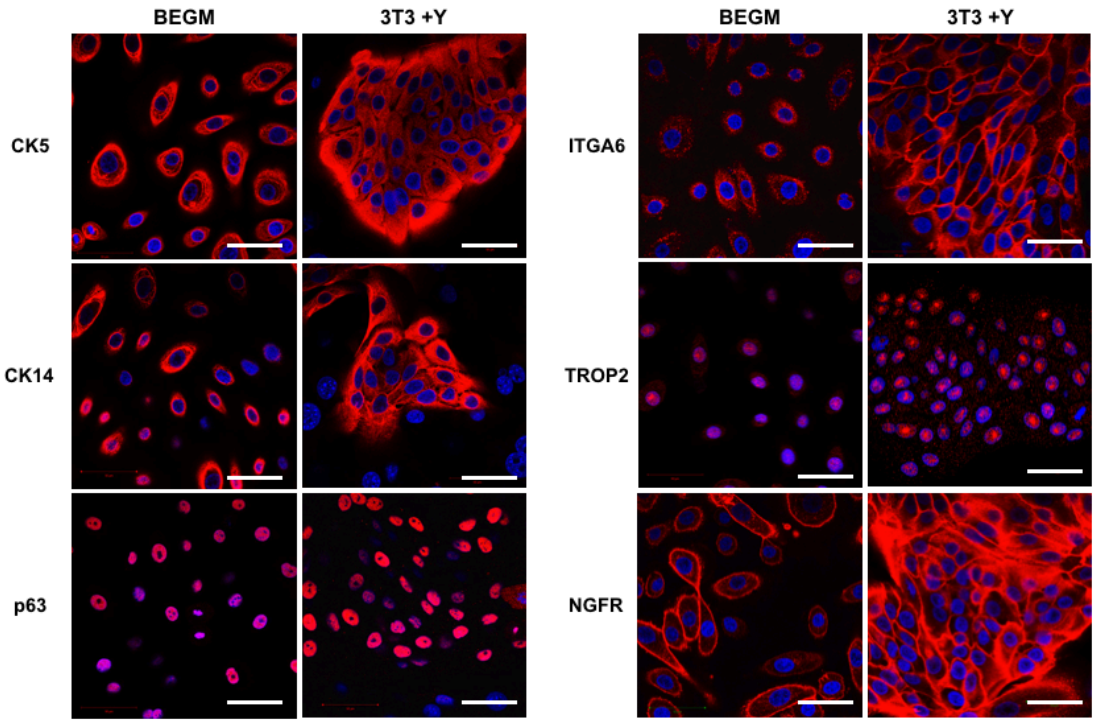

Figure 4.3: Immunofluorescence staining for basal cell markers in cells grown in either BEGM or 3T3+Y for one passage. Staining for each protein of interest is shown in red and DAPI (blue) is used as a counterstain. Scale bars = 50 µm.

To further these studies, qPCR and flow cytometry were used to assess changes in expression of specific airway basal cell genes and proteins, again using matched donor cells grown in BEGM and 3T3+Y. Higher levels of the putative stem cell markers integrin α6, NGFR and TROP2 were present on the surface of cells expanded in 3T3+Y compared with those expanded in BEGM (Figure 4.4A), confirming immunofluorescence staining in Figure 4.3. Expression of the associated genes varied between donors but consistent patterns of change did occur between culture conditions. Gene expression of TROP2 was significantly upregulated and there was a trend towards NGFR upregulation in basal cells expanded in 3T3+Y compared with BEGM (Figure 4.4B), supporting immunofluorescence staining in Figure 4.3 and flow cytometric staining in Figure 4.4A. However, integrin α6 was significantly downregulated at the level of gene expression (Figure 4.4B), suggesting that post-transcriptional regulation may underlie the increased surface expression observed in cells

cultured in 3T3+Y (Figure 4.3, Figure 4.4A). Expression of the ΔN-p63 isoforms expressed by basal epithelial stem cells [251, 257] was not significantly altered by culture conditions (Figure 4.4B).

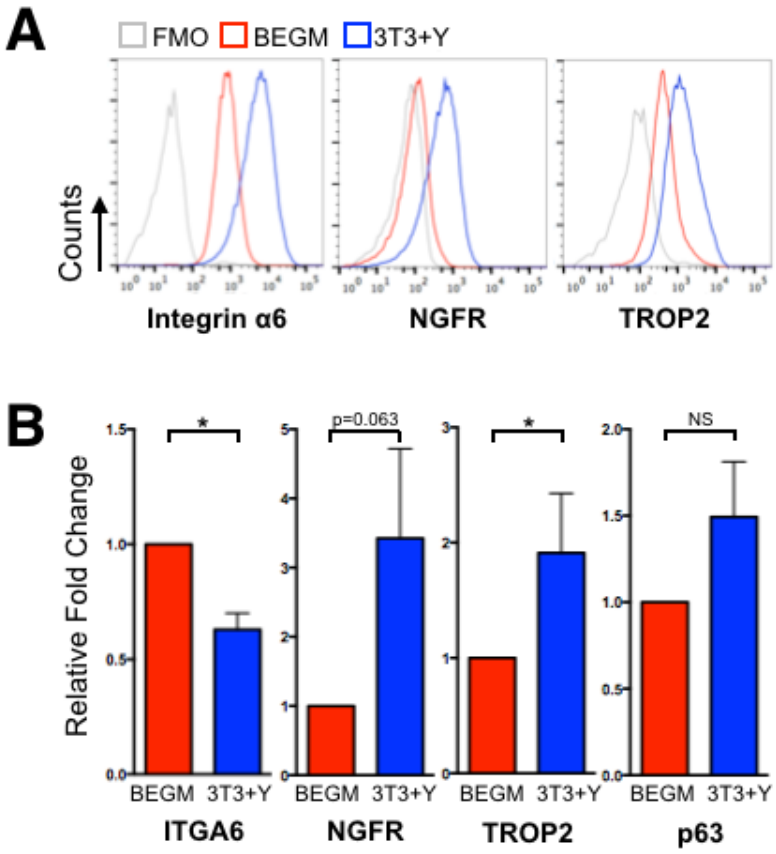

Figure 4.4: 3T3-J2 co-culture and ROCK inhibition expand basal epithelial stem cells. A) Flow cytometric analysis of airway basal stem cell marker expression on the surface of cells grown in bronchial epithelial growth medium (BEGM; red) or in 3T3-J2 co-culture with ROCK inhibition (3T3+Y; blue) for 4 days. Fluorescence minus one (FMO; grey) controls are shown for comparison. This experiment was repeated three times with different donor cell lines and representative plots for one donor cell line are shown. B) qPCR analysis of airway basal stem cell marker gene expression in airway epithelial cells grown in BEGM or in 3T3+Y for 7 days. Differences between groups were assessed using the Wilcoxon matched pairs signed ranked test (n≥6 donors; mean +/- SEM; * indicates $p<0.05$).

3T3+Y-expanded basal cells are karyotypically normal

To achieve representative airway *in vitro* models and to generate transplantable epithelium for tissue-engineering applications, it will be important to avoid the generation of genetic abnormalities during culture. Importantly, airway epithelial cells grown in 3T3+Y displayed a normal 46,XX or 46,XY karyotype after more than 6 weeks in culture (Figure 4.5A). However, deletions below ≈5 megabases are not reliably detected by conventional karyotyping so we obtained two biopsies from a single donor to compare the tissue of origin with matched cells grown in 3T3+Y in more detail. We investigated copy number change in these cells using multiplex ligation-dependent probe amplification (MLPA) [270] as gene-rich subtelomeric regions share significant homology between chromosomes making them vulnerable to inappropriate recombination during meiosis [271]. Our analysis revealed that both samples were normal with no evidence of subtelomeric copy number alterations after 6 weeks in culture (Figure 4.5B; Table 4.1).

Epithelial cells in culture cease to proliferate upon reaching confluency. One consequence of any genetic abnormalities acquired during culture could be the loss of this contact inhibition, which could indicate transformation of the cells. Consistent with the lack of karyotypic change in 3T3+Y-cultured basal cells, investigation of contact inhibition revealed that basal cells grown in 3T3+Y retained this contact inhibition capacity. When cells were seeded onto transwell membranes in differentiation medium (that is, when 3T3-J2 support and Y-27632 were withdrawn), a majority of cells were Ki67 after 2 days, showing high levels of cell proliferation. However, once cells were visibly confluent after 8 days of culture, no Ki67+ nuclei were detected by immunofluorescence (Figure 4.5C), showing that cells were contact inhibited and ceased to proliferate once confluence was reached.

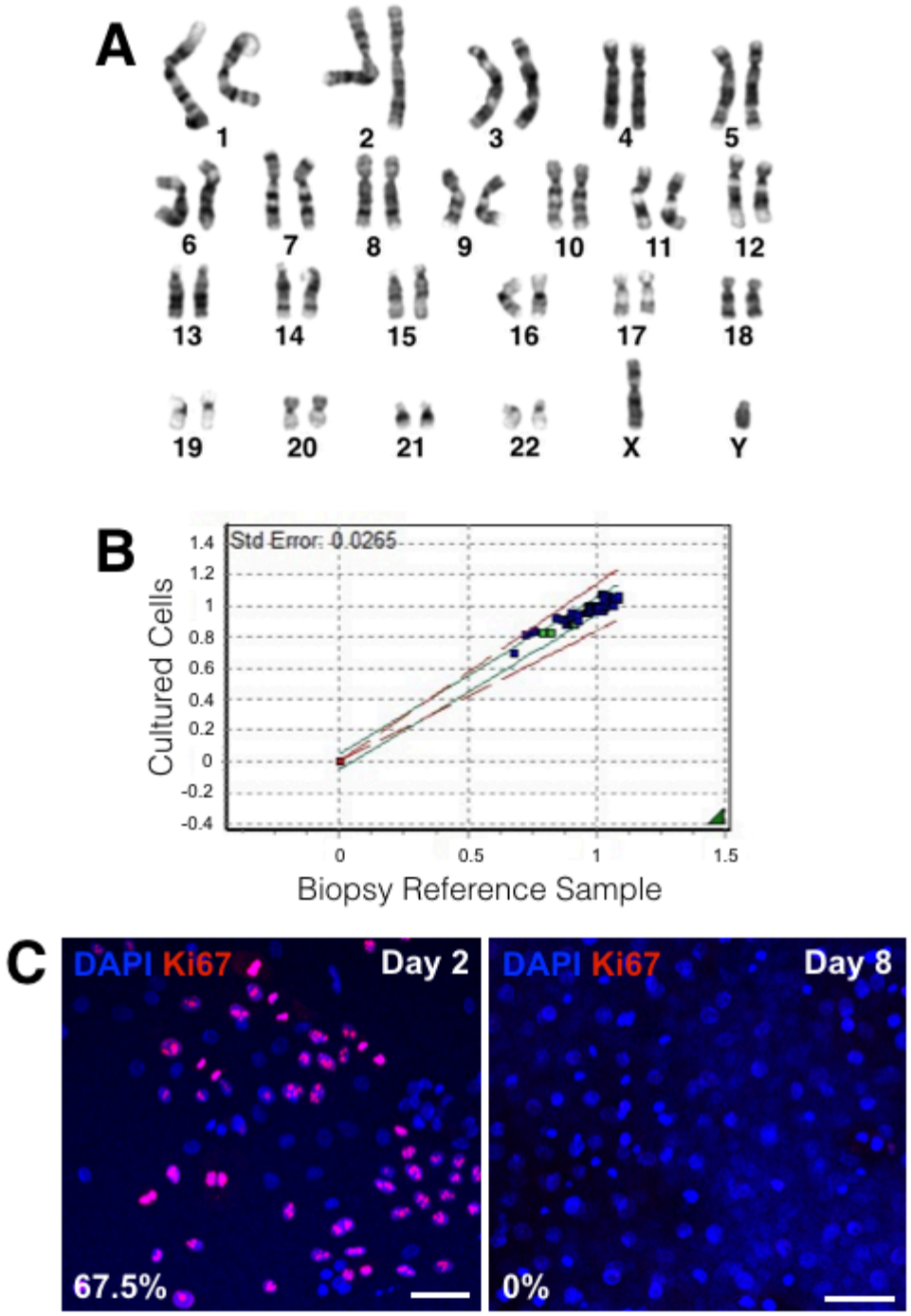

Figure 4.5: Airway epithelial cells are karyotypically normal after clinically relevant periods in culture. A) Representative karyotyping image for airway epithelial cells grown in 3T3+Y for >6 weeks. Normal karyotype was found in all 3 donor cell cultures tested. B) Multiplex ligation-dependent probe amplification (MLPA) analysis was performed in GeneMarker v2.4.0 to compare the normalised peak height ratio of a reference biopsy sample and donor-matched cells grown in 3T3+Y for 6 weeks. Clear correlation is demonstrated; no subtelomeric copy number changes were detected. C) Ki67 staining of cells grown in 3T3+Y for one month and then seeded onto transwell membranes. After 2 days (subconfluent) Ki67+ proliferating cells are seen but after 8 days (confluent for >48 hours) no Ki67 cells were detected. DAPI is used as a counterstain. Scale bars = 50 µm.

Probe	Bin Size	Cell Line-Biopsy Ratio
01p	126.8	1.021
01q	305.2	1.054
02p	134.2	1.117
02q	313.4	0.973
03p	141.8	1.137
03q	321.8	0.985
04p	150.5	1.044
04q	330.1	0.931
05p	158.8	0.952
05q	338.3	0.932
06p	166.0	1.114
06q	345.1	0.976
07p	173.0	0.957
07q	354.3	1.045
08p	179.9	1.069
08q	360.6	0.994
09p	186.6	0.984
09q	370.1	0.980
10p	194.3	1.040
10q	378.0	1.000
11p	201.8	1.067
11q	384.9	0.966
12p	209.6	1.011
12q	393.1	1.043
13p	219.2	0.966
13q	401.2	0.900
14p	228.6	1.000
14q	409.6	0.963
15p	236.4	0.995
15q	424.1	1.047
16p	243.7	1.152
16q	424.1	0.947
17p	252.6	0.991
17q	433.2	1.057
18p	259.0	0.996
18q	441.1	1.014
19p	266.6	0.905
19q	448.3	1.268
20p	275.3	0.998
20q	457.2	1.057
21p	282.9	0.962
21q	464.0	1.205
22p	288.4	1.000
22q	472.5	1.234
SHOX	296.9	0.933
SYBL1	481.5	1.092
X	100.9	1.020
Y1	105.2	-1
Y2	114.8	-1

Table 4.1: Table of individual probe ratios from multiplex ligation-dependent probe amplification (MLPA) comparison of matched donor cell line and reference patient biopsy.

Differentiation capacity of expanded basal cells is better maintained in 3T3+Y than in BEGM

Since basal cells expanded in 3T3+Y retain the capacity to form a stable, confluent epithelial layer, the capacity of these cells for *in vitro* airway differentiation was investigated. Firstly, cells were cultured at an air-liquid interface to establish their differentiation capabilities at either early (P1) or late (P4) passages. For comparison with earlier results using BEGM, matched cells grown in BEGM or 3T3+Y were compared. During expansion in either culture system, all basal cells were p63+ but, after ≥4 weeks in air-liquid interface, only a subset of cells retained p63 expression, indicating that differentiation occurred in all conditions (Figure 4.6A). Acetylated α-tubulin (ACT) staining of these cultures revealed extensive ciliation in cultures derived from early passage (P1) basal cells in either BEGM or 3T3+Y (Figure 4.6B). However, at late passage (P4) only the 3T3+Y-derived cultures persisted for the full 6 weeks of the experiment due to problems with epithelial integrity in BEGM-derived cultures. Importantly, very few ciliated cells were seen in late passage BEGM-derived cultures, indicating that basal cells expanded in BEGM lose their capacity for ciliated differentiation by passage 4 (Figure 4.6B). Interestingly, extensive ciliation comparable to P1 cultures was seen in late passage 3T3+Y-derived cultures, indicating that basal cells expanded in 3T3+Y maintain their differentiation capacity over passage.

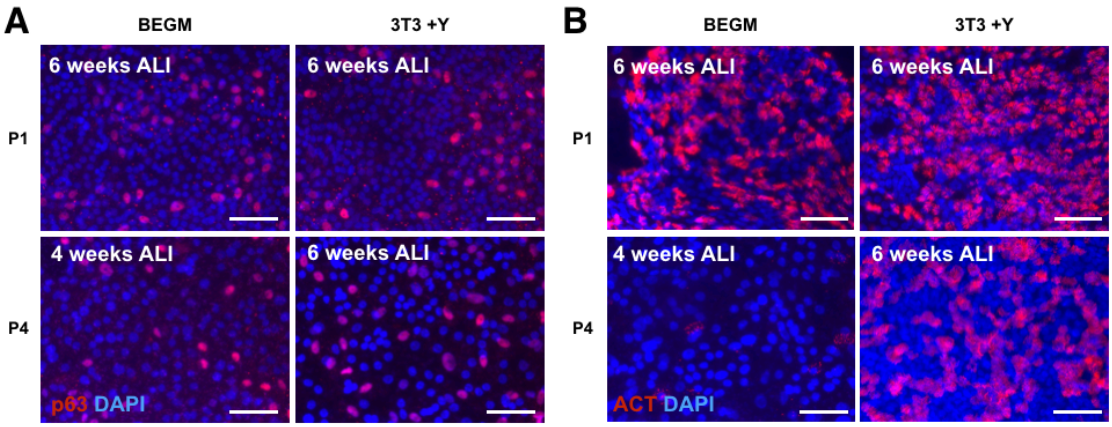

Figure 4.6: Air-liquid interface cultures reveal a decline in basal cell differentiation capacity over time in cells cultured in BEGM but not in 3T3+Y. A) Top-down immunofluorescence staining shows that a subset of cells expanded in all conditions express p63 after 6 weeks of air-liquid interface (ALI) culture. DAPI is used as a counterstain. Scale bars = 50 µm. B) Staining for acetylated α-tubulin (ACT) shows ciliated epithelial cells in air-liquid interface cultures derived from early passage bronchial epithelial growth medium (BEGM) and both early and late passage 3T3-J2 co-culture with ROCK inhibition (3T3+Y) cultures. DAPI is used as a counterstain. Scale bars = 50 µm.

Through collaboration with Professor Chris O'Callaghan's laboratory (Institute of Child Health, University College London), the functional capacity of the ciliated epithelium generated using air-liquid interface cultures from basal cells expanded in 3T3+Y was investigated. After 6 weeks, the cultures had very high transepithelial electrical resistance (TEER) values (Figure 4.7A), indicative of high epithelial integrity [272]. Further, high-speed video microscopy and scanning electron microscopy investigations revealed that the ciliary beat and frequency were within the normal range [273] (Figure 4.7A) and that ciliary ultrastructure [274] was normal (Figure 4.7B).

A

	Donor 1	Donor 2	Donor 3	Normal Range
TEER (Ohms)	1510.3 ± 32.0	1509.3 ± 22.8	3062.0 ± 40.5	>250
Ciliary Beat Frequency (Hz)	10.9 ± 1.0	16.8 ± 0.1	15.8 ± 0.7	7-16
Dyskinesia Score (%)	3.75	3.19	0	0-10

B

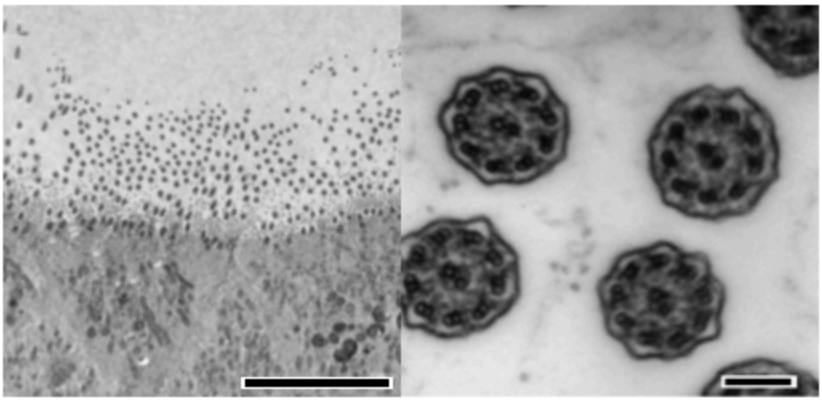

Figure 4.7: Ciliary function and ultrastructure are normal in 3T3+Y-derived air-liquid interface cultures. A) In air-liquid interface cultures, the transepithelial electrical resistance (TEER), ciliary beat frequency and ciliary beat pattern were characterised in collaboration with Professor Chris O'Callaghan's laboratory (Institute of Child Health, University College London). Results are shown as mean ± SEM. B) Transmission electron microscopy (TEM) shows a healthy well-ciliated strip of respiratory epithelium from air-liquid interface cultures. Normal columnar cells and microvilli are seen (scale bar = 10 µm). The electron micrograph on the right shows cilia in cross section. A normal ciliary ultrastructure is seen with the typical 9 + 2 arrangement of microtubules and inner and outer dynein arms (scale bar = 1 µm).

In addition to air-liquid interface assays, differentiation of cells grown in BEGM was compared with matched donor cells grown in 3T3+Y in a three-dimensional (3D) tracheosphere assay. Here, single cultured airway basal cells are grown in a 3D Matrigel matrix and form spheroids over the culture period. These undergo lumen formation and contain differentiated airway cell types at the luminal surface [15]. As in Figure 4.6, early (P1) and late (P4) passage cultures were compared to examine whether differentiation potential is maintained over passage. The size of tracheospheres derived from 3T3+Y basal cells was not affected by passage whereas tracheospheres derived from passage 4 BEGM cells were smaller than those derived from passage 1 BEGM cells (Figure 4.8A and Figure 4.8B). When differentiation status of tracheospheres was assessed, p63 was expressed in all of the cells on the basal surface of spheroids (Figure 4.8C), consistent with its expression in basal epithelial cells that contact the basement membrane *in vivo*. At early passage (P1), both BEGM and 3T3+Y cultures gave rise to tracheospheres with evidence of mucin 5B (MUC5B)+ goblet cells and ACT+ ciliated cells (Figure 4.8D). However, at late passage (P4), only cells cultured in 3T3+Y showed this multipotent differentiation capacity (Figure 4.8D). At late passage, the tracheospheres that did form (see Figure 4.8B) displayed abnormal lumen formation and did not show evidence of ciliated differentiation (Figure 4.8D).

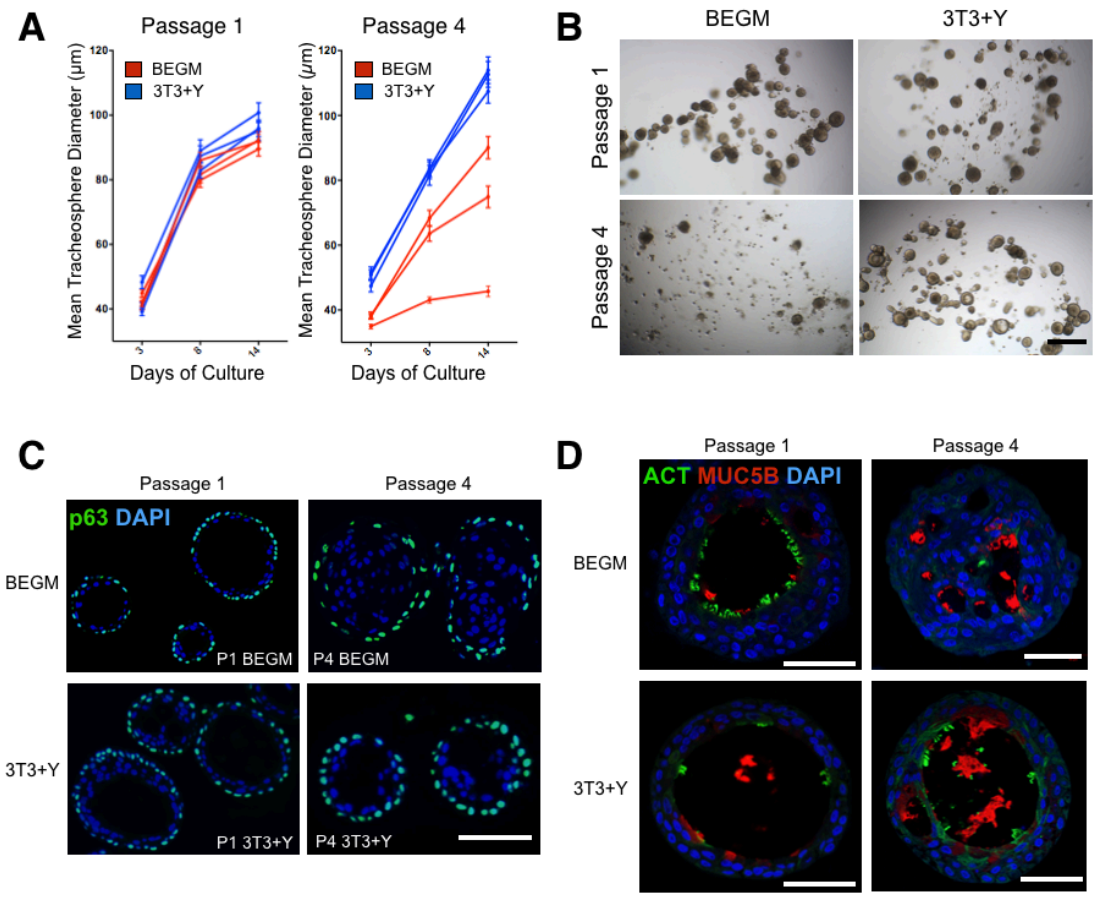

Figure 4.8: Airway basal cells expanded in 3T3+Y form well differentiated tracheospheres at later passage than those expanded in BEGM. A) Quantification of tracheosphere size at early (P1) and late (P4) passage in bronchial epithelial growth medium (BEGM) and 3T3-J2 co-culture with ROCK inhibition (3T3+Y). Mean +/- SEM is shown. B) Brightfield images show morphology of tracheospheres derived from basal cells cultured in BEGM or 3T3+Y for one passage (top row) or four passages (bottom row). Scale bar = 500 µm. C) Immunofluorescence staining shows tracheosphere p63 expression. Scale bar = 100 µm. D) Immunofluorescence staining of tracheospheres generated from cells grown in either BEGM (P1 and P4) or 3T3+Y (P1 and P4) for acetylated α-tubulin (ACT; green), mucin 5B (MUC5B; red) and DAPI (blue). Scale bars = 50 µm.

The multipotent differentiation capacity of airway basal cells grown in 3T3+Y was further investigated by adaptation of a second submerged airway differentiation protocol [239]. Here, cell suspensions were incubated in a non-adherent 96-well plate on a plate shaker and single aggregates of cells were formed (Figure 4.9A). This technique confers the benefit of having ciliated epithelial cells on the surface of airway spheroids, as opposed to in 3D tracheospheres where cilia are contained within the 3D structure, a factor that might limit their relevance in drug or toxicology exposure studies. After three weeks of culture, histology revealed a continuous epithelial structure containing acini (Figure 4.9B).

Immunofluorescence staining showed that aggregates contained MUC5B+ mucosecretory cells and were lined by ACT+ ciliated cells (Figure 4.9C), further indicating that basal cells expanded in 3T3+Y maintain their multipotent differentiation capacity.

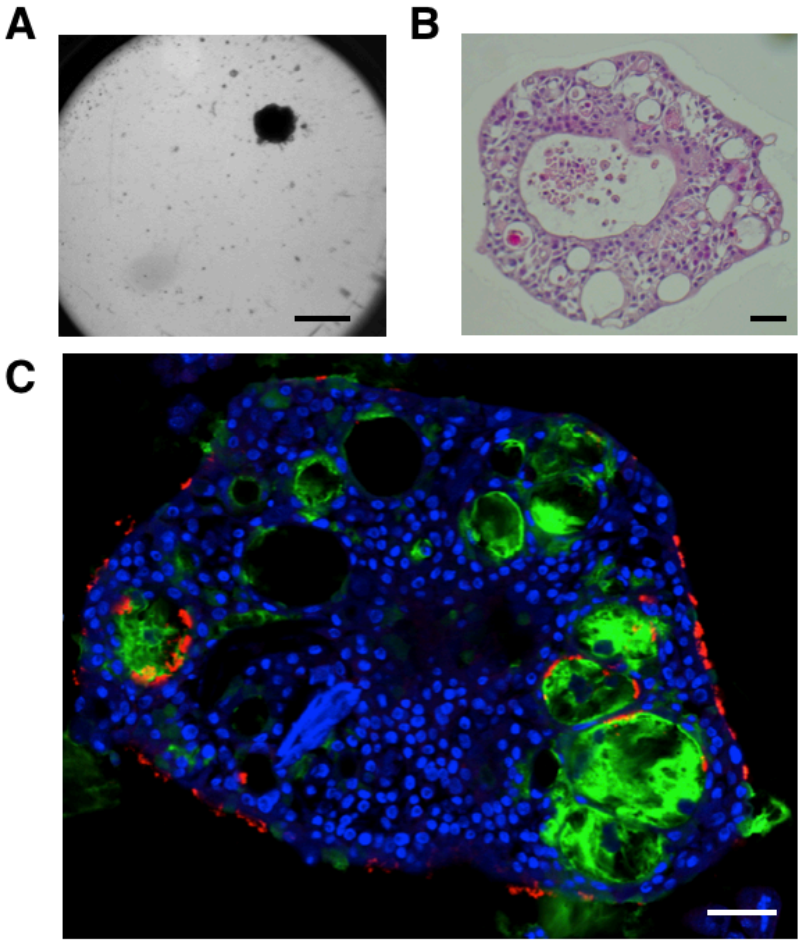

Figure 4.9: Differentiation of airway basal cells expanded in 3T3+Y using an aggregate culture method. A) Brightfield image showing cell aggregate in a 96-well plate well. Scale bar = 500 µm. B) Haemotoxylin and eosin staining of a cell aggregate after 23 days of culture. Scale bar = 50 µm. C) Immunofluorescence staining of a cell aggregate showing mucin 5B (MUC5B)+ mucus (green), acetylated α-tubulin (ACT)+ ciliated cells (red) and cell nuclei (DAPI; blue). Scale bar = 50 µm.

Microarray analysis

Given the remarkable effects of 3T3+Y culture on basal cell expansion *in vitro* and the maintenance of differentiation over longer periods in these cultures, genome-wide transcriptional profiling was performed using microarrays to explore the major pathways altered by 3T3+Y culture. After initial expansion in BEGM, four matched donor cell lines grown in either BEGM or 3T3+Y for 7 days were compared. Data were analysed using the significance analysis of microarrays method with a false discovery rate of 5%: 507 significantly differentially expressed transcripts were found, 297 of which were downregulated in 3T3+Y and 210 of which were upregulated. Significant differences were visualised in a cluster diagram (Figure 4.10A) that clearly shows clustering of expression according to culture condition rather than donor. Even when selected airway-relevant genes were analysed, independently of whether differences were significant, cells remained clustered according to culture condition rather than donor (Figure 4.10B).

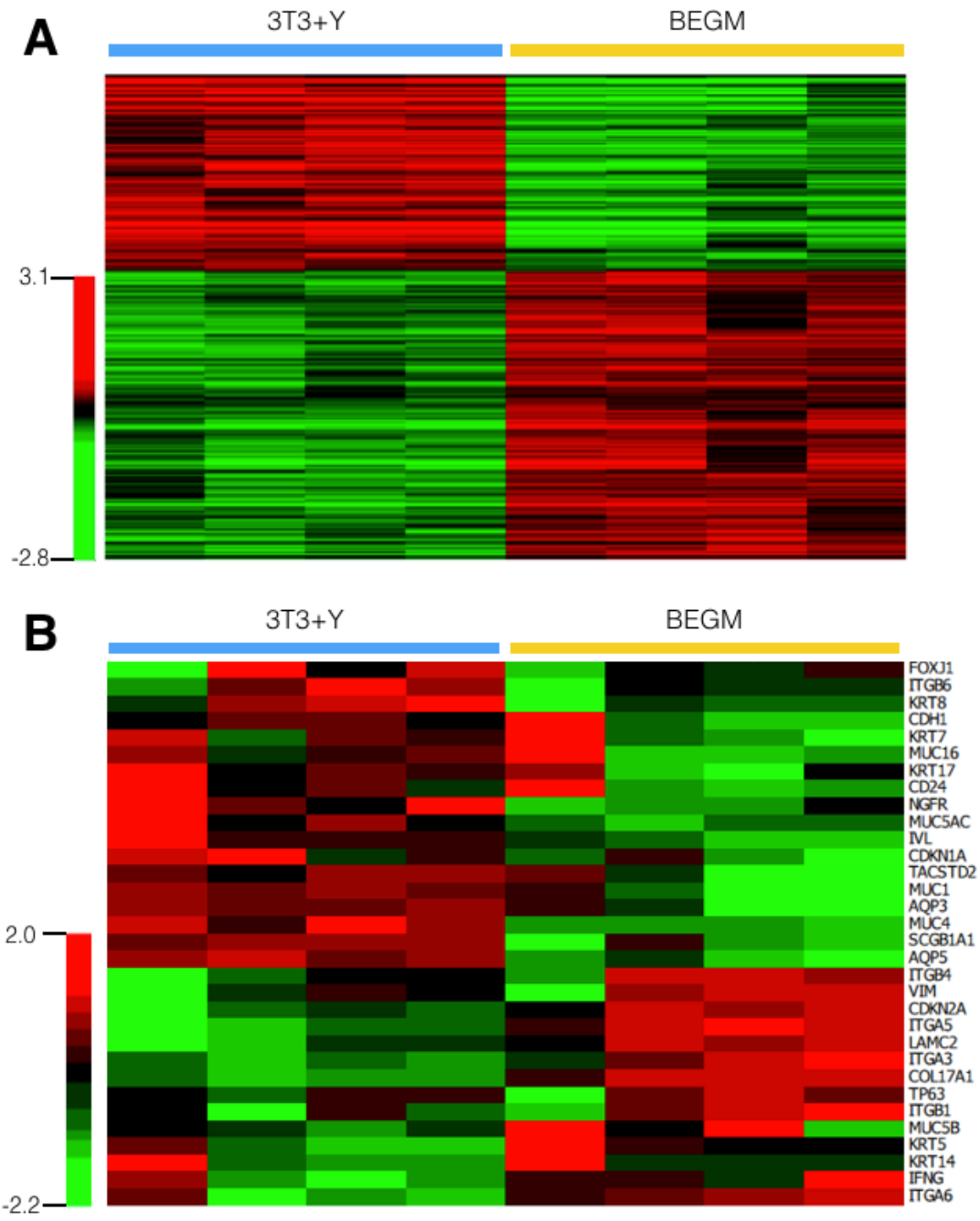

Figure 4.10: Microarray analysis reveals differentially expressed genes in matched donor cells expanded in 3T3+Y or BEGM. A) Cluster diagram plotting significantly differentially expressed genes between cells grown for one passage in either bronchial epithelial growth medium (BEGM) or in 3T3-J2 co-culture with ROCK inhibition (3T3+Y). B) Cluster diagram showing selected airway epithelial genes of interest, including markers of basal cells, goblet cells and ciliated cells. Selected airway-relevant genes are shown regardless of whether differences are significant. RNA isolation for microarray analysis was performed by Dr. Colin Butler.

To highlight pathways in which the genes whose expression changed significantly between culture conditions might be involved, we used Ingenuity Pathway Analysis and observed alterations in several pathways, including cell cycle regulation (Figure 4.11A), which correlated with the increased proliferation of basal cells in 3T3+Y shown in Figure 4.1. Functional analysis using the same software revealed significant upregulation of genes associated with cell movement and proliferation and decreased expression of genes associated with cell death in 3T3+Y (Figure 4.11B).

A

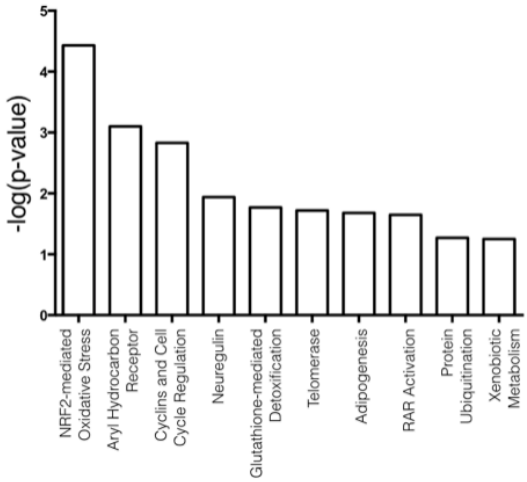

B

Function	-log(p-value)	Top unique genes (fold change)
Cell movement	5.106	SCGB3A1 (20), SERPINA3 (10.638), ID1 (6.25), AGR2 (5.263), MUC4 (4.348) APP (-4.36), CDH13 (-4.09), APOE (-3.25), LAMA3 (-2.95), COL17A1 (-2.52)
Proliferation	8.951	GABRP (12.195), CHP2 (5.882), ANXA10 (5.263), FOXA1 (3.448), AQP5 (3.333) TRIB3 (-6.35) DDIT3 (-4.32) CDH13 (-4.09), KLF9 (-3.14), TNFAIP3 (-3.12)
Cell death	9.703	CCNA1 (6.25), AGR2 (5.263), GPX2 (5.263), PLA2G10 (4.545), GSTA1 (3.571) SRPX (-5.02), NPC1 (-3.39), HERPUD1 (-2.77), FTH1 (-2.67), PHLDA1 (-2.46)

Figure 4.11: Pathway analysis of microarray comparisons. A) Ingenuity Pathway Analysis (IPA) was applied to investigate cell signalling pathways containing significantly differentially expressed genes. The IPA analysis –log(p-value) is plotted on the y-axis versus biological processes on the x axis. B) Functional analysis of differentially expressed genes was performed using IPA. The major functions altered by culture in 3T3-J2 co-culture with ROCK inhibition (3T3+Y) are shown, along with the relevant –log(p-value) and the top 10 relevant genes (5 upregulated and 5 downregulated). Genes already displayed in a function were subsequently ignored to avoid overlap.

In order to validate the results of the microarray, the expression of six differentially expressed genes was analysed in all samples by qPCR; these results showed a high correlation with the microarray (r = 0.96; Figure 4.12A). Further, the expression of secretoglobin family 3A member 1 (SCGB3A1), the most significantly different gene, was evaluated by western blotting. Antibody validation was performed by staining normal human tracheal epithelial sections and confirming its expected location in differentiated goblet cells (Figure 4.12B). Consistent with its upregulation in the microarray data, SCGB3A1 was strongly expressed in 3T3+Y but not in matched donor cells grown in BEGM (Figure 4.12C). The biological significance of this upregulation is unknown as the protein is not expressed in human basal cells *in vivo* (Figure 4.12B), although in mice SCGB3A1 expression may be increased during regeneration [275].

Overall, these results indicate that 3T3+Y allows the prolonged expansion of human airway basal epithelial cells with multipotent airway differentiation potential *in vitro*. Our microarray data provide a resource for future research to investigate the molecular basis of this improvement in cell culture conditions.

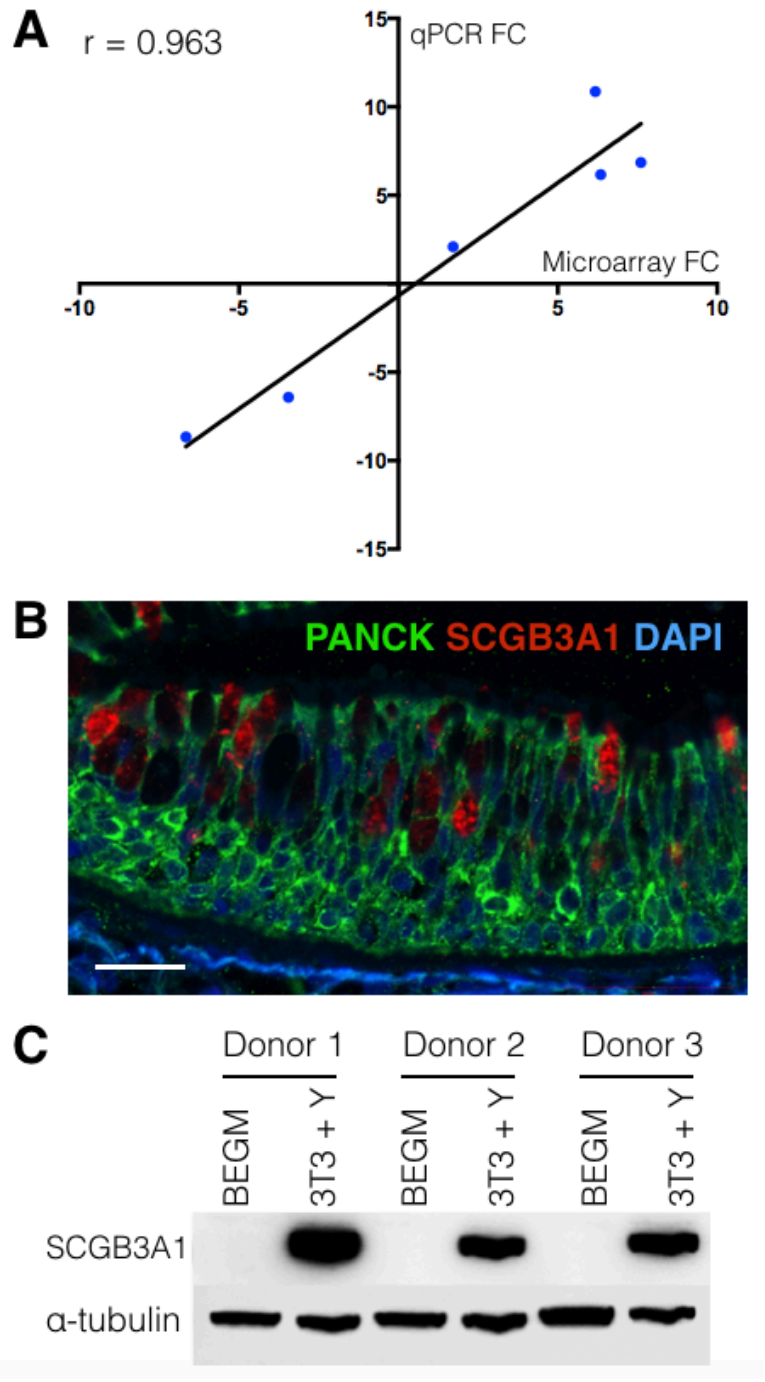

Figure 4.12: Validation of microarray data using qPCR and western blotting. A) Correlation between microarray fold change (3T3+Y/BEGM) and qPCR fold change (3T3+Y/BEGM). Pearson's r is shown. B) Immunofluorescence staining of normal human airway epithelium showing pan-cytokeratin (PANCK; green), secretoglobin family 3A member 1 (SCGB3A1; red) and cell nuclei (DAPI; blue). Scale bar = 20 µm. C) Western blot confirmation of upregulated SCGB3A1 expression in donor-matched cells grown in 3T3-J2 co-culture with ROCK inhibition (3T3+Y) compared with bronchial epithelial growth medium (BEGM).

4.4 Summary

- Human airway epithelial cells are rapidly expanded by co-culture with mitotically inactivated 3T3-J2 cells in the presence of a ROCK inhibitor (3T3+Y).
- 3T3+Y-expanded epithelial cells express markers of airway basal cells and show evidence of increased expression of genes associated with airway basal stem cells.
- Expanded basal cells are karyotypically normal and contact inhibited.
- After four passages, basal cells grown in BEGM proliferate more slowly and have demonstrably lost the capacity for multipotent airway epithelial differentiation. However, cells grown in 3T3+Y are still capable of forming epithelia containing both goblet and ciliated cells.
- Pathway analysis of microarray data comparing cells expanded in BEGM and 3T3+Y highlighted pathways that may be relevant to future investigations to unravel the mechanisms underpinning the success of 3T3+Y culture

5 . Improvements to the human airway basal epithelial cell co-culture system to improve suitability for tissue engineering

5.1 Background

Having established a protocol to expand human airway basal stem/progenitor cells in co-culture with 3T3-J2 fibroblasts and Rho-associated protein kinase (ROCK) inhibition (3T3+Y) and demonstrated the advantages of this system for extending the usefulness of these cells in differentiated primary airway cultures, improvements to the system were investigated. Firstly, if tissue-engineered airway transplantation is to enter clinical trials and eventually to produce novel therapeutic options, then GMP-compliance will be necessary. For this, co-culture of human epithelial cells with 3T3-J2 fibroblasts is not ideal due to the murine origin of the cells, although such methods have been approved in other epithelial organs [190, 194-196, 276]. The co-culture of airway epithelial cells with alternative stromal cells was investigated to establish whether stromal cells derived from patients could be used to create autologous, human feeder layers. Secondly, previous data were gathered using epithelial cells that were isolated in bronchial epithelial growth medium (BEGM) for one passage prior to investigation, so assessments of whether using 3T3+Y for the isolation of airway epithelial cells were made with the expectation that this would increase the culture success rate and reduce the amount of time required to establish cultures. In addition, we examined whether outgrowth from biopsy samples was the optimal way to isolate airway epithelial cells: we compared outgrowth from biopsy samples and from single cell suspensions generated by digestion of biopsy samples and endobronchial brushings. Finally, the potential use of 3T3-J2-conditioned medium instead of co-culture with feeder cells was investigated, as this would eliminate the need for direct contact with mouse cells and would therefore be more suitable to grow epithelial cells for tissue-engineering applications.

5.2 Aims

- To investigate whether human-derived stromal cells can replace 3T3-J2 cells in co-culture protocols.
- To investigate and to optimise the outgrowth of airway epithelial cells from endobronchial biopsy samples directly in 3T3+Y.
- To investigate whether 3T3-J2-conditioned medium can replace co-culture with 3T3-J2 feeder cells.

5.3 Results

Replacement of 3T3-J2 feeder cells with alternative stromal feeder cells

The ability to derive feeder cells on a patient-specific basis rather than to rely on a murine embryonic cell line is appealing for translational purposes, so plausible human feeder cell candidates were investigated as a 3T3-J2 replacement. Human lung fibroblasts were assessed given the ease of fibroblast isolation from small patient tissue samples [277] as well as human bone marrow-derived mesenchymal stromal cells (MSCs) because these have been used in an autologous fashion in previous tissue-engineered airway grafts [70, 71]. Feeder layers were prepared in the same way as for 3T3-J2 cells: that is, stromal cells were mitotically inactivated by 2-hour treatment with mitomycin C prior to epithelial cell seeding the following day, and epithelial growth medium containing 5 μM Y-27632 was used for co-cultures. Promisingly, colonies of epithelial cells with a similar morphology to those seen in co-culture with 3T3-J2 feeder layers emerged during the first passage in co-cultures with both MSCs and lung fibroblasts (Figure 5.1A), although epithelial cells appeared to proliferate more slowly on both of the human feeder layers. Unfortunately, after trypsinisation, substantial differences in both cell morphology and cell number appeared between the epithelial cells grown in co-culture with 3T3-J2 feeder layers and those grown in co-culture with either of the human alternatives (Figure 5.1A). Flow cytometry after passage one confirmed that integrin α6+/nerve growth factor receptor (NGFR)+/TROP2+ airway basal cells were expanded in all conditions (Figure 5.1C). Co-culture with alternative feeder cells induced higher levels of expression of these basal stem cell markers compared with BEGM, although not to the same level as co-culture in 3T3+Y in the case of NGFR and TROP2 expression. Although one further passage of these cells was possible (Figure 5.1B), these cells were not tested in terms of their differentiation capacity because the alternative

feeder layers did not improve cell expansion compared with BEGM (Figure 5.1B). Additionally, it was noted that neither human lung fibroblasts nor MSCs share the high trypsin sensitivity of 3T3-J2 cells so reliable separation of feeder cells and epithelial cells is another issue that would need to be addressed in attempts to replace 3T3-J2 feeder cells.

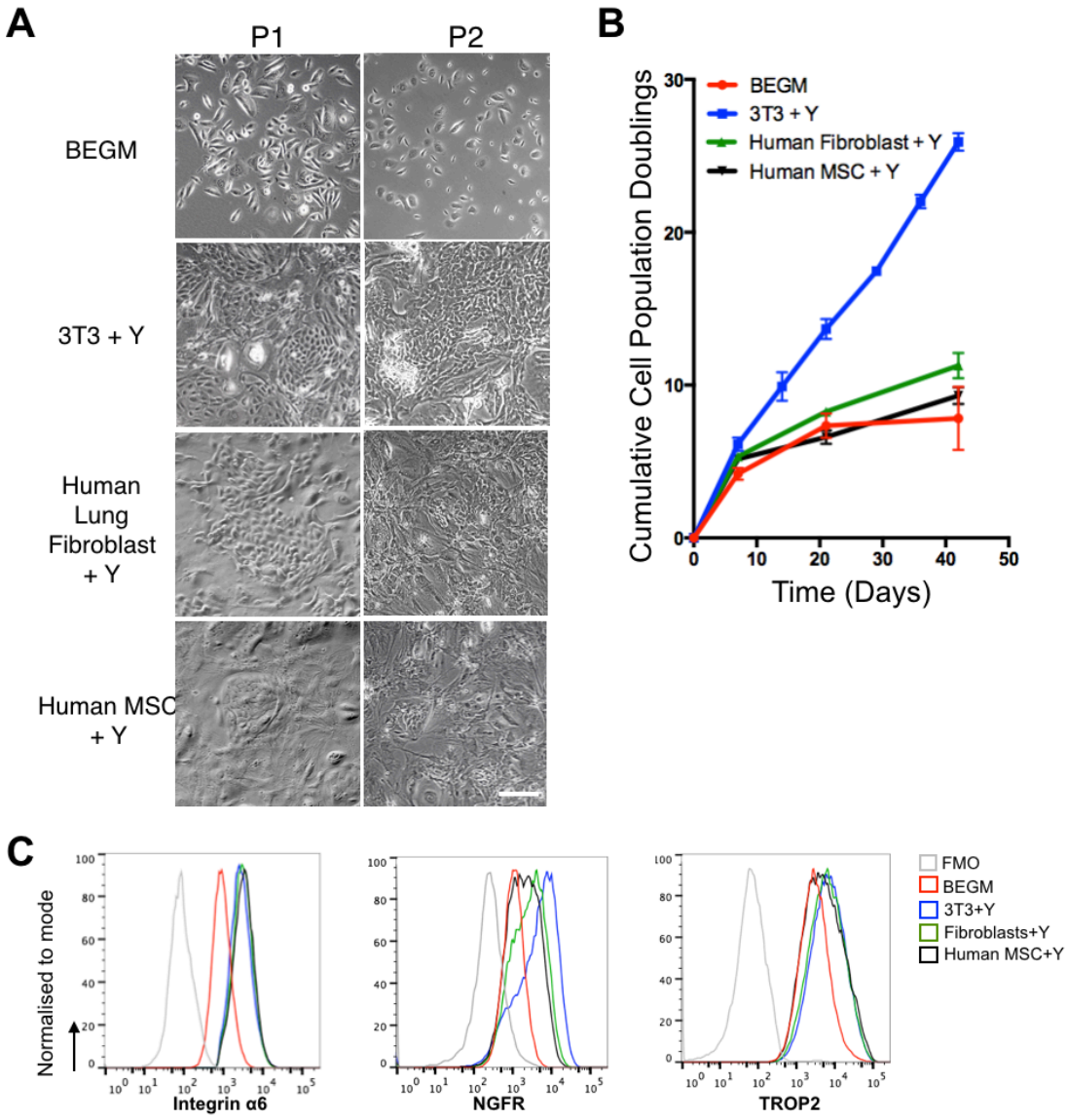

Figure 5.1: Mitotically inactivated allogeneic human bone marrow-derived MSCs or human lung fibroblast feeder layers cannot replace 3T3-J2 fibroblasts in human airway basal cell culture protocols. A) Representative brightfield images are shown for airway epithelial cells expanded in bronchial epithelial growth media (BEGM) or in co-culture with 3T3+Y, mitotically inactivated human lung fibroblasts + Y or mitotically inactivated human bone marrow-derived mesenchymal stromal cells (MSCs) + Y. Images were taken after one passage in these conditions (left) and after two passages (right). Scale bar = 50 µm. B) Cumulative cell population doublings for airway epithelial cells grown in these culture conditions are plotted over time (mean +/- SEM). C) Flow cytometry confirmed the similarity of expression of the basal cell proteins integrin α6, nerve growth factor receptor (NGFR) and TROP2 in cells cultured in these conditions. Epithelial cells were gated by selection of DAPI-, ITGA6+, CD90- cells (n = 3, representative plots shown).

Direct plating of biopsy samples in 3T3+Y

In the absence of an appropriate alternative to 3T3-J2 feeder cells, methods were sought to enhance the existing protocol. In all previous experiments, initial cell isolation occurred in BEGM and cells were subsequently divided into matched BEGM and 3T3+Y co-cultures for comparison of these methods. Given the advantages of 3T3+Y compared with BEGM in terms of proliferation and retention of basal progenitor cell properties, cell isolation directly in 3T3+Y was investigated. Results confirmed that, similarly to in BEGM, epithelial cells can be expanded from endobronchial biopsies plated in 3T3+Y as explants (Figure 5.2A). Also similarly to in BEGM, the cells that expand from biopsies are CK5+/p63+ basal epithelial cells (Figure 5.2B-5.2D).

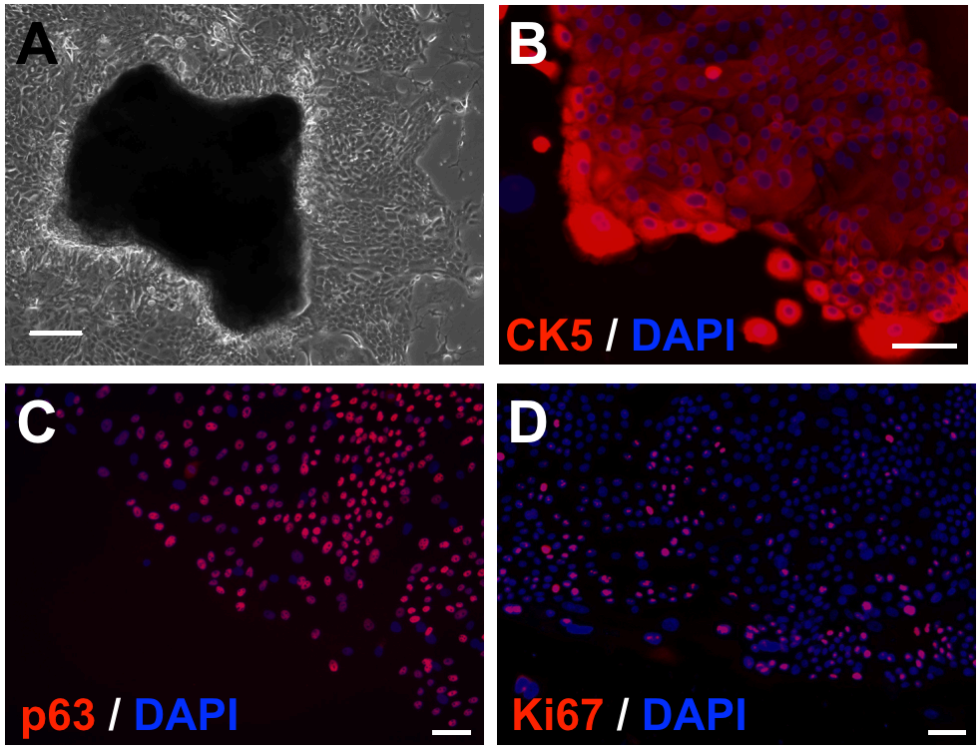

Figure 5.2: Direct expansion of human airway basal cells from endobronchial biopsy samples in 3T3+Y. A) Brightfield image showing epithelial cell outgrowth from endobronchial biopsy explant cultured in 3T3-J2 co-culture with ROCK inhibition (3T3+Y). Scale bar = 100 µm. B) Immunofluorescence staining for the basal cell marker cytokeratin 5 (CK5). Scale bar = 50 µm. C) Immunofluorescence staining for the basal cell marker p63. Scale bar = 50 µm. D) Immunofluorescence staining for the proliferation marker Ki67. Scale bar = 50 µm. DAPI is used as a counterstain.

Although airway basal cells could be expanded from explant biopsies directly in 3T3+Y, the culture time for satisfactory epithelial cell outgrowth from biopsies remained at 10-14 days, which is similar to the time taken for cell outgrowth from a biopsy in BEGM. Reducing this lag time is significant for translational applications as some tissue-engineering indications are urgent [71, 81]. In single, large explant biopsy cultures, epithelial cells effectively migrate from the biopsy as a continuous sheet across the culture plastic (Figure 5.3A). Seeding single cells was therefore investigated as an alternative with the aim that multiple epithelial cell colonies would form and proliferate, yielding a greater number of cells more quickly. This was achieved either through the enzymatic digestion of endobronchial biopsy samples to achieve a cell suspension that could then be plated in co-culture or through using a cell suspension derived directly from an endobronchial brushing sample. As expected, these new methods allow single basal cells to form independent colonies from the very beginning of culture and mean that the rapid expansion of cells begins earlier than from an explant biopsy. Indeed, cultures derived from either a biopsy following digestion or from a brushing yield significantly higher numbers of cells in 3T3+Y than those derived from an explant biopsy (Figure 5.3C). In all conditions, the expansion of integrin α6+/CK5+ airway basal epithelial cells was demonstrated using flow cytometry (Figure 5.3D).

Next, the success rate of cultures in these conditions was compared as, from experience of expanding cells in BEGM, we knew that not all biopsies that are plated in culture yield successful epithelial cell cultures. In our laboratory, the success rate of epithelial cell expansion from explant biopsies is around 50% in BEGM. Here, I show that 3T3+Y culture enables a greater culture success rate for biopsy explant than BEGM, with successful epithelial cultures established from 88% of biopsies grown in these conditions. The success rate for establishing cultures was particularly high in 3T3+Y when single cells were seeded

rather than explant biopsies, with 88% and 94% of digested biopsies and brushings, respectively, giving rise to epithelial cultures (Figure 5.3B).

Investigation of 3T3-J2-conditioned medium as a co-culture alternative

In these experiments the effect of using 3T3-J2-conditioned medium (CM+Y) in place of 3T3-J2 co-culture was investigated as this could be preferable in a translational setting: epithelial cells could be expanded without contamination with murine feeder cells even in the absence of a detailed understanding of the active components. To generate conditioned medium, 3T3-J2 feeder layers were prepared using mitomycin C, seeded at feeder density overnight and epithelial culture medium (without Y-27632) was added the following day. Medium was collected and replaced after 24 hours and collected again after 48 hours, based on a published protocol [278]. 5 μM Y-27632 was added to the conditioned medium and it was filtered and frozen at -80°C for future use. Basal airway epithelial cells expressing integrin α6 and CK5 could be isolated in 3T3-J2-conditioned medium containing 5 μM Y-27632 (Figure 5.3A and 5.3D) with the same (in the case of endobronchial brushings) or slightly lower (in the case of biopsy or digested biopsy samples) culture success rates than direct 3T3+Y co-culture (Figure 5.3B). Similar numbers of epithelial cells grew from biopsy explants or brushings in CM+Y compared with 3T3+Y. Interestingly, significantly fewer cells grow from digested biopsies when they were plated in CM+Y than when in 3T3+Y, suggesting that the full effect of co-culture is not replicated by the conditioned medium approach (Figure 5.3C).

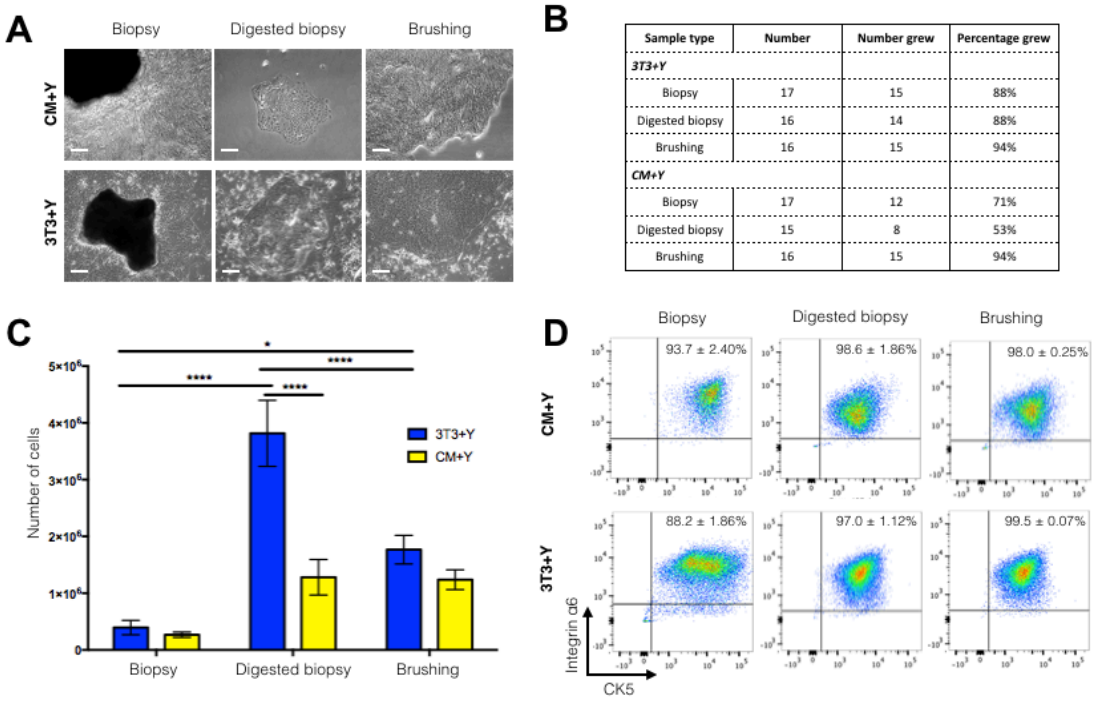

Sample type	Number	Number grew	Percentage grew
3T3+Y			
Biopsy	17	15	88%
Digested biopsy	16	14	88%
Brushing	16	15	94%
CM+Y			
Biopsy	17	12	71%
Digested biopsy	15	8	53%
Brushing	16	15	94%

Figure 5.3: Comparison of epithelial cell outgrowth from endobronchial biopsy samples and brushings in 3T3+Y and using 3T3-J2 feeder cell-conditioned medium. A) Brightfield images show successful epithelial cell outgrowth from explant endobronchial biopsy, enzymatically digested biopsy and endobronchial brushing samples. Scale bar = 50 µm. B) Comparison of culture success rate in either 3T3+Y co-culture with ROCK inhibition (3T3+Y) or using 3T3-J2-conditioned medium (CM+Y). C) Comparison of epithelial cell numbers generated after 12 days of culture in either 3T3+Y direct co-culture or 3T3-J2-conditioned medium. Statistical analysis was performed using a two-way ANOVA with Bonferroni post-test; mean +/- SEM; * indicated $p < 0.05$, **** $p<0.0001$; n = 8-14. D) Flow cytometric analysis shows that integrin α6- and CK5-expressing basal epithelial cells are expanded in all of these conditions.

Having isolated airway basal cells from biopsies, digested biopsies and brushings in 3T3+Y or in 3T3-J2-conditioned medium, these cells were passaged to confirm that further expansion was possible in line with previous findings using BEGM-isolated basal cells. Cells in all conditions could be expanded at passage one and colonies appeared morphologically similar, although some epithelial cells began to appear larger and flatter in 3T3-J2-conditioned medium, suggesting that the culture may not be as 'healthy' as that in 3T3+Y co-culture (Figure 5.4A). Passage one cells maintained their expression of the basal cell markers integrin α6 and CK5 (Figure 5.4B) and cells isolated and cultured in 3T3+Y co-culture maintained a proliferative advantage over those isolated and cultured in 3T3-J2-conditioned medium (Figure 5.4C).

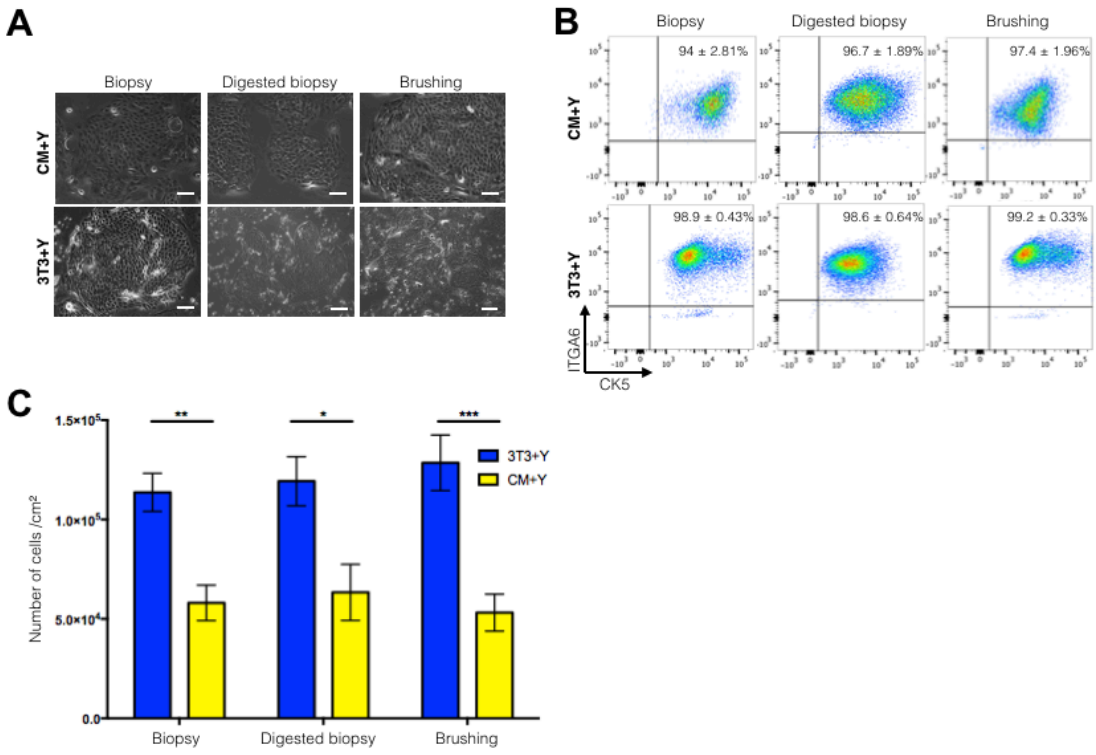

Figure 5.4: Comparison of epithelial cell expansion after passage in 3T3+Y and using 3T3-J2 feeder cell-conditioned medium. A) Brightfield images show the similar morphology of epithelial cells grown in 3T3-J2 co-culture (3T3+Y) and in 3T3-J2-conditioned medium (CM+Y) after one passage. Scale bar = 50 µm. B) Flow cytometric analysis confirms the maintenance of integrin α6 and cytokeratin 5 (CK5) expression in all conditions after one passage. C) Summary data show the increased number of cells generated from direct 3T3-J2 co-culture compared with culture in 3T3-J2-conditioned medium. Statistical analysis was performed using a two-way ANOVA with Bonferroni post-test; mean +/- SEM; * indicates $p < 0.05$; ** $p = 0.01$, **** $p<0.0001$; n = 6-13.

These conditioned medium experiments suggested that cell-cell contact between 3T3-J2 feeder cells and airway epithelial cells is necessary for the maximal proliferative effect of co-culture. This was in contrast to experiments performed in epidermal keratinocytes that suggest that secreted factors mediate the full effect of 3T3-J2 feeder cells and that cell-cell contact is not necessary [278]. To clarify this, the colony-forming efficiency of matched epithelial cells was compared when 3T3-J2s were in direct co-culture, 3T3-J2 cells were physically separated from epithelial cells by a transwell membrane or 3T3-J2-conditioned medium was used [279]. Results demonstrated that, while conditioned medium did allow the formation of epithelial colonies, it was less efficient than either condition in which 3T3-

J2 feeder cells were present (Figure 5.5). The similarity in the number of colonies formed in the conditions in which epithelial cells were in direct contact with the epithelial cells and in which they were separated by a transwell membrane supports the conclusion that diffusible factors co-operate with ROCK inhibition to improve epithelial cell expansion [278]. However, the difference between the number of epithelial cell colonies generated in 3T3-J2-conditioned medium and in cultures in which transwell separation was used implies that epithelial cells require a continuous supply of feeder cell factor(s), which was not recreated by the 3T3-J2-conditioned medium culture, in which cells were re-fed every two days. An interesting future experiment could demonstrate this conclusively by design of a bioreactor system in which epithelial growth medium flows across 3T3-J2 feeder cells in one chamber and then feeds epithelial cells in a physically separate adjacent chamber.

Overall, alternative adult human feeder cells that could be used in an autologous manner in patients were unable to recapitulate the effect of 3T3-J2 mouse embryonic feeder cells on the growth of airway basal cells. However, expanding epithelial cells from endobronchial biopsies and brushing samples directly in 3T3+Y, rather than initially in BEGM as previously has been done, allowed a further reduction in epithelial cell culture time. Additionally, a continuous supply of 3T3-J2 feeder cell-secreted factors appeared to be critical for the improvement in epithelial cell expansion.

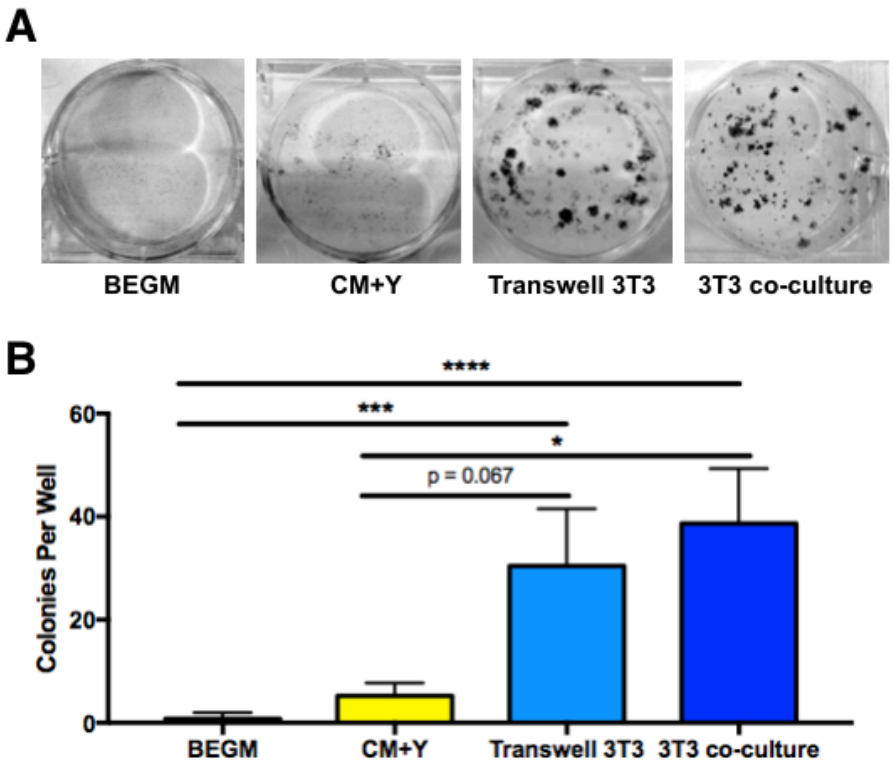

Figure 5.5: Colony-forming experiments reveal that a secreted factor mediates the effects of 3T3-J2 feeder cells on human epithelial cells. A) Representative images of colony-forming experiments comparing the effect of 3T3-J2-conditioned medium (CM+Y), co-culture with 3T3-J2 feeder cells physically separated from human epithelial cells by a transwell system and direct co-culture of 3T3-J2 feeder cells and human epithelial cells. B) Summary data of colony-forming experiments (3 donors repeated in triplicate; mean +/- SD). Statistical analysis was performed using a one-way ANOVA with Bonferroni post-test; mean +/- SEM; * indicates $p < 0.05$; *** $p = 0.001$, **** $p<0.0001$; n = 6-13.

5.4 Summary

- Feeder layers consisting of allogeneic human bone marrow MSCs or human lung fibroblasts do not successfully recreate the co-culture conditions provided by 3T3+Y.
- Human airway basal cells can be expanded by plating endobronchial biopsy samples directly in 3T3+Y.
- Plating single cell suspensions from either digested endobronchial biopsy samples or from endobronchial brushings in 3T3+Y expands the greatest number of epithelial cells in the shortest time.
- Although the remarkable effects of 3T3+Y are mediated by factors secreted by 3T3-J2 fibroblasts, 3T3-J2-conditioned medium could not fully recreate the effect of co-culture.

6 . Stromal-epithelial crosstalk between co-cultured 3T3-J2 fibroblasts and primary human basal cells

6.1 Background

Having established a methodology to expand large numbers of primary human airway epithelial cells using 3T3-J2 co-culture, I sought to characterise stromal-epithelial cell interactions during co-culture with a view to understanding their molecular basis. Data from Chapter 5 show that 3T3-J2 feeder cells mediate their effects through a secreted factor; however, the identity of this factor(s) remains unclear. Understanding the mechanisms underlying the effects of 3T3-J2 co-culture is important for several reasons. First, knowledge of the factor(s) that mediate the effects of 3T3-J2 fibroblasts would offer the potential to manufacture a medium containing the relevant factor(s) and to use this instead of 3T3-J2 co-culture to expand airway epithelial cells. This would be useful for epithelial cell research in general as it would remove the need to maintain 3T3-J2s and to differentially trypsinise them to avoid the risk of them contaminating downstream assays. In addition, it would be really useful for expanding epithelial cells for tissue-engineering applications as replacing the 3T3-J2 feeder layer with a defined medium would be much more compliant with good manufacturing practices. Second, understanding how 3T3-J2 feeder cells confer increased stem cell capacity and growth potential to epithelial cells may give clues as to the mechanisms behind stromal and epithelial cell crosstalk *in vivo*.

Despite many decades of research using 3T3-J2 co-culture to expand human epidermal keratinocytes *in vitro* [190], the factor(s) responsible for their remarkable effects on stem cell maintenance are still not completely understood and feeder-free alternative culture systems are still not able to replace feeder cells using defined factors [280]. I sought to characterise the nature of 3T3-J2 support for primary human airway basal cells and to identify factors from fibroblast feeder cells that affect epithelial cells. While not prohibitive,

co-culture with xenogeneic cells is not ideal for clinical translation of this culture system and understanding the signalling pathways involved might allow us to replace co-culture with an equally effective defined medium.

6.2 Aims

- To investigate the receptors that are activated on airway epithelial cells in response to the factors secreted by 3T3-J2 cells.
- To investigate the nature of feeder cell secretions that signal to airway epithelial cells in co-culture.
- To identify the downstream signalling pathways that are responsible for the 3T3-J2-secreted factor(s)'s mode of action.
- To investigate whether the growth advantages conferred on airway epithelial cells by co-culture with 3T3-J2 feeder cells can be reversed by inhibition of these signalling pathways.

6.3 Results

The HGF receptor, MET, is activated by 3T3-J2-conditioned medium

As the effects of 3T3-J2 cells appear to be mediated by secreted factors, a receptor tyrosine kinase activation array [281] was performed on primary human basal epithelial cells stimulated with medium conditioned by 3T3-J2 fibroblasts. Strong activation of the epidermal growth factor receptor (EGFR) and the insulin-like growth factor 1 receptor (IGF1R) was observed in cells stimulated with both base medium and conditioned medium, consistent with the inclusion of EGF and insulin in the base medium (Figure 6.1A). However, we found that the hepatocyte growth factor receptor (HGFR/MET) was strongly activated by conditioned medium but not by base medium alone (Figure 6.1A). MET activation by 3T3-J2-conditioned medium was validated by western blot, analysing three phosphorylation sites: tyrosine 1003 (Y1003), which leads to receptor ubiquitination and recycling via endosomal pathways [282], and Y1234/Y1235, which lies within the activation loop of MET's tyrosine kinase domain, were strongly phosphorylated, while Y1349, an autophosphorylation site (Figure 6.1B) that generates a multisubstrate-docking site [283], showed less marked phosphorylation (Figure 6.1C).

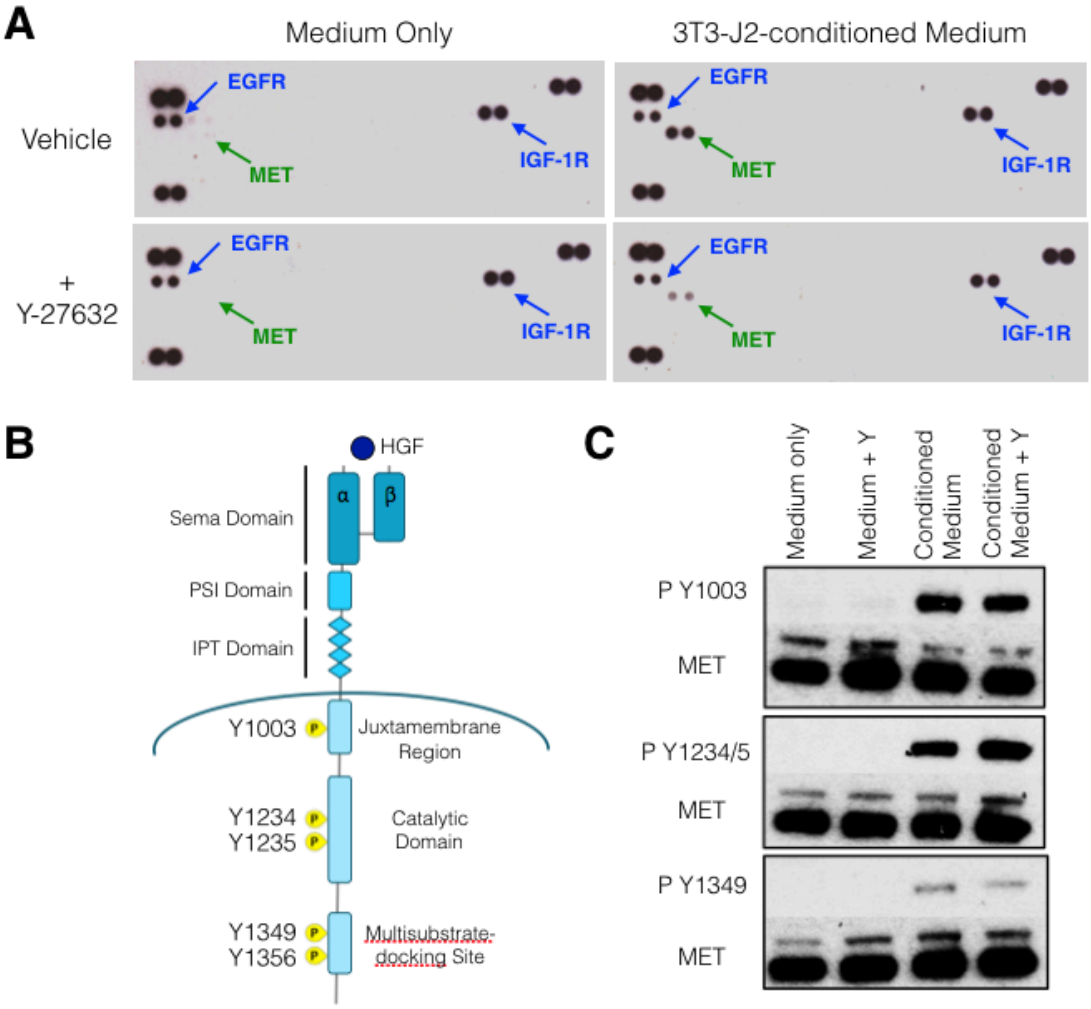

Figure 6.1: Activation of the HGF receptor, MET, by 3T3-J2-conditioned medium. A) Receptor tyrosine kinase array analysis of primary human airway epithelial cells stimulated for 30 minutes with 3T3-J2 feeder cell-conditioned medium. Specific activation of the hepatocyte growth factor (HGF) receptor, MET, on Y1234/Y1235 was observed in cells stimulated with 3T3-J2-conditioned medium both in the presence or in the absence of Rho-associated protein kinase (ROCK) inhibition using Y-27632. B) Schematic representation of MET receptor structure showing relevant phosphorylation sites. C) Western blot confirmation in independent lysates of MET phosphorylation following stimulation of primary human airway epithelial cells with 3T3-J2 feeder cell-conditioned medium for 30 minutes.

Having established that MET is phosphorylated in response to 3T3-J2-conditioned medium, I hypothesised that HGF, the ligand for MET, may be the 3T3-J2-secreted factor that confers increased growth potential in airway epithelial cells. Consistent with HGF-mediated crosstalk between fibroblasts and epithelial cells, the amount of HGF secreted into culture medium by feeder cells increased over time following mitotic inactivation (Figure 6.2A) and the amount of HGF mRNA in 3T3-J2 cells also increased during the first 24 hours following mitotic inactivation (Figure 6.2B).

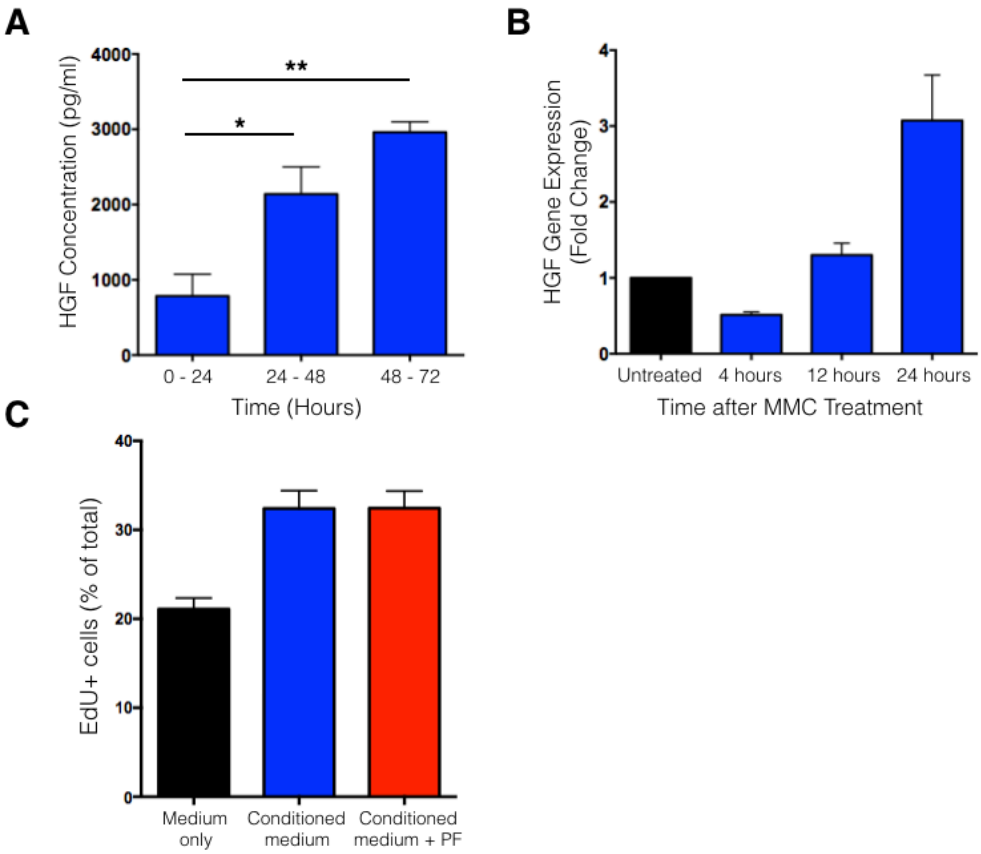

Figure 6.2: HGF is produced by 3T3-J2 feeder cells following mitotic inactivation but does not affect human airway basal cell proliferation. A) ELISA quantification of hepatocyte growth factor (HGF) secreted into culture medium by 3T3-J2 feeder cells following mitotic inactivation with mitomycin C (MMC). Medium was collected and replaced with fresh medium after 24 and 48 hours (n = 4; mean +/- SEM; * indicates $p < 0.05$, ** indicates $p < 0.01$). B) Quantification of HGF mRNA levels in 3T3-J2 feeder cells following mitotic inactivation with mitomycin C. (n = 3; mean +/- SEM). C) Flow cytometric analysis of EdU uptake in primary human airway epithelial cells treated with either epithelial culture medium alone, 3T3-J2-conditioned epithelial growth medium or the same medium containing 100 nM PF-0421903, a small molecule MET inhibitor (n = 3; mean +/- SEM).

Murine HGF activates intracellular signalling but does not affect basal cell proliferation

Previous work suggests that murine HGF does not exert biological effects in human cells as a result of a failure to initiate autophosphorylation of the multisubstrate-docking site [284]. To investigate whether this was true in our co-culture system, I investigated proliferation of airway epithelial cells by analysing EdU incorporation. 3T3-J2-conditioned medium induced an increase in the proliferation of epithelial cells compared with medium alone, which is consistent with data in Chapter 4 showing that 3T3-J2 co-culture increases the proliferation of epithelial cells. Consistent with the idea that murine HGF does not have an effect in human cells, I discovered that inhibition of MET, using the small molecule MET inhibitor PF-04217903 [248], did not reduce the increased epithelial cell proliferation induced by 3T3+Y-conditioned medium (Figure 6.2C).

However, upon investigation of the phosphorylation status of MET downstream effector proteins such as focal adhesion kinase (FAK; Figure 6.3A) and GRB2-associated-binding protein 1 (GAB1; Figure 6.3B), I identified phosphorylation sites that were activated by 3T3-J2-conditioned medium, hinting that a subset of intracellular MET signalling events might continue as a result of stimulation of the human MET receptor with murine HGF. Focal adhesion kinase was not investigated further as the phosphorylation site that appeared to be activated was a higher molecular weight than the total FAK protein (middle band in phospho-Y925 blot; Figure 6.3A and 6.3C). I was, however, able to identify the phosphorylated protein apparent in GAB1 blots as the related adapter protein GAB2 (Figure 6.3C); a finding that resulted from antibody cross-reactivity. As GAB2 is known to phosphorylate and activate the transcription factor signal transducer and activator of transcription 6 (STAT6) in differentiated airway goblet cells [285], the phosphorylation status of STAT6 in response to stimulation with 3T3-J2-conditioned medium was determined.

STAT6 was robustly phosphorylated in epithelial cells treated with conditioned medium with and without the ROCK inhibitor, while no STAT6 phosphorylation was observed in cells treated with medium only (Figure 6.3C). Importantly, the phosphorylation events of FAK, GAB2 and STAT6 were reversible by inhibition of MET using PF-04217903 (Figure 6.3C), suggesting that HGF is the factor responsible for activation of these proteins and that, although it is not responsible for the increased epithelial cell proliferation induced by 3T3-J2 co-culture, it might induce some functional response in epithelial cells.

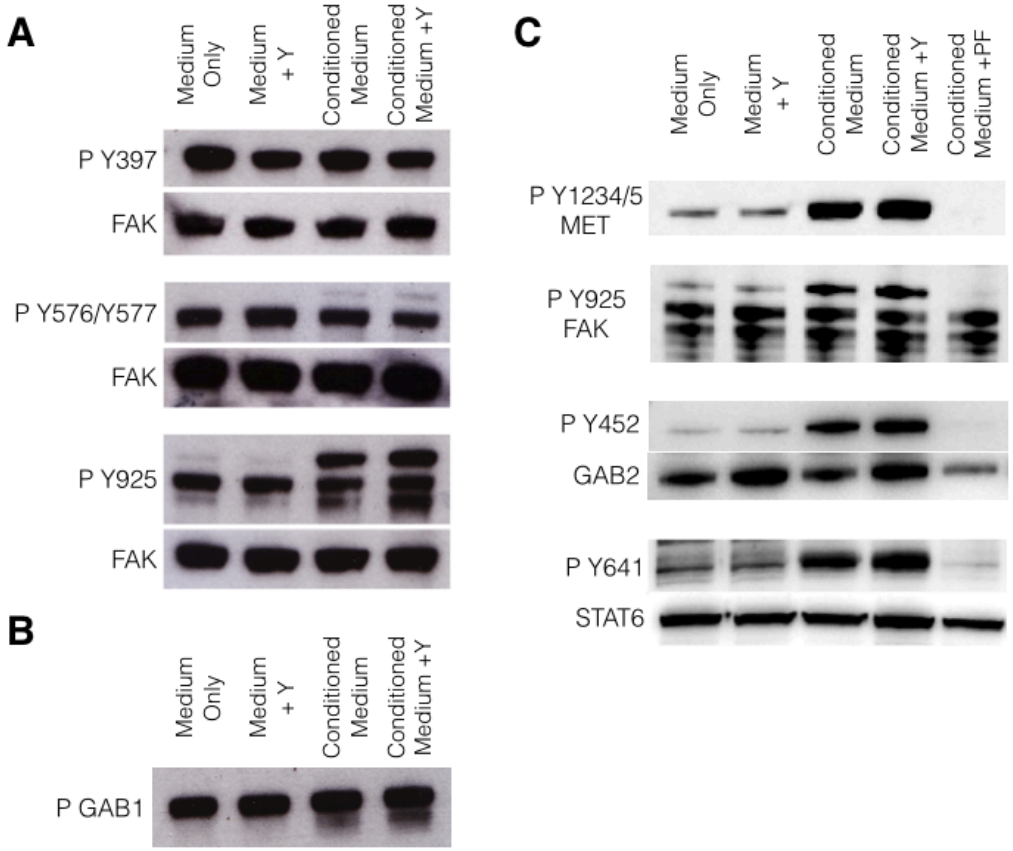

Figure 6.3: Activation of signalling pathways downstream of MET in human airway epithelial cells following stimulation with 3T3-J2-conditioned medium. A) Western blot analysis of focal adhesion kinase (FAK) phosphorylation following stimulation of human airway epithelial cells with 3T3-J2-conditioned medium for 30 minutes. B) Western blot analysis of GRB2-associated-binding protein 1 (GAB1) phosphorylation status following stimulation of human airway epithelial cells with 3T3-J2-conditioned medium for 30 minutes. C) Western blot analysis of MET, FAK, GAB2 and signal transducer and activator of transcription 6 (STAT6) phosphorylation status following stimulation of human airway epithelial cells with 3T3-J2-conditioned medium for 30 minutes in the presence of 100 nM PF-04217903, a small molecule MET inhibitor.

Human HGF phosphorylates STAT6 in human airway basal cells

The phosphorylation events described above could be explained by the presence of co-factors in conditioned medium or by the non-physiological action of murine HGF on the human MET receptor. To address this point, the same phosphorylation sites of MET, GAB2 and STAT6 were investigated in cells stimulated with recombinant human HGF. All sites were phosphorylated, including the autophosporylated multisubstrate-docking domain that was inefficiently activated by murine HGF in 3T3-J2-conditioned medium (Figure 6.4A). GAB2 and STAT6 activation in response to human HGF was dependent on MET as PF-0421903 again prevented their activation (Figure 6.4B). Experiments were initially performed using a high concentration of 50 ng/ml HGF but a titration of recombinant HGF concentration revealed that STAT6 was phosphorylated by concentrations of HGF above 5 ng/ml (Figure 6.4C). Phosphorylation of MET, GAB2 and STAT6 was maximal around 30 minutes following stimulation with HGF and was sustained for approximately 8 hours but had disappeared by 24 hours (Figure 6.5). Given the similarity of the timecourses for MET, GAB2 and STAT6, it is likely that availability of recombinant protein in the medium is the limiting factor causing the cessation of signalling (Figure 6.5).

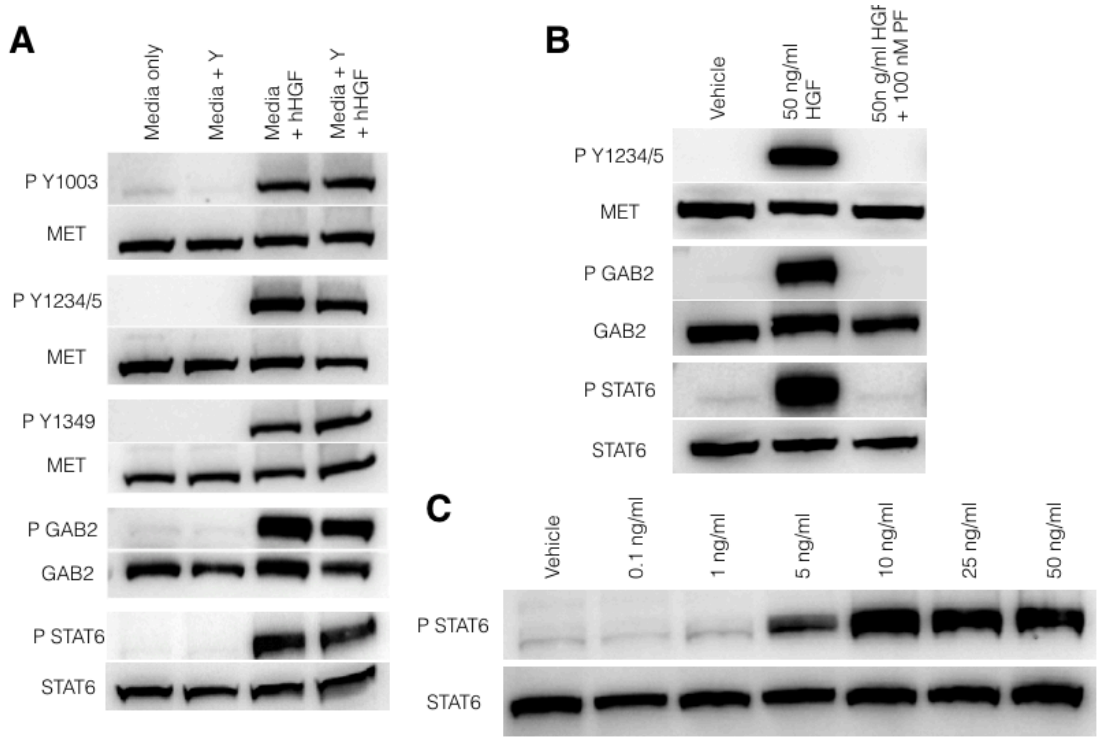

Figure 6.4: Phosphorylation of MET, GAB2 and STAT6 in response to recombinant human HGF. A) Western blot analysis of MET, GRB2-associated-binding protein 2 (GAB2) and signal transducer and activator of transcription 6 (STAT6) phosphorylation status in human airway epithelial cells stimulated with 50 ng/ml recombinant human hepatocyte growth factor (HGF) for 30 minutes. B) Western blot analyisis of MET, GAB2 and STAT6 phosphorylation status following stimulation of human airway epithelial cells with 50 ng/ml recombinant human HGF for 30 minutes in the presence of 100 nM PF-04217903, a small molecule MET inhibitor. C) Western blot analysis of STAT6 phosphorylation status in response to various doses of recombinant human HGF for 30 minutes.

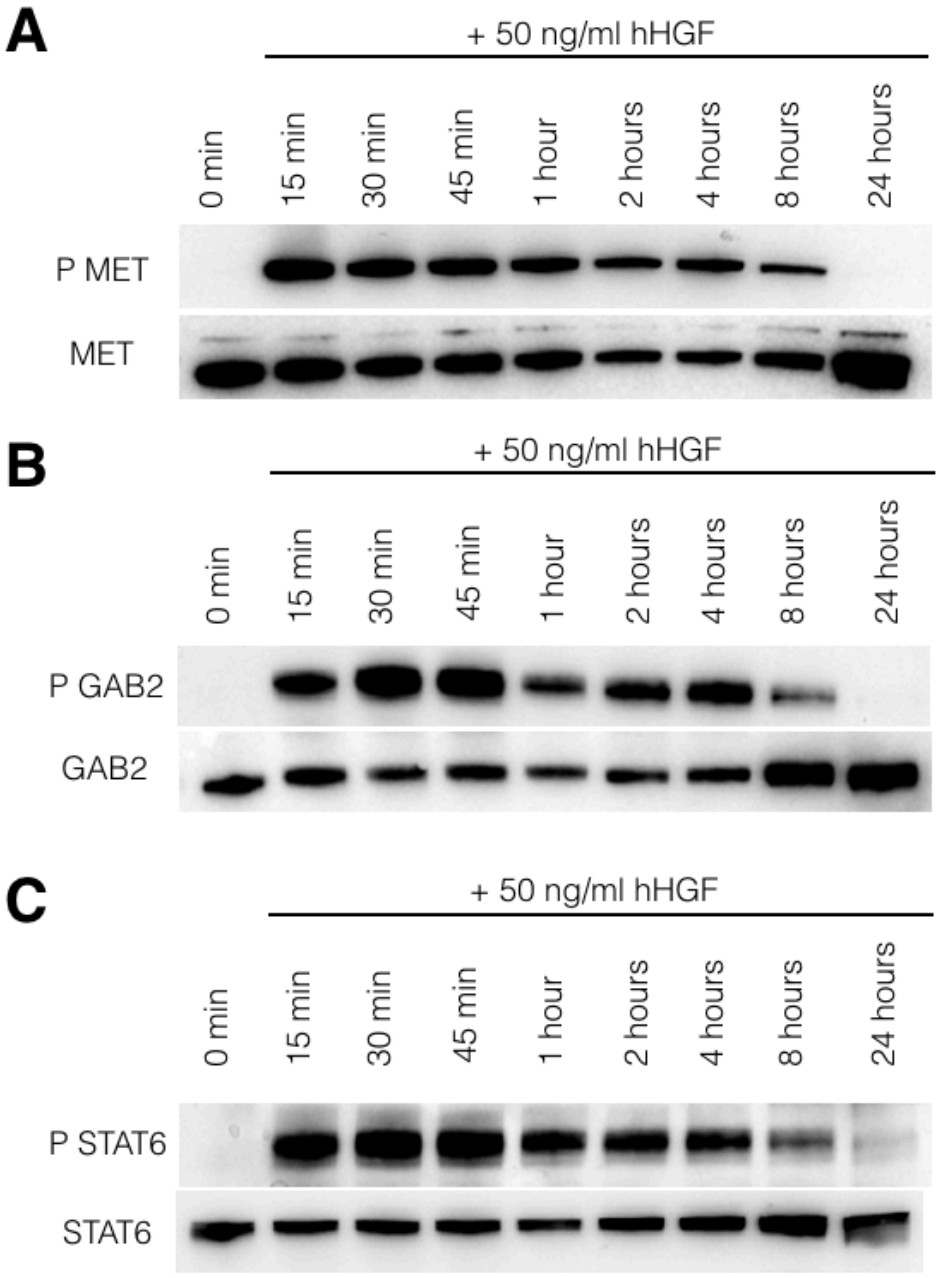

Figure 6.5: Timecourse of MET, GAB2 and STAT6 phosphorylation in human airway epithelial cells in response to recombinant human HGF. A) Western blot analysis of the phosphorylation status of MET over time following stimulation with 50 ng/ml recombinant human hepatocyte growth factor (HGF). B) Western blot analysis of the phosphorylation status of GRB2-associated-binding protein 2 (GAB2) over time following stimulation with 50 ng/ml recombinant human HGF. C) Western blot analysis of the phosphorylation status of signal tranducer and activator of transcription 6 (STAT6) over time following stimulation with 50 ng/ml recombinant human HGF.

HGF-induced STAT6 phosphorylation is not dependent on GAB2

Although cooperation between interleukin-4 (IL-4)/IL-13-driven STAT6 activation and MET signalling has previously been shown [286], the direct activation of STAT6 in response to HGF is novel so I next examined the mechanism of STAT6 activation. A previous report that GAB2 phosphorylates STAT6 downstream of IL-13 in airway epithelia [285] prompted the investigation of a MET-GAB2-STAT6 pathway, in which MET phosphorylates GAB2, which results in the phosphorylation of STAT6. I used siRNA to knock down GAB2 in airway epithelial cells. 3 nM siRNA caused some knowndown of GAB2 compared with non-silencing siRNA, but expression was almost entirely knocked down with 5 nM siRNA (Figure 6.6A) so this concentration with used for subsequent studies. Interestingly, knockdown of GAB2 using siRNA did not affect MET-induced STAT6 activation (Figure 6.6B), suggesting that phosphorylation of STAT6 is not dependent on GAB2.

As STAT3 binds directly to the MET receptor via its SH2 domain [287, 288] and STAT6 also contains an SH2 domain [289], co-immunoprecipitation experiments were performed to determine whether STAT6 binds to MET following the phosphorylation induced by stimulation with HGF. Successful pull-down of MET was achieved, as MET can clearly be seen in the immunoprecipitation fraction but not in the supernatant. However, neither STAT6 nor phosphorylated STAT6 could be detected in MET pull-downs (Figure 6.6C), suggesting that no complex of MET and STAT6 exists following stimulation with HGF.

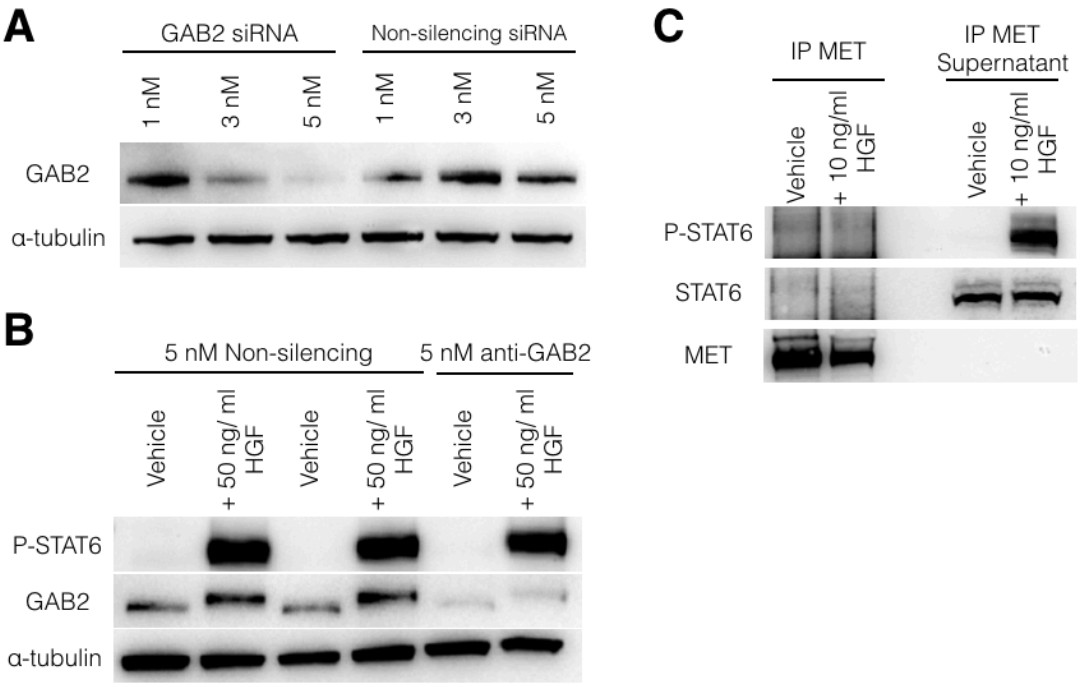

Figure 6.6: Investigation of the mechanism of HGF-induced STAT6 phosphorylation in human airway epithelial cells. A) Western blot analysis showing knockdown of GRB2-associated-binding protein 2 (GAB2) using 5 nM anti-GAB2 siRNA compared with non-silencing RNA. α-tubulin was used as a loading control. B) Western blot analysis of signal transducer and activator of transcription 6 (STAT6) phosphorylation status in cells treated with either 5 nM non-silencing siRNA or 5 nM anti-GAB2 siRNA. Unstimulated primary human airway epithelial cells were compared to matched cells stimulated with 50 ng/ml recombinant human hepatocyte growth factor (HGF). C) Western blot analysis of co-immunoprecipitation experiment. Unstimulated primary human airway epithelial cells were compared to matched cells stimulated with 10 ng/ml recombinant human HGF. MET was immunoprecipitated using Dynabeads and the supernatant retained. STAT6 was not co-immunoprecipitated with MET but was instead found in the unbound protein fraction.

HGF promotes GM-CSF and IL-8 secretion from human airway basal cells

As STAT6 controls the transcriptional response of epithelial cells following stimulation with IL-4 or IL-13 [290], the effect of HGF-induced STAT6 signalling on airway basal cell cytokine secretion was analysed using an array panel. Increased secretion of the neutrophil chemoattractants granulocyte/macrophage colony-stimulating factor (GM-CSF) and IL-8 [291, 292] was found following stimulation with HGF (Figure 6.7A). Interestingly, baseline secretion was restored in the presence of the MET inhibitor PF-0421903 or the STAT6 small molecule inhibitor AS-1517499 (Figure 6.7A) [293, 294]. These results were confirmed by ELISA in additional human donor cell cultures and the same pattern of secretion was observed (Figure 6.7B). At the level of gene expression, HGF treatment of serum-starved human airway basal cells causes upregulation of transcription of both GM-CSF (Figure 6.7C) and IL-8 (Figure 6.7D) and STAT6 inhibition appeared to cause a dose-dependent decrease in the expression of both of these genes (Figure 6.7C and 6.7D). Taken together, these results suggest that phosphorylation of MET and STAT6 following stimulation with HGF induces an increase in the expression and secretion of IL-8 and GM-CSF.

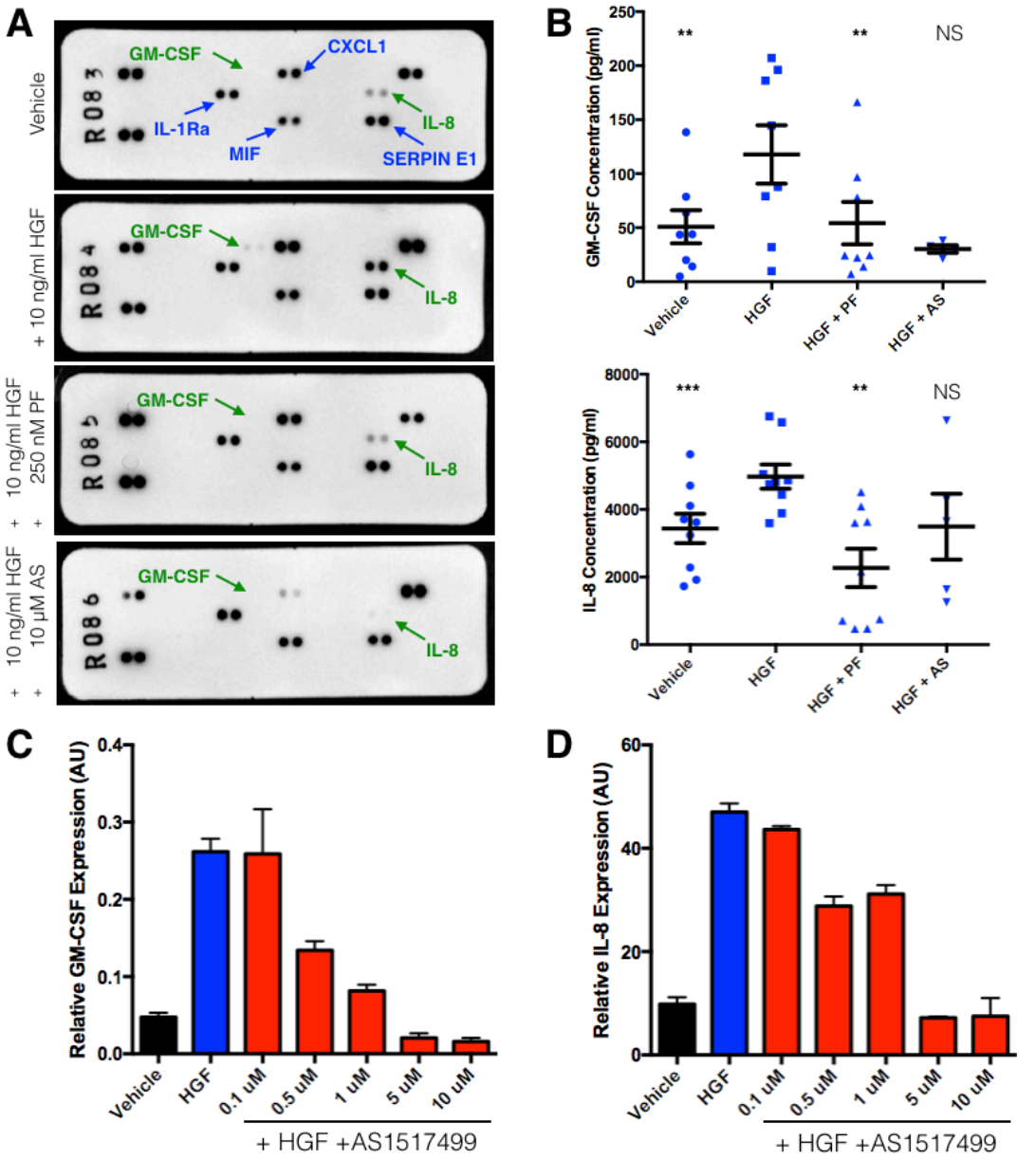

Figure 6.7: HGF causes an increase in the transcription and the secretion of GM-CSF and IL-8 in cultured human airway epithelial cells. A) Cytokine array analysis of primary human airway epithelial cells stimulated with either vehicle control, 10 ng/ml recombinant human hepatocyte growth factor (HGF), 10 ng/ml recombinant human HGF and 250 nM PF-04217903 (a MET inhibitor) or 10 ng/ml recombinant human HGF and 10 µM AS-1517499 (a STAT6 inhibitor). B) ELISA quantification of granulocyte/macrophage colony-stimulating factor (GM-CSF; upper) and interleukin-8 (IL-8; lower) secretion into culture medium in independent primary human airway epithelial cell cultures stimulated with either vehicle control, 10 ng/ml recombinant human HGF, 10 ng/ml recombinant human HGF and 250 nM PF-04217903 or 10 ng/ml recombinant human HGF and 10 µM AS-1517499 (n = 4-9 donors; mean +/- SEM). Statistical analysis was performed using a one-way ANOVA (with Bonferroni's post-test) comparing each group with HGF-treated cells; ** indicates $p < 0.01$, *** indicates $p < 0.001$. C) qPCR quantification of GM-CSF gene expression in primary human airway epithelial cells following stimulation with 10 ng/ml recombinant human HGF and various doses of AS-1517499 (n = 1 donor performed in technical triplicate; mean +/- SEM). D) qPCR quantification of IL-8 gene expression in primary human airway epithelial cells following stimulation with 10 ng/ml recombinant human HGF and various doses of AS-1517499 (n = 1 donor performed in technical triplicate; mean +/- SEM).

HGF-induced IL-8 expression is STAT6 independent

To confirm that induction of STAT6-dependent transcription is indeed induced by HGF stimulation, I established a luciferase reporter assay. As reporter assays are well established in cancer cell lines in our laboratory, the utility of using cancer cell lines as a system to study HGF-dependent STAT6-dependent transcription was investigated. HGF caused STAT6 phosphorylation in both A549 (lung adenocarcinoma) and A431 (epidermoid carcinoma) cancer cell lines but did not phosphorylate STAT6 in human lung fibroblasts (Figure 6.8A); these were included as a control due to their lack of expression of the HGF receptor MET [295]. These results show that HGF-dependent STAT6 phosphorylation is not restricted to primary airway epithelial cells but is also true for at least A549 and A431 cancer cell lines. These results also suggested that a cancer cell line could be used to further investigate STAT6-dependent transcription instead of primary airway epithelial cells. To do so, a STAT6 consensus sequence luciferase reporter vector – p4xSTAT6-Luc2P – was used. This construct contains four tandem repeats of STAT6/cEBP-binding sites (TTCN4GAA) from the human germline ε promoter sequence upstream of the luciferase gene. A431 cells transfected with this STAT6 luciferase reporter plasmid were incubated with either a vehicle control, 50 ng/ml recombinant human HGF or 50 ng/ml recombinant human IL-13, which was used as a positive control given that IL-13 is known to have a role in activating STAT6-dependent transcription in epithelial cells [59, 296]. After 3 hours, the activity of the luciferase reporter was assayed using a luminometer. Results showed that stimulation of cells with IL-13 induced strong expression of luciferase, while recombinant human HGF had no effect on the expression of luciferase (Figure 6.8B), indicating that HGF does not activate STAT6-dependent transcription at this time point. To ensure that HGF-induced STAT6 transcription does not occur at an earlier time point, this experiment was repeated at four earlier time points. IL-13 induced luciferase expression after 15 minutes but no induction of luciferase

expression was seen in response to HGF stimulation in any of the time points investigated (Figure 6.8C).

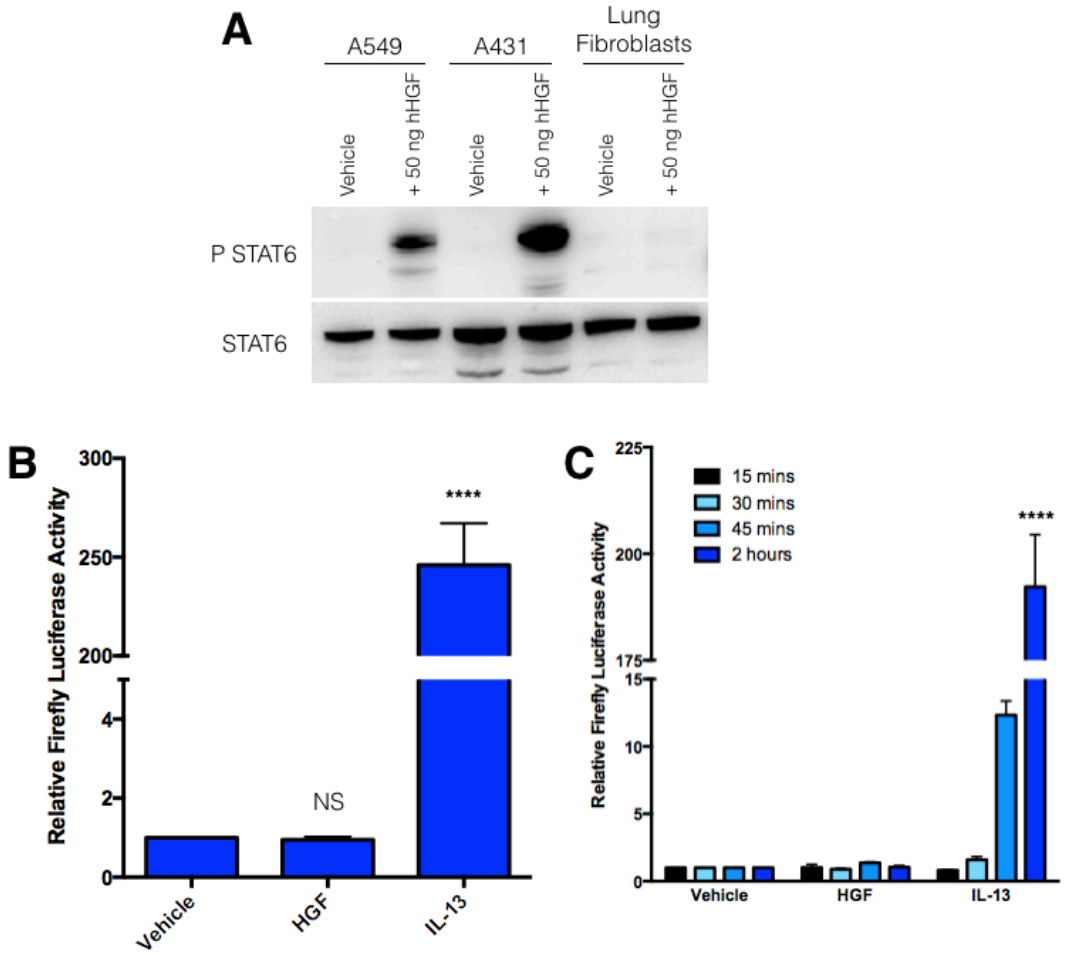

Figure 6.8: Establishment of a firefly luciferase STAT6 reporter assay in A431 cancer cells. A) Western blot analysis of STAT6 phosphorylation in the A549 cancer cell line, the A431 cancer cell line and primary human lung fibroblasts following stimulation with 50 ng/ml recombinant human hepatocyte growth factor (HGF). B) Quantification of firefly luciferase STAT6 reporter activity using luminescence in A431 cancer cells treated for 3 hours with either a vehicle control, 50 ng/ml recombinant human HGF or 50 ng/ml recombinant human interleukin-13 (IL-13). Values were normalised according to expression of a constitutively active renilla luciferase in order to account for variation in transfection efficiency. Statistical analysis comparing vehicle and HGF- or IL-13-treated groups was performed using a one-way ANOVA with Bonferroni post-test; n = 6 (mean +/- SEM); **** indicates P<0.0001. C) Quantification of firefly luciferase reporter STAT6 activity using luminescence in A431 cancer cells treated for 15 minutes, 30 minutes, 45 minutes or 2 hours with either a vehicle control, 50 ng/ml recombinant human HGF or 50 ng/ml recombinant human IL-13. Values were normalised according to expression of a constitutively active renilla luciferase in order to account for variation in transfection efficiency. Statistical analysis comparing vehicle and HGF- or IL-13-treated groups was performed using a two-way ANOVA with Bonferroni post-test; n = 3 (mean +/- SEM); unlabelled bars were not statistically significant, **** indicates P<0.0001.

These experiments contradicted earlier findings because STAT6 is robustly phosphorylated at Y641, the site associated with its dimerisation and translocation into the nucleus (that is, the activating phosphorylation site) [297], in response to HGF but does not activate STAT6-dependent transcription. In order to better understand what was happening, subcellular fractionation was established to cleanly resolve cytoplasmic and nuclear proteins (Figure 6.9A). This technique was then used to determine the location of STAT6 within cells following stimulation with either HGF or IL-13. This experiment revealed that either 30 minutes (Figure 6.9B) or 2 hours (Figure 6.9C) following stimulation, STAT6 was found in the nucleus of cells stimulated with IL-13 but remained in the cytoplasm of cells stimulated with HGF. Despite the presence of protease and phosphatase inhibitors, phosphorylated STAT6 was not detected well in these assays, presumably due to the different buffers used to process protein samples for subcellular fractionation but results for total STAT6 protein were conclusive. Interestingly, some STAT6 protein was seen in the nucleus of unstimulated cells, which is consistent with the fact that STAT6 is continually imported and exported out of the nucleus, independently of its phosphorylation status [298]. However, these results mean that it is unlikely that the inhibition of GM-CSF and IL-8 transcription seen previously with AS-1517499 is caused by on-target effects on STAT6 and suggest that induction of GM-CSF and IL-8 transcription in response to HGF is not STAT6 dependent. Indeed, these results suggest that alternative pathways are induced by HGF to cause GM-CSF and IL-8 transcription.

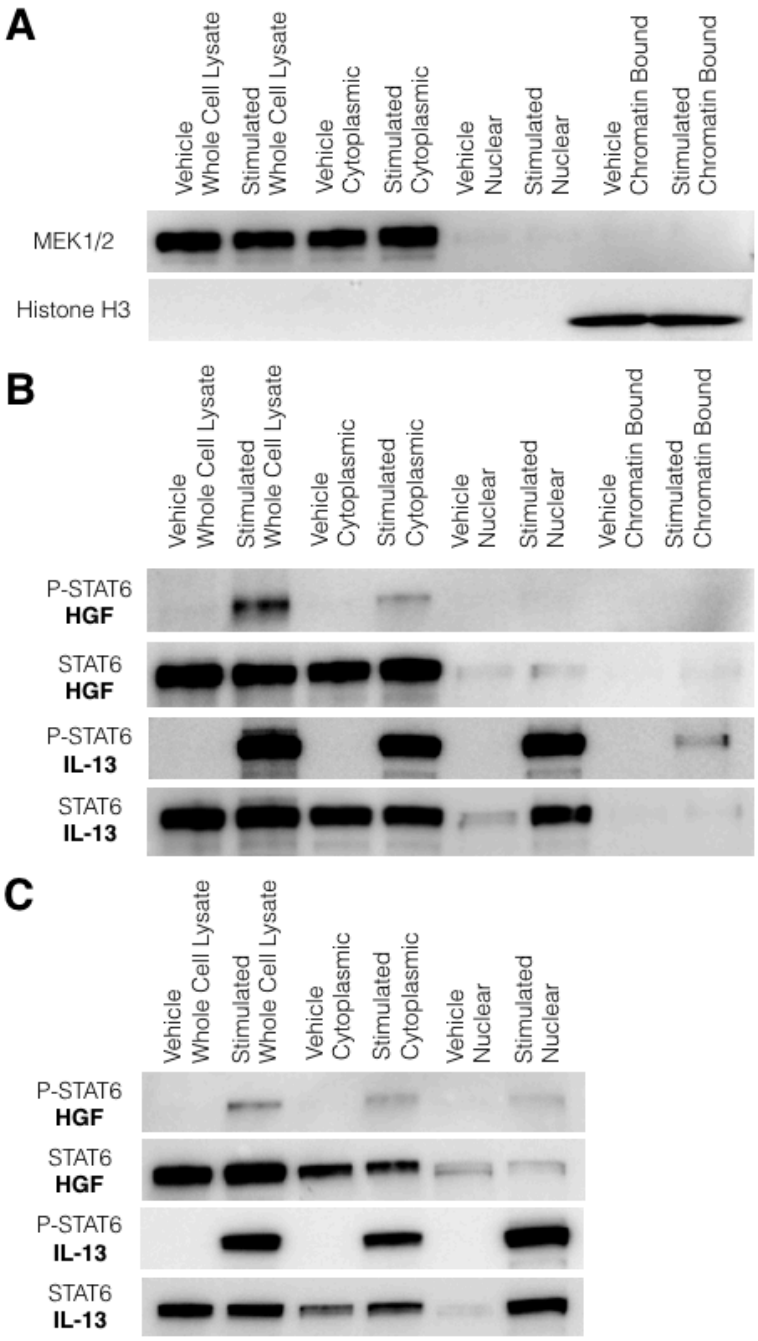

Figure 6.9: HGF causes the phosphorylation but not the nuclear translocation of STAT6. A) Western blot analysis of MEK1/2 (cytoplasmic) and histone H3 (nuclear and chromatin bound) in lysates processed using a subcellular fractionation kit to confirm that cytoplasmic, nuclear and chromatin-bound protein fractions were obtained. B) Western blot analysis of signal transducer and activator of transcription 6 (STAT6) phosphorylation status in primary human airway epithelial cells treated with either hepatocyte growth factor (HGF) or interleukin-13 (IL-13) for 30 minutes. Whole cell lysates were obtained using RIPA buffer and compared with independent lysates prepared using a subcellular fractionation kit. C) Western blot analysis of STAT6 phosphorylation status in primary human airway epithelial cells treated with either HGF or IL-13 for 2 hours.

Although results in Figure 6.9 suggest that induction of GM-CSF and IL-8 expression in response to HGF stimulation is not mediated by STAT6, previous experiments showed a downregulation of both GM-CSF and IL-8 protein (Figure 6.7A and 6.7B) and gene expression (Figure 6.7C and 6.7D) by the STAT6 small molecule inhibitor AS-1517499 following HGF stimulation. To reconcile these results, western blots were performed to investigate the phosphorylation status of MET and STAT6 in response to the 5 µM dose of AS-1517499 used in those experiments. These results show that MET phosphorylation itself is reduced by AS-1517499, suggesting that an off-target effect of this drug might be responsible for its apparent effect on GM-CSF and IL-8 expression, again indicating that the HGF-mediated induction of GM-CSF and IL-8 expression and secretion in epithelial cells is not dependent on STAT6.

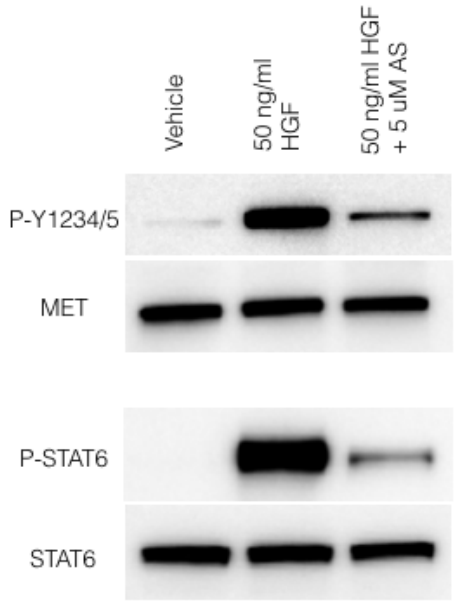

Figure 6.10: Non-specific inhibition of MET by the STAT6 inhibitor AS-1517499. Western blot analysis of MET and signal transducer and activator of transcription 6 (STAT6) phosphorylation status in primary human airway epithelial cells treated with a vehicle control, 50 ng/ml recombinant human hepatocyte growth factor (HGF) or 50 ng/ml recombinant human HGF and 5 µM AS-1517499 (a STAT6 inhibitor).

In order to investigate the requirements for IL-8 transcription in response to HGF, luciferase reporter constructs containing the IL-8 promoter were obtained. These plasmids include different lengths of the IL-8 promoter sequence such that the transcription factor-binding sites mediating transcriptional activation can be inferred [249, 250]. The -2000 construct includes IL-8 transcriptional regulatory elements including a STAT6 consensus sequence found 1850 bp upstream of the transcription start site [250]. Two truncated versions of this upstream region were analysed to tease out the transcriptional sites that mediate HGF-induced IL-8 transcription (Figure 6.11A). The -1400 plasmid lacks the STAT6-binding site but contains T-cell factor/lymphoid enhancer factor (TCF/LEF)-, interferon-regulatory factor 1 (IRF1)-, hepatocyte nuclear factor 1 (HNF1)- and glucocorticoid receptor (GR)-binding sites that are absent from the short -173 sequence, which contains activator protein 1 (AP-1)- and nuclear factor-κB (NF-κB*)*-binding domains (Figure 6.11B). Upon receipt of the plasmids from collaborators the inserts were checked by restriction enzyme digests, which demonstrated excised fragments of the predicted molecular weights (Figure 6.11C). A luciferase reporter assay using these plasmids showed that only stimulation of A431 cells transfected with the -173 IL-8 promoter sequence caused upregulation of luciferase activity following stimulation with HGF (Figure 6.11D). This result suggests that proximal transcription factors such as NF-κB and/or AP-1, which are known to respond to MET activation [299, 300], rather than STAT6, are candidate transcription factors responsible for the upregulation of IL-8 in primary human airway epithelial cells. Interestingly, they also suggest a possible repressive role for more distal transcriptional regulation in this process because although the -2000 and -1400 constructs contain the proximal sites, they did not respond significantly to HGF stimulation (Figure 6.11D).

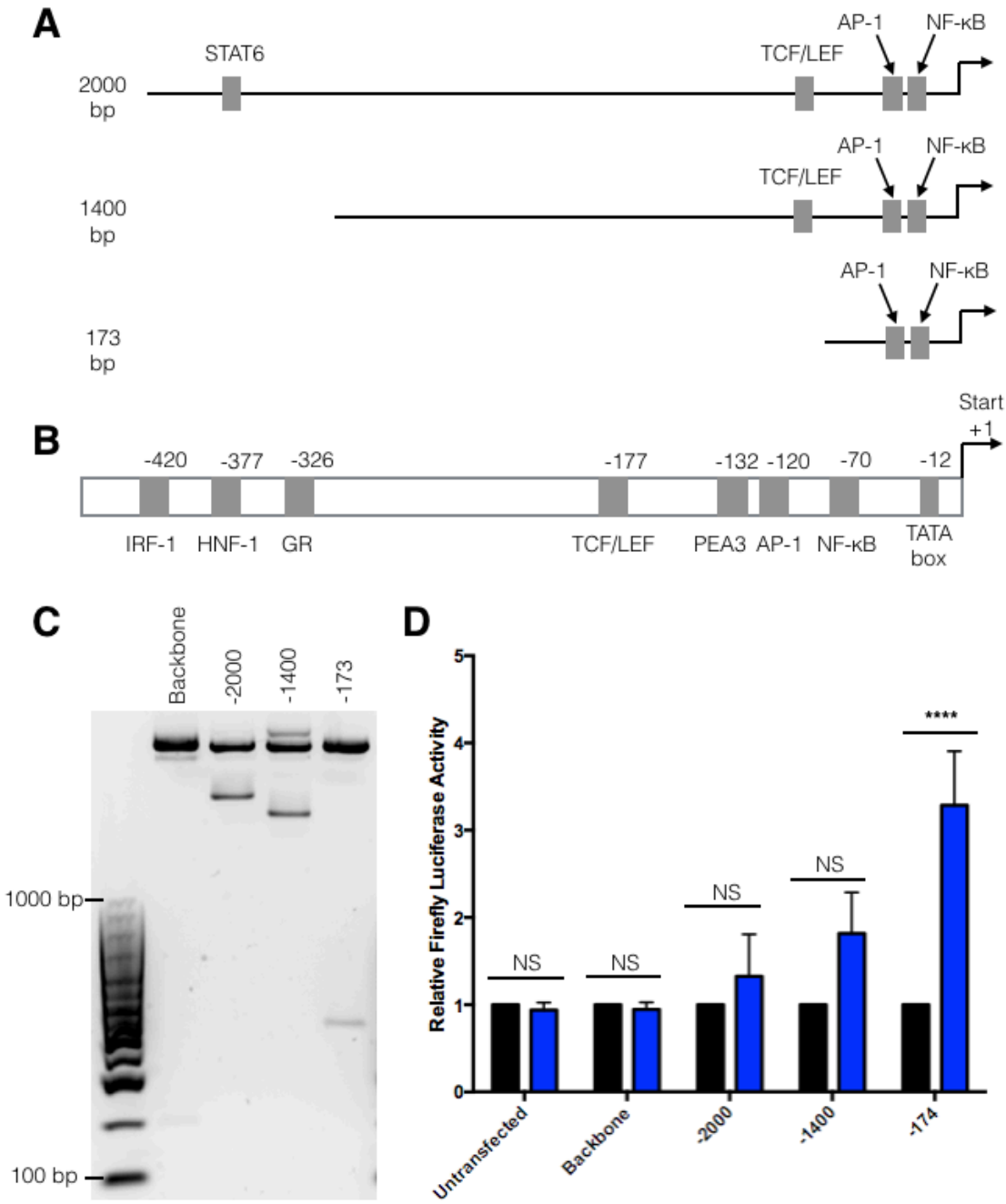

Figure 6.11: HGF-induced IL-8 transcription is mediated by NF-κB rather than by STAT6. A) Schematic representation of interleukin-8 (IL-8) promoter sequence firefly luciferase reporter constructs. B) Detailed schematic representation of the proximal promoter elements of IL-8. C) Validation of IL-8 promoter sequence plasmids by NotI and XhoI restriction enzyme digest. D) Quantification of firefly luciferase IL-8 promoter reporter activity using luminescence in A431 cancer cells treated for 30 minutes with either a vehicle control or 50 ng/ml recombinant human hepatocyte growth factor (HGF). Values were normalised according to expression of a constitutively active renilla luciferase in order to account for variation in transfection efficiency. Statistical analysis comparing vehicle and HGF-treated groups was performed using a two-way ANOVA with Bonferroni post-test; n = 3 (mean +/- SEM); **** indicates P<0.0001.

To conclude, murine HGF partially activates the human MET receptor but does not induce the increased proliferation that might be expected in human cells. However, phosphorylation of some substrates downstream of MET, including GAB2 and the novel MET target STAT6, occurs in response to both murine and human HGF. Human HGF also leads to phosphorylation of STAT6 downstream of the MET receptor but the functional relevance of this phosphorylation was not established as MET activation does not lead to transcriptional activation of STAT6-target genes. Furthermore, HGF-mediated upregulation of IL-8 was not dependent on STAT6.

6.4 Summary

- Our 3T3-J2 co-culture system was used to investigate stromal-epithelial cell interactions.
- HGF secreted from fibroblasts activates MET on human airway basal cells.
- MET activation leads to STAT6 phosphorylation but not to transcriptional activation of STAT6-target genes.
- MET signalling leads to the secretion of the potent neutrophil chemoattractants IL-8 and GM-CSF. HGF-induced IL-8 transcription occurs independently of STAT6.

7 . Conclusions and future directions

Limitations of traditional airway epithelial cell culture systems

The initial aim of this thesis was to investigate the suitability of protocols for human airway epithelial cell expansion for high-throughput *in vitro* assays relevant to drug screening, toxicology studies and personalised medicine [203] and for airway tissue-engineering applications [77]. Consistent with previous studies, epithelial cells expanded from bronchial biopsy samples using the established protocol for airway epithelial cell expansion, bronchial epithelial growth medium (BEGM), expressed basal stem cell markers [301] and were capable of differentiation at very early passages [222, 223]. However, a key early finding was that this protocol was largely unsuitable for our target studies.

BEGM protocols were initially developed using large cadaveric airway tissue samples [222] and in this work I showed that, even when cultures are initiated from the large numbers of airway epithelial cells that would be supplied by these samples, they are limited by diminishing proliferation over passage and by eventual senescence or terminal differentiation in these conditions [49, 117, 265, 267]. Previous studies demonstrate that the capacity of cultured basal cells to regenerate ciliated epithelium declines as a function of population doubling number [265]. Here, as cells were cultured from living patients through isolation of cells from endobronchial biopsy samples, the starting material necessarily contained a tiny fraction of the basal epithelial stem/progenitor cells obtained from whole airway samples. In these studies, the capacity of human basal cells to form either air-liquid interface differentiated epithelium or differentiated three-dimensional (3D) tracheospheres was compromised after four passages of BEGM culture, suggesting that the issue of limited proliferation, *in vitro* senescence and loss of differentiation capacity in passaged cells might be exacerbated by the limited starting material in biopsy-derived cultures. Indeed, previous

descriptions of such cultures have mainly focused on the initiation of basal cell culture and the earliest passages [219-221].

Improved airway epithelial cell culture using 3T3+Y

The work presented here furthers previous research in which epithelial cells have been cultured on 3T3-J2 feeder cells [189] and more recently using this culture system in the presence of Rho-associated protein kinase (ROCK) inhibitors [264]. While the ability to expand and differentiate airway basal cells in this system was previously shown [264], this is first detailed characterisation of the nature of basal cells expanded using the combination of mitotically inactivated murine embryonic fibroblast feeder layers and ROCK inhibition using Y-27632 (3T3+Y). Further, this thesis demonstrates the feasibility of expanding basal cells directly from primary human tissue in these conditions and shows that replacement of 3T3-J2 cells with cells that can be derived in an autologous manner, such as lung fibroblasts or bone marrow-derived mesenchymal stem cells (MSCs), is not successful.

The use of 3T3+Y culture conditions overcame the problems associated with culture in BEGM and allowed the expansion of meaningful cell numbers from small biopsies with a high success rate. This is important for a number of reasons. Firstly, this culture technique will provide an important alternative for studying airway epithelial cells cultured from different patients. Currently, these studies are limited by the cost of commercial primary cells and their limited lifespan in culture. Additionally, the high degree of inter-individual variability seen in studies using human airway epithelial cells means that experiments ideally require investigation of a range of donor cell cultures. 3T3+Y expansion and cryopreservation of primary cells that retain their characteristics for longer culture periods might enable serial investigation of the same donor cell cultures and might improve the

reliability of such investigations. Secondly, endobronchial biopsies are the route of tissue acquisition in patients receiving epithelial cell therapy as part of tracheal transplantation procedures [70] and, given the high number of epithelial cells required for successful scaffold seeding [302], BEGM-based strategies would require a number of biopsies that is clinically unachievable, particularly as patients requiring tissue-engineered airway replacement are likely to have severely damaged airway epithelium. 3T3+Y culture conditions overcome this problem, generating clinically useful numbers of cells that retain their differentiation capacity from a single biopsy sample. Finally, the culture of cells from living patients using a minimally invasive technique suggests the application of these protocols in the expanding area of personalised medicine [303]. In future, airway biopsies from patients with respiratory disease could be expanded in 3T3+Y culture and therapies could be tested for their *in vitro* efficacy in a patient-specific manner and used to inform clinical decision-making. It will be interesting to establish whether disease-specific basal cells retain their characteristics in diseases such as asthma and chronic obstructive pulmonary disease (COPD). Additionally, the expansion of primary lung tumour cells in 3T3+Y and the characterisation of the extent to which these mimic the heterogeneity [304] and the response to therapy of patient tumours will be of interest [305]. In this setting, the high success rate of epithelial cultures in 3T3+Y will be of particular importance as samples may only be available to researchers on one occasion.

Effects of combined 3T3+Y co-culture on cultured human airway epithelial cells

In an attempt to understand the mechanism of action of 3T3+Y, using microarray and pathway analysis, key pathways were identified that are changed in airway epithelial cells grown in 3T3+Y. These include cell cycle regulators, consistent with the increased proliferation of cells in 3T3+Y, oxidative stress pathway genes, which may be of significance

given that reactive oxygen species modulate human basal cell behaviour through NRF2 [306] and neuregulin signalling, consistent with a previous report that feeder cells cause epidermal growth factor receptor (EGFR) and human epidermal growth factor receptor 2 (HER2) phosphorylation in epidermal keratinocytes [307]. Additionally, telomerase signalling genes were significantly affected by co-culture. Although human telomerase reverse transcriptase (TERT) is not typically expressed in somatic cells, low expression levels are thought to slow telomere shortening in adult stem cells [308] and exogenous addition of *TERT* mRNA extends telomeres and the lifespan of epidermal keratinocytes *in vitro* [309]. Indeed, work from another member of the laboratory suggests that, while telomere lengths decrease over passage in BEGM, telomeres are maintained in 3T3+Y [310], suggesting that this might be one reason for the maintenance of stem cell capacity in these culture conditions. Although consistent with the behaviour of cells cultured in 3T3+Y, the array data give little mechanistic insight into the molecular basis of the effects of 3T3+Y. Future mechanistic studies are required to investigate the molecular basis of airway epithelial cell expansion in 3T3+Y and also to develop protocols for clinical airway epithelial cell expansion that are not dependent on murine cells.

Potential roles of 3T3-J2 feeder cells in 3T3+Y

3T3-J2 co-culture as a method to expand human epithelial cells was first described by Prof. Howard Green and colleagues in 1975 [188, 189], and expansion of epithelial cells from a range of non-epidermal organs, including the oesophagus [311], intestines [312] and lungs [313], has since been described. However, the specific contribution of 3T3-J2 feeder cells has never been determined and, as such, clinical products involving epidermal and limbal epithelial stem cell expansion remain dependent on these murine feeder cells as effective defined media alternatives are not available.

Data presented here suggest that a continual supply of soluble feeder cell products is required by epithelial cells for optimal expansion because co-culture levels of epithelial support were recreated in colony formation assays when feeder cells were separated from epithelial cells by a transwell membrane but not when feeder cell-conditioned medium was delivered three times per week. This is in agreement with previous observations that epidermal keratinocytes are not supported by 3T3-J2-conditioned medium [189, 314] but contradicts data showing that separation with a nitrocellulose membrane prevents the keratinocyte-stimulating effect of inactivated 3T3-J2 cells [314]. The association of the keratinocyte-stimulating effect of 3T3-J2 cells with the membrane of 3T3-J2 cells [314] suggests that different mechanisms of action may exist in different epithelial cell types as physical separation did not decrease colony formation in airway epithelial cell co-cultures.

I have shown that the supportive effects of 3T3-J2 fibroblasts cannot be recapitulated by mitotically inactivated human lung fibroblast or human mesenchymal stromal cell feeder layers [310], which could be used in an autologous manner in tissue-engineering applications. These investigations, however, cannot rule out that human embryonic fibroblast cell lines, such as MRC-5, might be able to recapitulate the effects of 3T3-J2 feeder cells or that non-inactivated stromal cells from human lungs might recapitulate the lung microenvironment *ex vivo*.

Despite the existence of cell therapies that use 3T3-J2-co-cultured human cells [190, 194-196, 198, 199], future work will establish the appropriate feeder-free culture conditions for human airway basal cells. This is likely to involve better characterisation of the complex protein (and non-protein) secretions of feeder cells as they undergo apoptosis [278], the mode of their delivery (for example, secreted protein, extracellular vesicles or another mechanism) and the optimisation of culture systems to deliver these *in vitro*.

Potential roles of the ROCK inhibitor Y-27632 in 3T3+Y

The results presented here show that addition of Y-27632 dramatically improves airway epithelial cell cultures in the presence of 3T3-J2 feeder cells, consistent with previous findings that Y-27362 increases the proliferation and the lentiviral transduction efficacy of mouse and human airway basal cells in culture [315]. While the effect of culture using alternative ROCK inhibitors has not been investigated here, it is likely that, at concentrations of less than 10 μM, the effects observed using Y-27632 are as a result of specific inhibition of ROCK1 and/or ROCK2 in airway epithelial cells rather than as a result of an off-target effect on proteins such as PRK2 and MSK1 [316] Indeed, in epidermal keratinocytes, Y-27632 can be replaced by fasudil hydrochloride (HA-1077; inhibits ROCK1, ROCK2 and cAMP-dependent protein kinase), HA-1000 hydrochloride (a metabolite of fasudil hydrochloride; a selective ROCK1 and ROCK2 inhibitor) or GSK-429286 (a selective ROCK1 and ROCK2 inhibitor) with no loss of efficacy [317].

The mechanism of Y-27632 has not been addressed in these studies; however, under conventional culture conditions, cumulative passage may reduce the number of stem/progenitor cells by inducing anoikis or terminal differentiation. In fact, inhibition of ROCK signalling might be an effective strategy against both of these possibilities. Firstly, ROCK activation is implicated in apoptotic pathways. The inhibitor used here, Y-27632, was identified in a screen of molecules to inhibit dissociation-induced apoptosis in cultured human embryonic stem cells [318]. Although ROCK activation occurs as a late event in the apoptotic signalling cascade [319], sudden high intensity ROCK activation as a result of acute stress, such as cell dissociation, may accelerate apoptosis [320]. ROCK inhibition also inhibits apoptosis induced by the loss of cadherin-dependent cell contacts in multiple cell types [318, 321, 322]. Secondly, RhoA/ROCK signals mediate terminal differentiation in epithelial cells

and inhibition of ROCK prevents differentiation [323]. In differentiation pathways, upstream activation of ROCK is caused by Notch 1, expression of which is low in ΔN-p63-expressing basal epithelial cells [324] and high in suprabasal keratinocytes expressing p53 and/or TA-p63 isoforms [325]. Gene expression analyses in epidermal keratinocytes show that inclusion of Y-27632 in cultures using 3T3-J2 feeder cells leads to downregulated expression of loricrin, filaggrin [317] and keratins that are expressed by differentiated keratinocytes and to upregulation of the Notch pathway inhibitory protein CHAC1 [307]. Indeed, calcium chelation by EDTA, routinely used in cell culture, leads to release of the Notch 1 intracellular fragment and to immediate ROCK activation [326]. As Notch signalling also mediates differentiation of airway basal cells [158], this might provide a plausible mechanism for the expansion of airway basal cells in 3T3+Y. Accordingly, small molecule inhibition of ROCK might act both to prevent dissociation-induced anoikis and to retain the proliferative fraction of undifferentiated epithelial stem/progenitor cells but further mechanistic studies are required to define its contribution and the requirements for additional activation and/or repression of other signalling pathways.

HGF signalling in cultured primary human airway epithelial cells

The data presented here suggest that secreted factors mediate the effect of 3T3-J2 co-culture but that they are required in constant supply for their effect. These data support the view that mechanisms of action involving direct cell-cell contact [278] or extracellular matrix deposition [327] can be ruled out. Searching for soluble mediators revealed that surprisingly few growth factor receptor-associated pathways are activated in human airway epithelial cells co-cultured with 3T3-J2 feeder cells, although one limitation of these experiments is that conditioned medium from mitotically inactivated fibroblasts was used rather than from co-cultures of epithelial cells and fibroblasts. This strategy allowed us to distinguish potential

contributions of feeder cells but could not identify feeder cell factors that are induced by epithelial-derived signals [328]. Nevertheless, hepatocyte growth factor (HGF)-MET signalling emerged as a promising candidate mediating feeder cell-epithelial cell crosstalk as it was secreted by feeder cells in increasing amounts following mitotic inactivation and activated MET on human epithelial cells. This is consistent with the physiological role of HGF-MET signalling, where mesenchyme-derived HGF signals to epithelial MET to mediate diverse responses such as proliferation, migration, survival and differentiation [283]. The identification of MET activation in human epithelial cells stimulated with 3T3-J2-conditioned medium was particularly interesting as murine HGF is not thought to bind efficiently to the human MET receptor [284]. Indeed, autophosphorylation of the MET receptor multisubstrate-docking site was reduced in response to murine HGF in 3T3-J2-conditioned medium compared with recombinant human HGF. Interestingly, inhibition of MET did not decrease proliferation caused by conditioned medium, suggesting that HGF signalling is unlikely to be responsible for this aspect of the improved epithelial cell culture conditions conferred by 3T3+Y.

Despite this, characterisation of signalling downstream of MET in response to 3T3-J2-conditioned medium identified the transcription factor signal transducer and activator of transcription 6 (STAT6) as a novel target of MET signalling, a finding validated using recombinant human HGF. STAT6 is a target of interleukin-4 (IL-4)/IL-13 [329] and this cytokine signalling pathway is directly involved in the pathogenesis of airway disease [290, 330]. In separate studies, HGF induced cultured proximal airway basal cell secretion of the neutrophil chemoattractants IL-8 and granulocyte/macrophage colony-stimulating factor (GM-CSF), consistent with recent findings that these cytokines are secreted in a MET-dependent manner in alveolar epithelial cells following influenza infection [331]. The hypothesis that HGF induction of IL-8 is dependent on STAT6 was tested but HGF could not

induce expression of luciferase from a STAT6 consensus sequence in a cancer cell line. In addition, phosphorylated STAT6 remained in the cytoplasm of human airway basal cells in response to HGF stimulation, in contrast to following activation by IL-13, which stimulates STAT6 nuclear translocation [61]. Further, HGF induced IL-8 promoter activation in luciferase assays in the absence of the upstream STAT6-binding sequence, suggesting that other transcription factors such as nuclear factor-κB (NF-κB) or activator protein 1 (AP-1), rather than STAT6, mediate the HGF-induced increase in IL-8 expression and secretion. Previous data show that cytoplasmic phosphorylated STAT6 cannot bind to DNA *in vitro* but that DNA-binding ability could be conferred by detergent treatment, suggesting the existence of a cytoplasmic inhibitor of phosphorylated STAT6 [332]. Although the identity of this inhibitor and the mechanism of inhibition are unknown, one possibility is that a bound factor both prevents the nuclear import of STAT6 and masks the DNA-binding site. Importin-α5 binds competitively to the STAT1 DNA-binding site [333], giving biological precedent to this hypothesis but experiments comparing proteins bound to phosphorylated STAT6 in response to HGF and IL-13 stimulation using co-immunoprecipitation and mass spectrometry are required to test this hypothesis. Overall, these results suggest that murine HGF cannot be considered to be completely inactive on human cells and that it may still have an unknown role in some of the effects of 3T3+Y on human airway epithelial cells but that other secreted factors most likely co-operate with ROCK inhibition to improve human airway basal cell phenotype in 3T3+Y. Although the classic proliferative and migratory effects of HGF are lacking following stimulation with murine HGF, some intracellular signalling proceeds, including the phosphorylation of STAT6, although the functional role of these signalling events remains to be explored.

Conclusion

The work presented here identifies problems in the use of existing cell culture protocols for *in vitro* investigations requiring large numbers of primary human airway epithelial cells and for potential tissue-engineering applications that require patient autologous epithelial cells because of the limited ability to expand basal cells that retain key stem/progenitor cell functions. I have characterised an alternative cell culture protocol involving co-culture of primary epithelial cells with 3T3-J2 mouse embryonic fibroblast feeder cells in medium containing a Rho-associated protein kinase (ROCK) inhibitor, Y-27632, and found that this system is better at retaining basal cell function in *in vitro* assays. As similar culture protocols have been applied clinically in the treatment of limbal stem cell deficiency and severe burns injury, I am hopeful that this protocol could be used to improve the prognosis of patients in future airway transplantation procedures and that these findings might be a platform to discover a feeder-free method to culture human airway epithelial cells with the efficiency required for functional transplantation. Finally, I have characterised the role of hepatocyte growth factor (HGF) signalling in feeder cell-epithelial cell crosstalk, finding that murine HGF activates the human MET receptor and downstream signalling processes involving phosphorylation of GRB2-associated-binding protein 2 (GAB2) and signal transducer and activator of transcription 6 (STAT6). However, the functional role of these signalling events is unclear.

8 . References

1. **Blanpain C, Horsley V, Fuchs E.** 2007. Epithelial stem cells: turning over new leaves. Cell **128:**445-458.
2. **Zorn AM, Wells JM.** 2009. Vertebrate endoderm development and organ formation. Annu Rev Cell Dev Biol **25:**221-251.
3. **Mercer RR, Russell ML, Roggli VL, Crapo JD.** 1994. Cell number and distribution in human and rat airways. Am J Respir Cell Mol Biol **10:**613-624.
4. **Giepmans BN, van Ijzendoorn SC.** 2009. Epithelial cell-cell junctions and plasma membrane domains. Biochim Biophys Acta **1788:**820-831.
5. **Gilcrease MZ.** 2007. Integrin signaling in epithelial cells. Cancer Lett **247:**1-25.
6. **Knight DA, Holgate ST.** 2003. The airway epithelium: structural and functional properties in health and disease. Respirology **8:**432-446.
7. **Wanner A, Salathe M, O'Riordan TG.** 1996. Mucociliary clearance in the airways. Am J Respir Crit Care Med **154:**1868-1902.
8. **Travis SM, Singh PK, Welsh MJ.** 2001. Antimicrobial peptides and proteins in the innate defense of the airway surface. Curr Opin Immunol **13:**89-95.
9. **Whitsett JA, Alenghat T.** 2015. Respiratory epithelial cells orchestrate pulmonary innate immunity. Nat Immunol **16:**27-35.
10. **Hiemstra PS, McCray PB, Jr., Bals R.** 2015. The innate immune function of airway epithelial cells in inflammatory lung disease. Eur Respir J **45:**1150-1162.
11. **Herriges M, Morrisey EE.** 2014. Lung development: orchestrating the generation and regeneration of a complex organ. Development **141:**502-513.
12. **Morrisey EE, Hogan BL.** 2010. Preparing for the first breath: genetic and cellular mechanisms in lung development. Dev Cell **18:**8-23.
13. **Hamilton N, Hynds RE, Butler CR, Giangreco A, Janes SM.** 2013. Lung Regeneration: The Developmental Biology Approach, p 707-717, Regenerative Medicine Applications in Organ Transplantation.
14. **Rackley CR, Stripp BR.** 2012. Building and maintaining the epithelium of the lung. J Clin Invest **122:**2724-2730.
15. **Rock JR, Onaitis MW, Rawlins EL, Lu Y, Clark CP, Xue Y, Randell SH, Hogan BL.** 2009. Basal cells as stem cells of the mouse trachea and human airway epithelium. Proc Natl Acad Sci U S A **106:**12771-12775.
16. **Van de Laar E, Clifford M, Hasenoeder S, Kim BR, Wang D, Lee S, Paterson J, Vu NM, Waddell TK, Keshavjee S, Tsao MS, Ailles L, Moghal N.** 2014. Cell surface marker profiling of human tracheal basal cells reveals distinct subpopulations,

identifies MST1/MSP as a mitogenic signal, and identifies new biomarkers for lung squamous cell carcinomas. Respir Res **15:**160.

17. **Shaykhiev R.** 2015. Multitasking basal cells: combining stem cell and innate immune duties. Eur Respir J **46:**894-897.
18. **Byers DE, Alexander-Brett J, Patel AC, Agapov E, Dang-Vu G, Jin X, Wu K, You Y, Alevy Y, Girard JP, Stappenbeck TS, Patterson GA, Pierce RA, Brody SL, Holtzman MJ.** 2013. Long-term IL-33-producing epithelial progenitor cells in chronic obstructive lung disease. J Clin Invest **123:**3967-3982.
19. **Amatngalim GD, van Wijck Y, de Mooij-Eijk Y, Verhoosel RM, Harder J, Lekkerkerker AN, Janssen RA, Hiemstra PS.** 2015. Basal cells contribute to innate immunity of the airway epithelium through production of the antimicrobial protein RNase 7. J Immunol **194:**3340-3350.
20. **Park KS, Korfhagen TR, Bruno MD, Kitzmiller JA, Wan H, Wert SE, Khurana Hershey GK, Chen G, Whitsett JA.** 2007. SPDEF regulates goblet cell hyperplasia in the airway epithelium. J Clin Invest **117:**978-988.
21. **Chen G, Korfhagen TR, Xu Y, Kitzmiller J, Wert SE, Maeda Y, Gregorieff A, Clevers H, Whitsett JA.** 2009. SPDEF is required for mouse pulmonary goblet cell differentiation and regulates a network of genes associated with mucus production. J Clin Invest **119:**2914-2924.
22. **Bernacki SH, Nelson AL, Abdullah L, Sheehan JK, Harris A, Davis CW, Randell SH.** 1999. Mucin gene expression during differentiation of human airway epithelia in vitro. Muc4 and muc5b are strongly induced. Am J Respir Cell Mol Biol **20:**595-604.
23. **You Y, Huang T, Richer EJ, Schmidt JE, Zabner J, Borok Z, Brody SL.** 2004. Role of f-box factor foxj1 in differentiation of ciliated airway epithelial cells. Am J Physiol Lung Cell Mol Physiol **286:**L650-657.
24. **Horani A, Ferkol TW, Dutcher SK, Brody SL.** 2015. Genetics and biology of primary ciliary dyskinesia. Paediatr Respir Rev doi:S1526-0542(15)00086-X [pii] 10.1016/j.prrv.2015.09.001.
25. **Brooks ER, Wallingford JB.** 2014. Multiciliated cells. Curr Biol **24:**R973-982.
26. **Chilvers MA, O'Callaghan C.** 2000. Analysis of ciliary beat pattern and beat frequency using digital high speed imaging: comparison with the photomultiplier and photodiode methods. Thorax **55:**314-317.
27. **Werner C, Onnebrink JG, Omran H.** 2015. Diagnosis and management of primary ciliary dyskinesia. Cilia **4:**2.

28. **Clara M.** 1937. On the histobiology of the bronchial epithelium. Zeitschrift fur mikroskopisch-anatomische Forschung **41:**321-347.
29. **Winkelmann A, Noack T.** 2010. The Clara cell: a "Third Reich eponym"? Eur Respir J **36:**722-727.
30. **Singh G, Katyal SL.** 1997. Clara cells and Clara cell 10 kD protein (CC10). Am J Respir Cell Mol Biol **17:**141-143.
31. **Massaro GD, Singh G, Mason R, Plopper CG, Malkinson AM, Gail DB.** 1994. Biology of the Clara cell. Am J Physiol **266:**L101-106.
32. **Kuo CS, Krasnow MA.** 2015. Formation of a Neurosensory Organ by Epithelial Cell Slithering. Cell **163:**394-405.
33. **Noguchi M, Sumiyama K, Morimoto M.** 2015. Directed Migration of Pulmonary Neuroendocrine Cells toward Airway Branches Organizes the Stereotypic Location of Neuroepithelial Bodies. Cell Rep **13:**2679-2686.
34. **Pearse AG, Takor T.** 1979. Embryology of the diffuse neuroendocrine system and its relationship to the common peptides. Fed Proc **38:**2288-2294.
35. **Song H, Yao E, Lin C, Gacayan R, Chen MH, Chuang PT.** 2012. Functional characterization of pulmonary neuroendocrine cells in lung development, injury, and tumorigenesis. Proc Natl Acad Sci U S A **109:**17531-17536.
36. **Branchfield K, Nantie L, Verheyden JM, Sui P, Wienhold MD, Sun X.** 2016. Pulmonary neuroendocrine cells function as airway sensors to control lung immune response. Science **351:**707-710.
37. **Gu X, Karp PH, Brody SL, Pierce RA, Welsh MJ, Holtzman MJ, Ben-Shahar Y.** 2014. Chemosensory functions for pulmonary neuroendocrine cells. Am J Respir Cell Mol Biol **50:**637-646.
38. **Boers JE, den Brok JL, Koudstaal J, Arends JW, Thunnissen FB.** 1996. Number and proliferation of neuroendocrine cells in normal human airway epithelium. Am J Respir Crit Care Med **154:**758-763.
39. **Griscom NT, Wohl ME.** 1986. Dimensions of the growing trachea related to age and gender. AJR Am J Roentgenol **146:**233-237.
40. **Tyler WS.** 1983. Comparative subgross anatomy of lungs. Pleuras, interlobular septa, and distal airways. Am Rev Respir Dis **128:**S32-36.
41. **Rock JR, Randell SH, Hogan BL.** 2010. Airway basal stem cells: a perspective on their roles in epithelial homeostasis and remodeling. Dis Model Mech **3:**545-556.

42. **Irvin CG, Bates JH.** 2003. Measuring the lung function in the mouse: the challenge of size. Respir Res **4:**4.

43. **Jemal A, Bray F, Center MM, Ferlay J, Ward E, Forman D.** 2011. Global cancer statistics. CA Cancer J Clin **61:**69-90.

44. **Succony L, Janes SM.** 2014. Airway stem cells and lung cancer. QJM **107:**607-612.

45. **Hynds RE, Giangreco A.** 2015. Stem cells of the distal bronchiolar airways, p 113-126, Stem Cells in the Lung.

46. **Jeremy George P, Banerjee AK, Read CA, O'Sullivan C, Falzon M, Pezzella F, Nicholson AG, Shaw P, Laurent G, Rabbitts PH.** 2007. Surveillance for the detection of early lung cancer in patients with bronchial dysplasia. Thorax **62:**43-50.

47. **Parkin DM.** 2011. 2. Tobacco-attributable cancer burden in the UK in 2010. Br J Cancer **105 Suppl 2:**S6-S13.

48. **Spiro SG, Tanner NT, Silvestri GA, Janes SM, Lim E, Vansteenkiste JF, Pirker R.** 2010. Lung cancer: progress in diagnosis, staging and therapy. Respirology **15:**44-50.

49. **Danahay H, Pessotti AD, Coote J, Montgomery BE, Xia D, Wilson A, Yang H, Wang Z, Bevan L, Thomas C, Petit S, London A, LeMotte P, Doelemeyer A, Velez-Reyes GL, Bernasconi P, Fryer CJ, Edwards M, Capodieci P, Chen A, Hild M, Jaffe AB.** 2015. Notch2 is required for inflammatory cytokine-driven goblet cell metaplasia in the lung. Cell Rep **10:**239-252.

50. **Rogers DF.** 2007. Physiology of airway mucus secretion and pathophysiology of hypersecretion. Respir Care **52:**1134-1146; discussion 1146-1139.

51. **Elizur A, Cannon CL, Ferkol TW.** 2008. Airway inflammation in cystic fibrosis. Chest **133:**489-495.

52. **Barnes PJ.** 2013. New anti-inflammatory targets for chronic obstructive pulmonary disease. Nat Rev Drug Discov **12:**543-559.

53. **Barnes PJ.** 2008. Immunology of asthma and chronic obstructive pulmonary disease. Nat Rev Immunol **8:**183-192.

54. **Erle DJ, Sheppard D.** 2014. The cell biology of asthma. J Cell Biol **205:**621-631.

55. **Snippert HJ, Haegebarth A, Kasper M, Jaks V, van Es JH, Barker N, van de Wetering M, van den Born M, Begthel H, Vries RG, Stange DE, Toftgard R, Clevers H.** 2010. Lgr6 marks stem cells in the hair follicle that generate all cell lineages of the skin. Science **327:**1385-1389.

56. **Kelly-Welch A, Hanson EM, Keegan AD.** 2005. Interleukin-13 (IL-13) pathway. Sci STKE **2005:**cm8.

57. **Kelly-Welch A, Hanson EM, Keegan AD.** 2005. Interleukin-4 (IL-4) pathway. Sci STKE **2005:**cm9.

58. **Elo LL, Jarvenpaa H, Tuomela S, Raghav S, Ahlfors H, Laurila K, Gupta B, Lund RJ, Tahvanainen J, Hawkins RD, Oresic M, Lahdesmaki H, Rasool O, Rao KV, Aittokallio T, Lahesmaa R.** 2010. Genome-wide profiling of interleukin-4 and STAT6 transcription factor regulation of human Th2 cell programming. Immunity **32:**852-862.

59. **Kanai A, Suzuki K, Tanimoto K, Mizushima-Sugano J, Suzuki Y, Sugano S.** 2011. Characterization of STAT6 target genes in human B cells and lung epithelial cells. DNA Res **18:**379-392.

60. **Tomita K, Caramori G, Ito K, Sano H, Lim S, Oates T, Cosio B, Chung KF, Tohda Y, Barnes PJ, Adcock IM.** 2012. STAT6 expression in T cells, alveolar macrophages and bronchial biopsies of normal and asthmatic subjects. J Inflamm (Lond) **9:**5.

61. **Matsukura S, Stellato C, Plitt JR, Bickel C, Miura K, Georas SN, Casolaro V, Schleimer RP.** 1999. Activation of eotaxin gene transcription by NF-kappa B and STAT6 in human airway epithelial cells. J Immunol **163:**6876-6883.

62. **Striz I, Mio T, Adachi Y, Heires P, Robbins RA, Spurzem JR, Illig MJ, Romberger DJ, Rennard SI.** 1999. IL-4 induces ICAM-1 expression in human bronchial epithelial cells and potentiates TNF-alpha. Am J Physiol **277:**L58-64.

63. **Kuperman DA, Huang X, Koth LL, Chang GH, Dolganov GM, Zhu Z, Elias JA, Sheppard D, Erle DJ.** 2002. Direct effects of interleukin-13 on epithelial cells cause airway hyperreactivity and mucus overproduction in asthma. Nat Med **8:**885-889.

64. **Mascareno E, Dhar M, Siddiqui MA.** 1998. Signal transduction and activator of transcription (STAT) protein-dependent activation of angiotensinogen promoter: a cellular signal for hypertrophy in cardiac muscle. Proc Natl Acad Sci U S A **95:**5590-5594.

65. **Oki S, Otsuki N, Kohsaka T, Azuma M.** 2000. Stat6 activation and Th2 cell differentiation [correction of proliferation] driven by CD28 [correction of CD28 signals]. Eur J Immunol **30:**1416-1424.

66. **Patel BK, Wang LM, Lee CC, Taylor WG, Pierce JH, LaRochelle WJ.** 1996. Stat6 and Jak1 are common elements in platelet-derived growth factor and interleukin-4 signal transduction pathways in NIH 3T3 fibroblasts. J Biol Chem **271:**22175-22182.

67. **Ott LM, Weatherly RA, Detamore MS.** 2011. Overview of tracheal tissue engineering: clinical need drives the laboratory approach. Ann Biomed Eng **39:**2091-2113.

68. **Kotloff RM, Thabut G.** 2011. Lung transplantation. Am J Respir Crit Care Med **184:**159-171.

69. **Ren X, Ott HC.** 2014. On the road to bioartificial organs. Pflugers Arch **466:**1847-1857.

70. **Macchiarini P, Jungebluth P, Go T, Asnaghi MA, Rees LE, Cogan TA, Dodson A, Martorell J, Bellini S, Parnigotto PP, Dickinson SC, Hollander AP, Mantero S, Conconi MT, Birchall MA.** 2008. Clinical transplantation of a tissue-engineered airway. Lancet **372:**2023-2030.

71. **Elliott MJ, De Coppi P, Speggiorin S, Roebuck D, Butler CR, Samuel E, Crowley C, McLaren C, Fierens A, Vondrys D, Cochrane L, Jephson C, Janes S, Beaumont NJ, Cogan T, Bader A, Seifalian AM, Hsuan JJ, Lowdell MW, Birchall MA.** 2012. Stem-cell-based, tissue engineered tracheal replacement in a child: a 2-year follow-up study. Lancet **380:**994-1000.

72. **Delaere P, Vranckx J, Verleden G, De Leyn P, Van Raemdonck D.** 2010. Tracheal allotransplantation after withdrawal of immunosuppressive therapy. N Engl J Med **362:**138-145.

73. **Crowley C, Birchall M, Seifalian AM.** 2014. Trachea transplantation: from laboratory to patient. J Tissue Eng Regen Med doi:10.1002/term.1847.

74. **Brouwer KM, Hoogenkamp HR, Daamen WF, van Kuppevelt TH.** 2013. Regenerative medicine for the respiratory system: distant future or tomorrow's treatment? Am J Respir Crit Care Med **187:**468-475.

75. **Jungebluth P, Alici E, Baiguera S, Le Blanc K, Blomberg P, Bozoky B, Crowley C, Einarsson O, Grinnemo KH, Gudbjartsson T, Le Guyader S, Henriksson G, Hermanson O, Juto JE, Leidner B, Lilja T, Liska J, Luedde T, Lundin V, Moll G, Nilsson B, Roderburg C, Stromblad S, Sutlu T, Teixeira AI, Watz E, Seifalian A, Macchiarini P.** 2011. Tracheobronchial transplantation with a stem-cell-seeded bioartificial nanocomposite: a proof-of-concept study. Lancet **378:**1997-2004.

76. **Delaere PR, Vranckx JJ, Den Hondt M.** 2014. Tracheal allograft after withdrawal of immunosuppressive therapy. N Engl J Med **370:**1568-1570.

77. **Hamilton N, Bullock AJ, Macneil S, Janes SM, Birchall M.** 2014. Tissue engineering airway mucosa: a systematic review. Laryngoscope **124:**961-968.

78. **Fishman JM, Wiles K, Lowdell MW, De Coppi P, Elliott MJ, Atala A, Birchall MA.** 2014. Airway tissue engineering: an update. Expert Opin Biol Ther **14:**1477-1491.

79. **Santacruz JF, Mehta AC.** 2009. Airway complications and management after lung transplantation: ischemia, dehiscence, and stenosis. Proc Am Thorac Soc **6:**79-93.

80. **Berg M, Ejnell H, Kovacs A, Nayakawde N, Patil PB, Joshi M, Aziz L, Radberg G, Hajizadeh S, Olausson M, Sumitran-Holgersson S.** 2014. Replacement of a tracheal stenosis with a tissue-engineered human trachea using autologous stem cells: a case report. Tissue Eng Part A **20:**389-397.

81. **Hamilton NJ, Kanani M, Roebuck DJ, Hewitt RJ, Cetto R, Culme-Seymour EJ, Toll E, Bates AJ, Comerford AP, McLaren CA, Butler CR, Crowley C, McIntyre D, Sebire NJ, Janes SM, O'Callaghan C, Mason C, De Coppi P, Lowdell MW, Elliott MJ, Birchall MA.** 2015. Tissue-Engineered Tracheal Replacement in a Child: A 4-Year Follow-Up Study. Am J Transplant **15:**2750-2757.

82. **Franklin WA, Folkvord JM, Varella-Garcia M, Kennedy T, Proudfoot S, Cook R, Dempsey EC, Helm K, Bunn PA, Miller YE.** 1996. Expansion of bronchial epithelial cell populations by in vitro culture of explants from dysplastic and histologically normal sites. Am J Respir Cell Mol Biol **15:**297-304.

83. **Kummer W, Lips KS, Pfeil U.** 2008. The epithelial cholinergic system of the airways. Histochem Cell Biol **130:**219-234.

84. **Bayart E, Cohen-Haguenauer O.** 2013. Technological overview of iPS induction from human adult somatic cells. Curr Gene Ther **13:**73-92.

85. **Serra M, Brito C, Correia C, Alves PM.** 2012. Process engineering of human pluripotent stem cells for clinical application. Trends Biotechnol **30:**350-359.

86. **Moore KA, Lemischka IR.** 2006. Stem cells and their niches. Science **311:**1880-1885.

87. **Bonfanti P, Claudinot S, Amici AW, Farley A, Blackburn CC, Barrandon Y.** 2010. Microenvironmental reprogramming of thymic epithelial cells to skin multipotent stem cells. Nature **466:**978-982.

88. **Clevers H.** 2015. STEM CELLS. What is an adult stem cell? Science **350:**1319-1320.

89. **Jacobson LO, Simmons EL, Marks EK, Robson MJ, Bethard WF, Gaston EO.** 1950. The role of the spleen in radiation injury and recovery. J Lab Clin Med **35:**746-770.

90. **Lorenz E, Uphoff D, Reid TR, Shelton E.** 1951. Modification of irradiation injury in mice and guinea pigs by bone marrow injections. J Natl Cancer Inst **12:**197-201.

91. **Ford CE, Hamerton JL, Barnes DW, Loutit JF.** 1956. Cytological identification of radiation-chimaeras. Nature **177:**452-454.

92. **Becker AJ, Mc CE, Till JE.** 1963. Cytological demonstration of the clonal nature of spleen colonies derived from transplanted mouse marrow cells. Nature **197:**452-454.

93. **Potten CS.** 1981. Cell replacement in epidermis (keratopoiesis) via discrete units of proliferation. Int Rev Cytol **69:**271-318.

94. **Fuchs E.** 2009. The tortoise and the hair: slow-cycling cells in the stem cell race. Cell **137:**811-819.

95. **Notta F, Zandi S, Takayama N, Dobson S, Gan OI, Wilson G, Kaufmann KB, McLeod J, Laurenti E, Dunant CF, McPherson JD, Stein LD, Dror Y, Dick JE.** 2016. Distinct routes of lineage development reshape the human blood hierarchy across ontogeny. Science **351:**aab2116.

96. **Clayton E, Doupe DP, Klein AM, Winton DJ, Simons BD, Jones PH.** 2007. A single type of progenitor cell maintains normal epidermis. Nature **446:**185-189.

97. **Doupe DP, Klein AM, Simons BD, Jones PH.** 2010. The ordered architecture of murine ear epidermis is maintained by progenitor cells with random fate. Dev Cell **18:**317-323.

98. **Jones P, Simons BD.** 2008. Epidermal homeostasis: do committed progenitors work while stem cells sleep? Nat Rev Mol Cell Biol **9:**82-88.

99. **Potten CS, Loeffler M.** 1990. Stem cells: attributes, cycles, spirals, pitfalls and uncertainties. Lessons for and from the crypt. Development **110:**1001-1020.

100. **Stange DE, Koo BK, Huch M, Sibbel G, Basak O, Lyubimova A, Kujala P, Bartfeld S, Koster J, Geahlen JH, Peters PJ, van Es JH, van de Wetering M, Mills JC, Clevers H.** 2013. Differentiated Troy+ chief cells act as reserve stem cells to generate all lineages of the stomach epithelium. Cell **155:**357-368.

101. **Nakagawa T, Sharma M, Nabeshima Y, Braun RE, Yoshida S.** 2010. Functional hierarchy and reversibility within the murine spermatogenic stem cell compartment. Science **328:**62-67.

102. **Tata PR, Mou H, Pardo-Saganta A, Zhao R, Prabhu M, Law BM, Vinarsky V, Cho JL, Breton S, Sahay A, Medoff BD, Rajagopal J.** 2013. Dedifferentiation of committed epithelial cells into stem cells in vivo. Nature **503:**218-223.

103. **Rawlins EL, Hogan BL.** 2006. Epithelial stem cells of the lung: privileged few or opportunities for many? Development **133:**2455-2465.

104. **Kajstura J, Rota M, Hall SR, Hosoda T, D'Amario D, Sanada F, Zheng H, Ogorek B, Rondon-Clavo C, Ferreira-Martins J, Matsuda A, Arranto C, Goichberg P, Giordano**

G, Haley KJ, Bardelli S, Rayatzadeh H, Liu X, Quaini F, Liao R, Leri A, Perrella MA, Loscalzo J, Anversa P. 2011. Evidence for human lung stem cells. N Engl J Med **364:**1795-1806.

105. **Teixeira VH, Nadarajan P, Graham TA, Pipinikas CP, Brown JM, Falzon M, Nye E, Poulsom R, Lawrence D, Wright NA, McDonald S, Giangreco A, Simons BD, Janes SM.** 2013. Stochastic homeostasis in human airway epithelium is achieved by neutral competition of basal cell progenitors. Elife **2:**e00966.
106. **Liu Q, Huang X, Zhang H, Tian X, He L, Yang R, Yan Y, Wang QD, Gillich A, Zhou B.** 2015. c-kit(+) cells adopt vascular endothelial but not epithelial cell fates during lung maintenance and repair. Nat Med **21:**866-868.
107. **Rawlins EL, Hogan BL.** 2008. Ciliated epithelial cell lifespan in the mouse trachea and lung. Am J Physiol Lung Cell Mol Physiol **295:**L231-234.
108. **Breuer R, Zajicek G, Christensen TG, Lucey EC, Snider GL.** 1990. Cell kinetics of normal adult hamster bronchial epithelium in the steady state. Am J Respir Cell Mol Biol **2:**51-58.
109. **Evans MJ, Shami SG, Cabral-Anderson LJ, Dekker NP.** 1986. Role of nonciliated cells in renewal of the bronchial epithelium of rats exposed to NO2. Am J Pathol **123:**126-133.
110. **Randell SH, Comment CE, Ramaekers FC, Nettesheim P.** 1991. Properties of rat tracheal epithelial cells separated based on expression of cell surface alpha-galactosyl end groups. Am J Respir Cell Mol Biol **4:**544-554.
111. **Hong KU, Reynolds SD, Watkins S, Fuchs E, Stripp BR.** 2004. Basal cells are a multipotent progenitor capable of renewing the bronchial epithelium. Am J Pathol **164:**577-588.
112. **Hong KU, Reynolds SD, Watkins S, Fuchs E, Stripp BR.** 2004. In vivo differentiation potential of tracheal basal cells: evidence for multipotent and unipotent subpopulations. Am J Physiol Lung Cell Mol Physiol **286:**L643-649.
113. **Schoch KG, Lori A, Burns KA, Eldred T, Olsen JC, Randell SH.** 2004. A subset of mouse tracheal epithelial basal cells generates large colonies in vitro. Am J Physiol Lung Cell Mol Physiol **286:**L631-642.
114. **Watson JK, Rulands S, Wilkinson AC, Wuidart A, Ousset M, Van Keymeulen A, Gottgens B, Blanpain C, Simons BD, Rawlins EL.** 2015. Clonal Dynamics Reveal Two Distinct Populations of Basal Cells in Slow-Turnover Airway Epithelium. Cell Rep **12:**90-101.

115. **Mori M, Mahoney JE, Stupnikov MR, Paez-Cortez JR, Szymaniak AD, Varelas X, Herrick DB, Schwob J, Zhang H, Cardoso WV.** 2015. Notch3-Jagged signaling controls the pool of undifferentiated airway progenitors. Development **142:**258-267.

116. **Rawlins EL, Okubo T, Xue Y, Brass DM, Auten RL, Hasegawa H, Wang F, Hogan BL.** 2009. The role of Scgb1a1+ Clara cells in the long-term maintenance and repair of lung airway, but not alveolar, epithelium. Cell Stem Cell **4:**525-534.

117. **Gray TE, Guzman K, Davis CW, Abdullah LH, Nettesheim P.** 1996. Mucociliary differentiation of serially passaged normal human tracheobronchial epithelial cells. Am J Respir Cell Mol Biol **14:**104-112.

118. **Engelhardt JF, Schlossberg H, Yankaskas JR, Dudus L.** 1995. Progenitor cells of the adult human airway involved in submucosal gland development. Development **121:**2031-2046.

119. **Avril-Delplanque A, Casal I, Castillon N, Hinnrasky J, Puchelle E, Peault B.** 2005. Aquaporin-3 expression in human fetal airway epithelial progenitor cells. Stem Cells **23:**992-1001.

120. **Shaykhiev R, Zuo WL, Chao I, Fukui T, Witover B, Brekman A, Crystal RG.** 2013. EGF shifts human airway basal cell fate toward a smoking-associated airway epithelial phenotype. Proc Natl Acad Sci U S A **110:**12102-12107.

121. **Evans MJ, Cabral-Anderson LJ, Freeman G.** 1978. Role of the Clara cell in renewal of the bronchiolar epithelium. Lab Invest **38:**648-653.

122. **Fanucchi MV, Murphy ME, Buckpitt AR, Philpot RM, Plopper CG.** 1997. Pulmonary cytochrome P450 monooxygenase and Clara cell differentiation in mice. Am J Respir Cell Mol Biol **17:**302-314.

123. **Giangreco A, Arwert EN, Rosewell IR, Snyder J, Watt FM, Stripp BR.** 2009. Stem cells are dispensable for lung homeostasis but restore airways after injury. Proc Natl Acad Sci U S A **106:**9286-9291.

124. **Ayers MM, Jeffery PK.** 1988. Proliferation and differentiation in mammalian airway epithelium. Eur Respir J **1:**58-80.

125. **Evans MJ, Hackney JD.** 1972. Cell proliferation in lungs of mice exposed to elevated concentrations of oxygen. Aerosp Med **43:**620-622.

126. **Stripp BR, Maxson K, Mera R, Singh G.** 1995. Plasticity of airway cell proliferation and gene expression after acute naphthalene injury. Am J Physiol **269:**L791-799.

127. **van Rongen E, Thames HD, Jr., Travis EL.** 1993. Recovery from radiation damage in mouse lung: interpretation in terms of two rates of repair. Radiat Res **133:**225-233.

128. **O'Brien KA, Suverkropp C, Kanekal S, Plopper CG, Buckpitt AR.** 1989. Tolerance to multiple doses of the pulmonary toxicant, naphthalene. Toxicol Appl Pharmacol **99:**487-500.

129. **Van Winkle LS, Buckpitt AR, Nishio SJ, Isaac JM, Plopper CG.** 1995. Cellular response in naphthalene-induced Clara cell injury and bronchiolar epithelial repair in mice. Am J Physiol **269:**L800-818.

130. **West JA, Pakehham G, Morin D, Fleschner CA, Buckpitt AR, Plopper CG.** 2001. Inhaled naphthalene causes dose dependent Clara cell cytotoxicity in mice but not in rats. Toxicol Appl Pharmacol **173:**114-119.

131. **Mahvi D, Bank H, Harley R.** 1977. Morphology of a naphthalene-induced bronchiolar lesion. Am J Pathol **86:**558-572.

132. **Plopper CG, Macklin J, Nishio SJ, Hyde DM, Buckpitt AR.** 1992. Relationship of cytochrome P-450 activity to Clara cell cytotoxicity. III. Morphometric comparison of changes in the epithelial populations of terminal bronchioles and lobar bronchi in mice, hamsters, and rats after parenteral administration of naphthalene. Lab Invest **67:**553-565.

133. **Hong KU, Reynolds SD, Giangreco A, Hurley CM, Stripp BR.** 2001. Clara cell secretory protein-expressing cells of the airway neuroepithelial body microenvironment include a label-retaining subset and are critical for epithelial renewal after progenitor cell depletion. Am J Respir Cell Mol Biol **24:**671-681.

134. **Kim CF, Jackson EL, Woolfenden AE, Lawrence S, Babar I, Vogel S, Crowley D, Bronson RT, Jacks T.** 2005. Identification of bronchioalveolar stem cells in normal lung and lung cancer. Cell **121:**823-835.

135. **Kumar PA, Hu Y, Yamamoto Y, Hoe NB, Wei TS, Mu D, Sun Y, Joo LS, Dagher R, Zielonka EM, Wang de Y, Lim B, Chow VT, Crum CP, Xian W, McKeon F.** 2011. Distal airway stem cells yield alveoli in vitro and during lung regeneration following H1N1 influenza infection. Cell **147:**525-538.

136. **Zuo W, Zhang T, Wu DZ, Guan SP, Liew AA, Yamamoto Y, Wang X, Lim SJ, Vincent M, Lessard M, Crum CP, Xian W, McKeon F.** 2015. p63(+)Krt5(+) distal airway stem cells are essential for lung regeneration. Nature **517:**616-620.

137. **Boers JE, Ambergen AW, Thunnissen FB.** 1999. Number and proliferation of clara cells in normal human airway epithelium. Am J Respir Crit Care Med **159:**1585-1591.

138. **Koo BK, Clevers H.** 2014. Stem cells marked by the R-spondin receptor LGR5. Gastroenterology **147:**289-302.

139. **Oeztuerk-Winder F, Guinot A, Ochalek A, Ventura JJ.** 2012. Regulation of human lung alveolar multipotent cells by a novel p38alpha MAPK/miR-17-92 axis. EMBO J **31:**3431-3441.

140. **Schofield R.** 1978. The relationship between the spleen colony-forming cell and the haemopoietic stem cell. Blood Cells **4:**7-25.

141. **Sato T, van Es JH, Snippert HJ, Stange DE, Vries RG, van den Born M, Barker N, Shroyer NF, van de Wetering M, Clevers H.** 2011. Paneth cells constitute the niche for Lgr5 stem cells in intestinal crypts. Nature **469:**415-418.

142. **Rompolas P, Greco V.** 2014. Stem cell dynamics in the hair follicle niche. Semin Cell Dev Biol **25-26:**34-42.

143. **Yin H, Price F, Rudnicki MA.** 2013. Satellite cells and the muscle stem cell niche. Physiol Rev **93:**23-67.

144. **Kirby ED, Kuwahara AA, Messer RL, Wyss-Coray T.** 2015. Adult hippocampal neural stem and progenitor cells regulate the neurogenic niche by secreting VEGF. Proc Natl Acad Sci U S A **112:**4128-4133.

145. **Watt FM, Hogan BL.** 2000. Out of Eden: stem cells and their niches. Science **287:**1427-1430.

146. **Lane SW, Williams DA, Watt FM.** 2014. Modulating the stem cell niche for tissue regeneration. Nat Biotechnol **32:**795-803.

147. **Jones DL, Wagers AJ.** 2008. No place like home: anatomy and function of the stem cell niche. Nat Rev Mol Cell Biol **9:**11-21.

148. **Borthwick DW, Shahbazian M, Krantz QT, Dorin JR, Randell SH.** 2001. Evidence for stem-cell niches in the tracheal epithelium. Am J Respir Cell Mol Biol **24:**662-670.

149. **Liu X, Engelhardt JF.** 2008. The glandular stem/progenitor cell niche in airway development and repair. Proc Am Thorac Soc **5:**682-688.

150. **Lynch TJ, Engelhardt JF.** 2014. Progenitor cells in proximal airway epithelial development and regeneration. J Cell Biochem **115:**1637-1645.

151. **Giangreco A, Reynolds SD, Stripp BR.** 2002. Terminal bronchioles harbor a unique airway stem cell population that localizes to the bronchoalveolar duct junction. Am J Pathol **161:**173-182.

152. **Reynolds SD, Giangreco A, Power JH, Stripp BR.** 2000. Neuroepithelial bodies of pulmonary airways serve as a reservoir of progenitor cells capable of epithelial regeneration. Am J Pathol **156:**269-278.

153. **Hoyt RF, Jr., McNelly NA, McDowell EM, Sorokin SP.** 1991. Neuroepithelial bodies stimulate proliferation of airway epithelium in fetal hamster lung. Am J Physiol **260:**L234-240.

154. **Hoyt RF, Jr., McNelly NA, Sorokin SP.** 1990. Dynamics of neuroepithelial body (NEB) formation in developing hamster lung: light microscopic autoradiography after 3H-thymidine labeling in vivo. Anat Rec **227:**340-350.

155. **Reynolds SD, Hong KU, Giangreco A, Mango GW, Guron C, Morimoto Y, Stripp BR.** 2000. Conditional clara cell ablation reveals a self-renewing progenitor function of pulmonary neuroendocrine cells. Am J Physiol Lung Cell Mol Physiol **278:**L1256-1263.

156. **Vallath S, Hynds RE, Succony L, Janes SM, Giangreco A.** 2014. Targeting EGFR signalling in chronic lung disease: therapeutic challenges and opportunities. Eur Respir J **44:**513-522.

157. **Vermeer PD, Einwalter LA, Moninger TO, Rokhlina T, Kern JA, Zabner J, Welsh MJ.** 2003. Segregation of receptor and ligand regulates activation of epithelial growth factor receptor. Nature **422:**322-326.

158. **Rock JR, Gao X, Xue Y, Randell SH, Kong YY, Hogan BL.** 2011. Notch-dependent differentiation of adult airway basal stem cells. Cell Stem Cell **8:**639-648.

159. **Guseh JS, Bores SA, Stanger BZ, Zhou Q, Anderson WJ, Melton DA, Rajagopal J.** 2009. Notch signaling promotes airway mucous metaplasia and inhibits alveolar development. Development **136:**1751-1759.

160. **Morimoto M, Liu Z, Cheng HT, Winters N, Bader D, Kopan R.** 2010. Canonical Notch signaling in the developing lung is required for determination of arterial smooth muscle cells and selection of Clara versus ciliated cell fate. J Cell Sci **123:**213-224.

161. **Tsao PN, Vasconcelos M, Izvolsky KI, Qian J, Lu J, Cardoso WV.** 2009. Notch signaling controls the balance of ciliated and secretory cell fates in developing airways. Development **136:**2297-2307.

162. **Pardo-Saganta A, Law BM, Tata PR, Villoria J, Saez B, Mou H, Zhao R, Rajagopal J.** 2015. Injury induces direct lineage segregation of functionally distinct airway basal stem/progenitor cell subpopulations. Cell Stem Cell **16:**184-197.

163. **Lafkas D, Shelton A, Chiu C, de Leon Boenig G, Chen Y, Stawicki SS, Siltanen C, Reichelt M, Zhou M, Wu X, Eastham-Anderson J, Moore H, Roose-Girma M, Chinn Y, Hang JQ, Warming S, Egen J, Lee WP, Austin C, Wu Y, Payandeh J, Lowe JB,**

Siebel CW. 2015. Therapeutic antibodies reveal Notch control of transdifferentiation in the adult lung. Nature **528:**127-131.

164. **Lewis J.** 1998. Notch signalling and the control of cell fate choices in vertebrates. Semin Cell Dev Biol **9:**583-589.

165. **Pardo-Saganta A, Tata PR, Law BM, Saez B, Chow R, Prabhu M, Gridley T, Rajagopal J.** 2015. Parent stem cells can serve as niches for their daughter cells. Nature **523:**597-601.

166. **El Agha E, Herold S, Al Alam D, Quantius J, MacKenzie B, Carraro G, Moiseenko A, Chao CM, Minoo P, Seeger W, Bellusci S.** 2014. Fgf10-positive cells represent a progenitor cell population during lung development and postnatally. Development **141:**296-306.

167. **Bellusci S, Grindley J, Emoto H, Itoh N, Hogan BL.** 1997. Fibroblast growth factor 10 (FGF10) and branching morphogenesis in the embryonic mouse lung. Development **124:**4867-4878.

168. **Volckaert T, Dill E, Campbell A, Tiozzo C, Majka S, Bellusci S, De Langhe SP.** 2011. Parabronchial smooth muscle constitutes an airway epithelial stem cell niche in the mouse lung after injury. J Clin Invest **121:**4409-4419.

169. **Volckaert T, Campbell A, De Langhe S.** 2013. c-Myc regulates proliferation and Fgf10 expression in airway smooth muscle after airway epithelial injury in mouse. PLoS One **8:**e71426.

170. **McQualter JL, Yuen K, Williams B, Bertoncello I.** 2010. Evidence of an epithelial stem/progenitor cell hierarchy in the adult mouse lung. Proc Natl Acad Sci U S A **107:**1414-1419.

171. **McQualter JL, McCarty RC, Van der Velden J, O'Donoghue RJ, Asselin-Labat ML, Bozinovski S, Bertoncello I.** 2013. TGF-beta signaling in stromal cells acts upstream of FGF-10 to regulate epithelial stem cell growth in the adult lung. Stem Cell Res **11:**1222-1233.

172. **Tadokoro T, Wang Y, Barak LS, Bai Y, Randell SH, Hogan BL.** 2014. IL-6/STAT3 promotes regeneration of airway ciliated cells from basal stem cells. Proc Natl Acad Sci U S A **111:**E3641-3649.

173. **Driskell RR, Watt FM.** 2015. Understanding fibroblast heterogeneity in the skin. Trends Cell Biol **25:**92-99.

174. **Ding BS, Nolan DJ, Guo P, Babazadeh AO, Cao Z, Rosenwaks Z, Crystal RG, Simons M, Sato TN, Worgall S, Shido K, Rabbany SY, Rafii S.** 2011. Endothelial-derived

angiocrine signals induce and sustain regenerative lung alveolarization. Cell **147:**539-553.

175. **Lee JH, Bhang DH, Beede A, Huang TL, Stripp BR, Bloch KD, Wagers AJ, Tseng YH, Ryeom S, Kim CF.** 2014. Lung stem cell differentiation in mice directed by endothelial cells via a BMP4-NFATc1-thrombospondin-1 axis. Cell **156:**440-455.

176. **Masterson JC, Molloy EL, Gilbert JL, McCormack N, Adams A, O'Dea S.** 2011. Bone morphogenetic protein signalling in airway epithelial cells during regeneration. Cell Signal **23:**398-406.

177. **Katayama Y, Battista M, Kao WM, Hidalgo A, Peired AJ, Thomas SA, Frenette PS.** 2006. Signals from the sympathetic nervous system regulate hematopoietic stem cell egress from bone marrow. Cell **124:**407-421.

178. **van der Velden VH, Hulsmann AR.** 1999. Autonomic innervation of human airways: structure, function, and pathophysiology in asthma. Neuroimmunomodulation **6:**145-159.

179. **Belvisi MG.** 2002. Overview of the innervation of the lung. Curr Opin Pharmacol **2:**211-215.

180. **Xie W, Fisher JT, Lynch TJ, Luo M, Evans TI, Neff TL, Zhou W, Zhang Y, Ou Y, Bunnett NW, Russo AF, Goodheart MJ, Parekh KR, Liu X, Engelhardt JF.** 2011. CGRP induction in cystic fibrosis airways alters the submucosal gland progenitor cell niche in mice. J Clin Invest **121:**3144-3158.

181. **Gomi K, Arbelaez V, Crystal RG, Walters MS.** 2015. Activation of NOTCH1 or NOTCH3 signaling skews human airway basal cell differentiation toward a secretory pathway. PLoS One **10:**e0116507.

182. **Curradi G, Walters MS, Ding BS, Rafii S, Hackett NR, Crystal RG.** 2012. Airway basal cell vascular endothelial growth factor-mediated cross-talk regulates endothelial cell-dependent growth support of human airway basal cells. Cell Mol Life Sci **69:**2217-2231.

183. **Ding BS, Gomi K, Rafii S, Crystal RG, Walters MS.** 2015. Endothelial MMP14 is required for endothelial-dependent growth support of human airway basal cells. J Cell Sci **128:**2983-2988.

184. **Ruiz EJ, Oeztuerk-Winder F, Ventura JJ.** 2014. A paracrine network regulates the cross-talk between human lung stem cells and the stroma. Nat Commun **5:**3175.

185. **Kuilman T, Michaloglou C, Mooi WJ, Peeper DS.** 2010. The essence of senescence. Genes Dev **24:**2463-2479.

186. **Ramirez RD, Morales CP, Herbert BS, Rohde JM, Passons C, Shay JW, Wright WE.** 2001. Putative telomere-independent mechanisms of replicative aging reflect inadequate growth conditions. Genes Dev **15:**398-403.

187. **Todaro GJ, Green H.** 1963. Quantitative studies of the growth of mouse embryo cells in culture and their development into established lines. J Cell Biol **17:**299-313.

188. **Rheinwald JG, Green H.** 1975. Formation of a keratinizing epithelium in culture by a cloned cell line derived from a teratoma. Cell **6:**317-330.

189. **Rheinwald JG, Green H.** 1975. Serial cultivation of strains of human epidermal keratinocytes: the formation of keratinizing colonies from single cells. Cell **6:**331-343.

190. **Green H.** 2008. The birth of therapy with cultured cells. Bioessays **30:**897-903.

191. **Banks-Schlegel S, Green H.** 1980. Formation of epidermis by serially cultivated human epidermal cells transplanted as an epithelium to athymic mice. Transplantation **29:**308-313.

192. **O'Connor NE, Mulliken JB, Banks-Schlegel S, Kehinde O, Green H.** 1981. Grafting of burns with cultured epithelium prepared from autologous epidermal cells. Lancet **1:**75-78.

193. **Gallico GG, 3rd, O'Connor NE, Compton CC, Kehinde O, Green H.** 1984. Permanent coverage of large burn wounds with autologous cultured human epithelium. N Engl J Med **311:**448-451.

194. **Mavilio F, Pellegrini G, Ferrari S, Di Nunzio F, Di Iorio E, Recchia A, Maruggi G, Ferrari G, Provasi E, Bonini C, Capurro S, Conti A, Magnoni C, Giannetti A, De Luca M.** 2006. Correction of junctional epidermolysis bullosa by transplantation of genetically modified epidermal stem cells. Nat Med **12:**1397-1402.

195. **De Rosa L, Carulli S, Cocchiarella F, Quaglino D, Enzo E, Franchini E, Giannetti A, De Santis G, Recchia A, Pellegrini G, De Luca M.** 2014. Long-term stability and safety of transgenic cultured epidermal stem cells in gene therapy of junctional epidermolysis bullosa. Stem Cell Reports **2:**1-8.

196. **Hernon CA, Dawson RA, Freedlander E, Short R, Haddow DB, Brotherston M, MacNeil S.** 2006. Clinical experience using cultured epithelial autografts leads to an alternative methodology for transferring skin cells from the laboratory to the patient. Regen Med **1:**809-821.

197. **Schermer A, Galvin S, Sun TT.** 1986. Differentiation-related expression of a major 64K corneal keratin in vivo and in culture suggests limbal location of corneal epithelial stem cells. J Cell Biol **103:**49-62.

198. **Rama P, Bonini S, Lambiase A, Golisano O, Paterna P, De Luca M, Pellegrini G.** 2001. Autologous fibrin-cultured limbal stem cells permanently restore the corneal surface of patients with total limbal stem cell deficiency. Transplantation **72:**1478-1485.

199. **Pellegrini G, Traverso CE, Franzi AT, Zingirian M, Cancedda R, De Luca M.** 1997. Long-term restoration of damaged corneal surfaces with autologous cultivated corneal epithelium. Lancet **349:**990-993.

200. **Pellegrini G, De Luca M.** 2014. Eyes on the prize: limbal stem cells and corneal restoration. Cell Stem Cell **15:**121-122.

201. **Griffith LG, Swartz MA.** 2006. Capturing complex 3D tissue physiology in vitro. Nat Rev Mol Cell Biol **7:**211-224.

202. **Schmeichel KL, Bissell MJ.** 2003. Modeling tissue-specific signaling and organ function in three dimensions. J Cell Sci **116:**2377-2388.

203. **Hynds RE, Giangreco A.** 2013. Concise review: the relevance of human stem cell-derived organoid models for epithelial translational medicine. Stem Cells **31:**417-422.

204. **Emerman JT, Pitelka DR.** 1977. Maintenance and induction of morphological differentiation in dissociated mammary epithelium on floating collagen membranes. In Vitro **13:**316-328.

205. **Barcellos-Hoff MH, Aggeler J, Ram TG, Bissell MJ.** 1989. Functional differentiation and alveolar morphogenesis of primary mammary cultures on reconstituted basement membrane. Development **105:**223-235.

206. **Sato T, Vries RG, Snippert HJ, van de Wetering M, Barker N, Stange DE, van Es JH, Abo A, Kujala P, Peters PJ, Clevers H.** 2009. Single Lgr5 stem cells build crypt-villus structures in vitro without a mesenchymal niche. Nature **459:**262-265.

207. **Sato T, Stange DE, Ferrante M, Vries RG, Van Es JH, Van den Brink S, Van Houdt WJ, Pronk A, Van Gorp J, Siersema PD, Clevers H.** 2011. Long-term expansion of epithelial organoids from human colon, adenoma, adenocarcinoma, and Barrett's epithelium. Gastroenterology **141:**1762-1772.

208. **Van Haute L, De Block G, Liebaers I, Sermon K, De Rycke M.** 2009. Generation of lung epithelial-like tissue from human embryonic stem cells. Respir Res **10:**105.

209. **Wang D, Haviland DL, Burns AR, Zsigmond E, Wetsel RA.** 2007. A pure population of lung alveolar epithelial type II cells derived from human embryonic stem cells. Proc Natl Acad Sci U S A **104:**4449-4454.

210. **Mou H, Zhao R, Sherwood R, Ahfeldt T, Lapey A, Wain J, Sicilian L, Izvolsky K, Musunuru K, Cowan C, Rajagopal J.** 2012. Generation of multipotent lung and airway progenitors from mouse ESCs and patient-specific cystic fibrosis iPSCs. Cell Stem Cell **10:**385-397.

211. **Huang SX, Islam MN, O'Neill J, Hu Z, Yang YG, Chen YW, Mumau M, Green MD, Vunjak-Novakovic G, Bhattacharya J, Snoeck HW.** 2014. Efficient generation of lung and airway epithelial cells from human pluripotent stem cells. Nat Biotechnol **32:**84-91.

212. **Wong AP, Bear CE, Chin S, Pasceri P, Thompson TO, Huan LJ, Ratjen F, Ellis J, Rossant J.** 2012. Directed differentiation of human pluripotent stem cells into mature airway epithelia expressing functional CFTR protein. Nat Biotechnol **30:**876-882.

213. **Whitsett JA, Clark JC, Picard L, Tichelaar JW, Wert SE, Itoh N, Perl AK, Stahlman MT.** 2002. Fibroblast growth factor 18 influences proximal programming during lung morphogenesis. J Biol Chem **277:**22743-22749.

214. **Firth AL, Dargitz CT, Qualls SJ, Menon T, Wright R, Singer O, Gage FH, Khanna A, Verma IM.** 2014. Generation of multiciliated cells in functional airway epithelia from human induced pluripotent stem cells. Proc Natl Acad Sci U S A **111:**E1723-1730.

215. **Dye BR, Hill DR, Ferguson MA, Tsai YH, Nagy MS, Dyal R, Wells JM, Mayhew CN, Nattiv R, Klein OD, White ES, Deutsch GH, Spence JR.** 2015. In vitro generation of human pluripotent stem cell derived lung organoids. Elife **4**.

216. **Konishi S, Gotoh S, Tateishi K, Yamamoto Y, Korogi Y, Nagasaki T, Matsumoto H, Muro S, Hirai T, Ito I, Tsukita S, Mishima M.** 2016. Directed Induction of Functional Multi-ciliated Cells in Proximal Airway Epithelial Spheroids from Human Pluripotent Stem Cells. Stem Cell Reports **6:**18-25.

217. **Tobin SC, Kim K.** 2012. Generating pluripotent stem cells: differential epigenetic changes during cellular reprogramming. FEBS Lett **586:**2874-2881.

218. **Lechner JF, Haugen A, McClendon IA, Pettis EW.** 1982. Clonal growth of normal adult human bronchial epithelial cells in a serum-free medium. In Vitro **18:**633-642.

219. **Kelsen SG, Mardini IA, Zhou S, Benovic JL, Higgins NC.** 1992. A technique to harvest viable tracheobronchial epithelial cells from living human donors. Am J Respir Cell Mol Biol **7:**66-72.

220. **de Jong PM, van Sterkenburg MA, Kempenaar JA, Dijkman JH, Ponec M.** 1993. Serial culturing of human bronchial epithelial cells derived from biopsies. In Vitro Cell Dev Biol Anim **29A:**379-387.

221. **Goulet F, Boulet LP, Chakir J, Tremblay N, Dube J, Laviolette M, Boutet M, Xu W, Germain L, Auger FA.** 1996. Morphologic and functional properties of bronchial cells isolated from normal and asthmatic subjects. Am J Respir Cell Mol Biol **15:**312-318.

222. **Fulcher ML, Gabriel S, Burns KA, Yankaskas JR, Randell SH.** 2005. Well-differentiated human airway epithelial cell cultures. Methods Mol Med **107:**183-206.

223. **Fulcher ML, Randell SH.** 2013. Human nasal and tracheo-bronchial respiratory epithelial cell culture. Methods Mol Biol **945:**109-121.

224. **Karp PH, Moninger TO, Weber SP, Nesselhauf TS, Launspach JL, Zabner J, Welsh MJ.** 2002. An in vitro model of differentiated human airway epithelia. Methods for establishing primary cultures. Methods Mol Biol **188:**115-137.

225. **Whitcutt MJ, Adler KB, Wu R.** 1988. A biphasic chamber system for maintaining polarity of differentiation of cultured respiratory tract epithelial cells. In Vitro Cell Dev Biol **24:**420-428.

226. **de Jong PM, van Sterkenburg MA, Hesseling SC, Kempenaar JA, Mulder AA, Mommaas AM, Dijkman JH, Ponec M.** 1994. Ciliogenesis in human bronchial epithelial cells cultured at the air-liquid interface. Am J Respir Cell Mol Biol **10:**271-277.

227. **Koo JS, Yoon JH, Gray T, Norford D, Jetten AM, Nettesheim P.** 1999. Restoration of the mucous phenotype by retinoic acid in retinoid-deficient human bronchial cell cultures: changes in mucin gene expression. Am J Respir Cell Mol Biol **20:**43-52.

228. **Yoon JH, Koo JS, Norford D, Guzman K, Gray T, Nettesheim P.** 1999. Lysozyme expression during metaplastic squamous differentiation of retinoic acid-deficient human tracheobronchial epithelial cells. Am J Respir Cell Mol Biol **20:**573-581.

229. **Mathis C, Poussin C, Weisensee D, Gebel S, Hengstermann A, Sewer A, Belcastro V, Xiang Y, Ansari S, Wagner S, Hoeng J, Peitsch MC.** 2013. Human bronchial epithelial cells exposed in vitro to cigarette smoke at the air-liquid interface resemble bronchial epithelium from human smokers. Am J Physiol Lung Cell Mol Physiol **304:**L489-503.

230. **Fessart D, Begueret H, Delom F.** 2013. Three-dimensional culture model to distinguish normal from malignant human bronchial epithelial cells. Eur Respir J **42:**1345-1356.

231. **Hegab AE, Ha VL, Darmawan DO, Gilbert JL, Ooi AT, Attiga YS, Bisht B, Nickerson DW, Gomperts BN.** 2012. Isolation and in vitro characterization of basal and submucosal gland duct stem/progenitor cells from human proximal airways. Stem Cells Transl Med **1:**719-724.

232. **Wu X, Peters-Hall JR, Bose S, Pena MT, Rose MC.** 2011. Human bronchial epithelial cells differentiate to 3D glandular acini on basement membrane matrix. Am J Respir Cell Mol Biol **44:**914-921.

233. **Watt F, Broad S, Prowse D.** 2006. Cultivation and Retroviral Infection of Human Epidermal Keratinocytes. *In* Celis JE (ed), Cell Biology: A Laboratory Handbook, Third ed, vol 1.

234. **Sage EK, Kolluri KK, McNulty K, Lourenco Sda S, Kalber TL, Ordidge KL, Davies D, Gary Lee YC, Giangreco A, Janes SM.** 2014. Systemic but not topical TRAIL-expressing mesenchymal stem cells reduce tumour growth in malignant mesothelioma. Thorax **69:**638-647.

235. **Welm BE, Dijkgraaf GJ, Bledau AS, Welm AL, Werb Z.** 2008. Lentiviral transduction of mammary stem cells for analysis of gene function during development and cancer. Cell Stem Cell **2:**90-102.

236. **Dull T, Zufferey R, Kelly M, Mandel RJ, Nguyen M, Trono D, Naldini L.** 1998. A third-generation lentivirus vector with a conditional packaging system. J Virol **72:**8463-8471.

237. **Hirst RA, Rutman A, Williams G, O'Callaghan C.** 2010. Ciliated air-liquid cultures as an aid to diagnostic testing of primary ciliary dyskinesia. Chest **138:**1441-1447.

238. **Jorissen M, Van der Schueren B, Tyberghein J, Van der Berghe H, Cassiman JJ.** 1989. Ciliogenesis and coordinated ciliary beating in human nasal epithelial cells cultured in vitro. Acta Otorhinolaryngol Belg **43:**67-73.

239. **Jorissen M, Van der Schueren B, Van den Berghe H, Cassiman JJ.** 1989. The preservation and regeneration of cilia on human nasal epithelial cells cultured in vitro. Arch Otorhinolaryngol **246:**308-314.

240. **Laoukili J, Perret E, Willems T, Minty A, Parthoens E, Houcine O, Coste A, Jorissen M, Marano F, Caput D, Tournier F.** 2001. IL-13 alters mucociliary differentiation and ciliary beating of human respiratory epithelial cells. J Clin Invest **108:**1817-1824.

241. **Willems T, Jorissen M.** 2004. Sequential monolayer-suspension culture of human airway epithelial cells. J Cyst Fibros **3 Suppl 2:**53-54.

242. **van Kuppeveld FJ, van der Logt JT, Angulo AF, van Zoest MJ, Quint WG, Niesters HG, Galama JM, Melchers WJ.** 1992. Genus- and species-specific identification of mycoplasmas by 16S rRNA amplification. Appl Environ Microbiol **58:**2606-2615.

243. **Evans IC, Barnes JL, Garner IM, Pearce DR, Maher TM, Shiwen X, Renzoni EA, Wells AU, Denton CP, Laurent GJ, Abraham DJ, McAnulty RJ.** 2016. Epigenetic regulation of cyclooxygenase-2 by methylation of c8orf4 in pulmonary fibrosis. Clin Sci (Lond) **130:**575-586.

244. **Yuan Z, Kolluri KK, Sage EK, Gowers KH, Janes SM.** 2015. Mesenchymal stromal cell delivery of full-length tumor necrosis factor-related apoptosis-inducing ligand is superior to soluble type for cancer therapy. Cytotherapy **17:**885-896.

245. **Tusher VG, Tibshirani R, Chu G.** 2001. Significance analysis of microarrays applied to the ionizing radiation response. Proc Natl Acad Sci U S A **98:**5116-5121.

246. **Benjamini Y, Hochberg Y.** 1995. Controlling the False Discovery Rate: A Practical and Powerful Approach to Multiple Testing. Journal of the Royal Statistical Society Series B (Methodological) **57:**289-300.

247. **Eisen MB, Spellman PT, Brown PO, Botstein D.** 1998. Cluster analysis and display of genome-wide expression patterns. Proc Natl Acad Sci U S A **95:**14863-14868.

248. **Zou HY, Li Q, Lee JH, Arango ME, Burgess K, Qiu M, Engstrom LD, Yamazaki S, Parker M, Timofeevski S, Cui JJ, McTigue M, Los G, Bender SL, Smeal T, Christensen JG.** 2012. Sensitivity of selected human tumor models to PF-04217903, a novel selective c-Met kinase inhibitor. Mol Cancer Ther **11:**1036-1047.

249. **Levy L, Neuveut C, Renard CA, Charneau P, Branchereau S, Gauthier F, Van Nhieu JT, Cherqui D, Petit-Bertron AF, Mathieu D, Buendia MA.** 2002. Transcriptional activation of interleukin-8 by beta-catenin-Tcf4. J Biol Chem **277:**42386-42393.

250. **Raingeaud J, Pierre J.** 2005. Interleukin-4 downregulates TNFalpha-induced IL-8 production in keratinocytes. FEBS Lett **579:**3953-3959.

251. **Arason AJ, Jonsdottir HR, Halldorsson S, Benediktsdottir BE, Bergthorsson JT, Ingthorsson S, Baldursson O, Sinha S, Gudjonsson T, Magnusson MK.** 2014. deltaNp63 has a role in maintaining epithelial integrity in airway epithelium. PLoS One **9:**e88683.

252. **Stripp BR, Huffman JA, Bohinski RJ.** 1994. Structure and regulation of the murine Clara cell secretory protein gene. Genomics **20:**27-35.

253. **Marshall CB, Mays DJ, Beeler JS, Rosenbluth JM, Boyd KL, Santos Guasch GL, Shaver TM, Tang LJ, Liu Q, Shyr Y, Venters BJ, Magnuson MA, Pietenpol JA.** 2016. p73 Is Required for Multiciliogenesis and Regulates the Foxj1-Associated Gene Network. Cell Rep **14:**2289-2300.

254. **Hogan BL, Barkauskas CE, Chapman HA, Epstein JA, Jain R, Hsia CC, Niklason L, Calle E, Le A, Randell SH, Rock J, Snitow M, Krummel M, Stripp BR, Vu T, White ES, Whitsett JA, Morrisey EE.** 2014. Repair and regeneration of the respiratory system: complexity, plasticity, and mechanisms of lung stem cell function. Cell Stem Cell **15:**123-138.

255. **Ghosh M, Brechbuhl HM, Smith RW, Li B, Hicks DA, Titchner T, Runkle CM, Reynolds SD.** 2011. Context-dependent differentiation of multipotential keratin 14-expressing tracheal basal cells. Am J Respir Cell Mol Biol **45:**403-410.

256. **Cole BB, Smith RW, Jenkins KM, Graham BB, Reynolds PR, Reynolds SD.** 2010. Tracheal Basal cells: a facultative progenitor cell pool. Am J Pathol **177:**362-376.

257. **Warner SM, Hackett TL, Shaheen F, Hallstrand TS, Kicic A, Stick SM, Knight DA.** 2013. Transcription factor p63 regulates key genes and wound repair in human airway epithelial basal cells. Am J Respir Cell Mol Biol **49:**978-988.

258. **Scholzen T, Gerdes J.** 2000. The Ki-67 protein: from the known and the unknown. J Cell Physiol **182:**311-322.

259. **Guo A, Jahoda CA.** 2009. An improved method of human keratinocyte culture from skin explants: cell expansion is linked to markers of activated progenitor cells. Exp Dermatol **18:**720-726.

260. **Atherton HC, Jones G, Danahay H.** 2003. IL-13-induced changes in the goblet cell density of human bronchial epithelial cell cultures: MAP kinase and phosphatidylinositol 3-kinase regulation. Am J Physiol Lung Cell Mol Physiol **285:**L730-739.

261. **Bals R, Beisswenger C, Blouquit S, Chinet T.** 2004. Isolation and air-liquid interface culture of human large airway and bronchiolar epithelial cells. J Cyst Fibros **3 Suppl 2:**49-51.

262. **Chapman S, Liu X, Meyers C, Schlegel R, McBride AA.** 2010. Human keratinocytes are efficiently immortalized by a Rho kinase inhibitor. J Clin Invest **120:**2619-2626.

263. **Liu X, Ory V, Chapman S, Yuan H, Albanese C, Kallakury B, Timofeeva OA, Nealon C, Dakic A, Simic V, Haddad BR, Rhim JS, Dritschilo A, Riegel A, McBride A, Schlegel R.**

2012. ROCK inhibitor and feeder cells induce the conditional reprogramming of epithelial cells. Am J Pathol **180:**599-607.

264. **Suprynowicz FA, Upadhyay G, Krawczyk E, Kramer SC, Hebert JD, Liu X, Yuan H, Cheluvaraju C, Clapp PW, Boucher RC, Jr., Kamonjoh CM, Randell SH, Schlegel R.** 2012. Conditionally reprogrammed cells represent a stem-like state of adult epithelial cells. Proc Natl Acad Sci U S A **109:**20035-20040.

265. **Ghosh M, Ahmad S, Jian A, Li B, Smith RW, Helm KM, Seibold MA, Groshong SD, White CW, Reynolds SD.** 2013. Human tracheobronchial basal cells. Normal versus remodeling/repairing phenotypes in vivo and in vitro. Am J Respir Cell Mol Biol **49:**1127-1134.

266. **Yu XM, Li CW, Chao SS, Li YY, Yan Y, Zhao XN, Yu FG, Liu J, Shen L, Pan XL, Shi L, Wang de Y.** 2014. Reduced growth and proliferation dynamics of nasal epithelial stem/progenitor cells in nasal polyps in vitro. Sci Rep **4:**4619.

267. **Araya J, Cambier S, Markovics JA, Wolters P, Jablons D, Hill A, Finkbeiner W, Jones K, Broaddus VC, Sheppard D, Barzcak A, Xiao Y, Erle DJ, Nishimura SL.** 2007. Squamous metaplasia amplifies pathologic epithelial-mesenchymal interactions in COPD patients. J Clin Invest **117:**3551-3562.

268. **Hackett NR, Shaykhiev R, Walters MS, Wang R, Zwick RK, Ferris B, Witover B, Salit J, Crystal RG.** 2011. The human airway epithelial basal cell transcriptome. PLoS One **6:**e18378.

269. **Hegab AE, Ha VL, Gilbert JL, Zhang KX, Malkoski SP, Chon AT, Darmawan DO, Bisht B, Ooi AT, Pellegrini M, Nickerson DW, Gomperts BN.** 2011. Novel stem/progenitor cell population from murine tracheal submucosal gland ducts with multipotent regenerative potential. Stem Cells **29:**1283-1293.

270. **Schouten JP, McElgunn CJ, Waaijer R, Zwijnenburg D, Diepvens F, Pals G.** 2002. Relative quantification of 40 nucleic acid sequences by multiplex ligation-dependent probe amplification. Nucleic Acids Res **30:**e57.

271. **Darnfors C, Flodin A, Andersson K, Caisander G, Lindqvist J, Hyllner J, Wahlstrom J, Sartipy P.** 2005. High-resolution analysis of the subtelomeric regions of human embryonic stem cells. Stem Cells **23:**483-488.

272. **Schamberger AC, Staab-Weijnitz CA, Mise-Racek N, Eickelberg O.** 2015. Cigarette smoke alters primary human bronchial epithelial cell differentiation at the air-liquid interface. Sci Rep **5:**8163.

273. **Smith CM, Kulkarni H, Radhakrishnan P, Rutman A, Bankart MJ, Williams G, Hirst RA, Easton AJ, Andrew PW, O'Callaghan C.** 2014. Ciliary dyskinesia is an early feature of respiratory syncytial virus infection. Eur Respir J **43:**485-496.

274. **Chilvers MA, Rutman A, O'Callaghan C.** 2003. Functional analysis of cilia and ciliated epithelial ultrastructure in healthy children and young adults. Thorax **58:**333-338.

275. **Reynolds SD, Reynolds PR, Pryhuber GS, Finder JD, Stripp BR.** 2002. Secretoglobins SCGB3A1 and SCGB3A2 define secretory cell subsets in mouse and human airways. Am J Respir Crit Care Med **166:**1498-1509.

276. **Pellegrini G, Rama P, Di Rocco A, Panaras A, De Luca M.** 2014. Concise review: hurdles in a successful example of limbal stem cell-based regenerative medicine. Stem Cells **32:**26-34.

277. **Kotaru C, Schoonover KJ, Trudeau JB, Huynh ML, Zhou X, Hu H, Wenzel SE.** 2006. Regional fibroblast heterogeneity in the lung: implications for remodeling. Am J Respir Crit Care Med **173:**1208-1215.

278. **Palechor-Ceron N, Suprynowicz FA, Upadhyay G, Dakic A, Minas T, Simic V, Johnson M, Albanese C, Schlegel R, Liu X.** 2013. Radiation induces diffusible feeder cell factor(s) that cooperate with ROCK inhibitor to conditionally reprogram and immortalize epithelial cells. Am J Pathol **183:**1862-1870.

279. **Jensen KB, Driskell RR, Watt FM.** 2010. Assaying proliferation and differentiation capacity of stem cells using disaggregated adult mouse epidermis. Nat Protoc **5:**898-911.

280. **Lamb R, Ambler CA.** 2013. Keratinocytes propagated in serum-free, feeder-free culture conditions fail to form stratified epidermis in a reconstituted skin model. PLoS One **8:**e52494.

281. **Wang L, Schulz TC, Sherrer ES, Dauphin DS, Shin S, Nelson AM, Ware CB, Zhan M, Song CZ, Chen X, Brimble SN, McLean A, Galeano MJ, Uhl EW, D'Amour KA, Chesnut JD, Rao MS, Blau CA, Robins AJ.** 2007. Self-renewal of human embryonic stem cells requires insulin-like growth factor-1 receptor and ERBB2 receptor signaling. Blood **110:**4111-4119.

282. **Lefebvre J, Ancot F, Leroy C, Muharram G, Lemiere A, Tulasne D.** 2012. Met degradation: more than one stone to shoot a receptor down. FASEB J **26:**1387-1399.

283. **Organ SL, Tsao MS.** 2011. An overview of the c-MET signaling pathway. Ther Adv Med Oncol **3:**S7-S19.

284. **Ikebuchi F, Oka K, Mizuno S, Fukuta K, Hayata D, Ohnishi H, Nakamura T.** 2013. Dissociation of c-Met phosphotyrosine sites in human cells in response to mouse hepatocyte growth factor but not human hepatocyte growth factor: the possible roles of different amino acids in different species. Cell Biochem Funct **31:**298-304.

285. **Zhang X, Zhang Y, Tao B, Wang D, Cheng H, Wang K, Zhou R, Xie Q, Ke Y.** 2012. Docking protein Gab2 regulates mucin expression and goblet cell hyperplasia through TYK2/STAT6 pathway. FASEB J **26:**4603-4613.

286. **Day RM, Soon L, Breckenridge D, Bridges B, Patel BK, Wang LM, Corey SJ, Bottaro DP.** 2002. Mitogenic synergy through multilevel convergence of hepatocyte growth factor and interleukin-4 signaling pathways. Oncogene **21:**2201-2211.

287. **Boccaccio C, Ando M, Tamagnone L, Bardelli A, Michieli P, Battistini C, Comoglio PM.** 1998. Induction of epithelial tubules by growth factor HGF depends on the STAT pathway. Nature **391:**285-288.

288. **Trusolino L, Bertotti A, Comoglio PM.** 2010. MET signalling: principles and functions in development, organ regeneration and cancer. Nat Rev Mol Cell Biol **11:**834-848.

289. **Mikita T, Daniel C, Wu P, Schindler U.** 1998. Mutational analysis of the STAT6 SH2 domain. J Biol Chem **273:**17634-17642.

290. **Walford HH, Doherty TA.** 2013. STAT6 and lung inflammation. JAKSTAT **2:**e25301.

291. **Yoshimura T, Matsushima K, Oppenheim JJ, Leonard EJ.** 1987. Neutrophil chemotactic factor produced by lipopolysaccharide (LPS)-stimulated human blood mononuclear leukocytes: partial characterization and separation from interleukin 1 (IL 1). J Immunol **139:**788-793.

292. **Gomez-Cambronero J, Horn J, Paul CC, Baumann MA.** 2003. Granulocyte-macrophage colony-stimulating factor is a chemoattractant cytokine for human neutrophils: involvement of the ribosomal p70 S6 kinase signaling pathway. J Immunol **171:**6846-6855.

293. **Chiba Y, Todoroki M, Nishida Y, Tanabe M, Misawa M.** 2009. A novel STAT6 inhibitor AS1517499 ameliorates antigen-induced bronchial hypercontractility in mice. Am J Respir Cell Mol Biol **41:**516-524.

294. **Nagashima S, Yokota M, Nakai E, Kuromitsu S, Ohga K, Takeuchi M, Tsukamoto S, Ohta M.** 2007. Synthesis and evaluation of 2-{[2-(4-hydroxyphenyl)-ethyl]amino}pyrimidine-5-carboxamide derivatives as novel STAT6 inhibitors. Bioorg Med Chem **15:**1044-1055.

295. **Panganiban RA, Day RM.** 2011. Hepatocyte growth factor in lung repair and pulmonary fibrosis. Acta Pharmacol Sin **32:**12-20.

296. **Quelle FW, Shimoda K, Thierfelder W, Fischer C, Kim A, Ruben SM, Cleveland JL, Pierce JH, Keegan AD, Nelms K, et al.** 1995. Cloning of murine Stat6 and human Stat6, Stat proteins that are tyrosine phosphorylated in responses to IL-4 and IL-3 but are not required for mitogenesis. Mol Cell Biol **15:**3336-3343.

297. **Wurster AL, Tanaka T, Grusby MJ.** 2000. The biology of Stat4 and Stat6. Oncogene **19:**2577-2584.

298. **Chen HC, Reich NC.** 2010. Live cell imaging reveals continuous STAT6 nuclear trafficking. J Immunol **185:**64-70.

299. **Rahmani M, Nadori F, Durand-Schneider AM, Lardeux B, Bernuau D.** 1999. Hepatocyte growth factor activates the AP-1 complex: a comparison between normal and transformed rat hepatocytes. J Hepatol **30:**916-925.

300. **Muller M, Morotti A, Ponzetto C.** 2002. Activation of NF-kappaB is essential for hepatocyte growth factor-mediated proliferation and tubulogenesis. Mol Cell Biol **22:**1060-1072.

301. **Comer DM, Elborn JS, Ennis M.** 2012. Comparison of nasal and bronchial epithelial cells obtained from patients with COPD. PLoS One **7:**e32924.

302. **Crowley C, Klanrit P, Butler CR, Varanou A, Plate M, Hynds RE, Chambers RC, Seifalian AM, Birchall MA, Janes SM.** 2016. Surface modification of a POSS-nanocomposite material to enhance cellular integration of a synthetic bioscaffold. Biomaterials **83:**283-293.

303. **Chan IS, Ginsburg GS.** 2011. Personalized medicine: progress and promise. Annu Rev Genomics Hum Genet **12:**217-244.

304. **Jamal-Hanjani M, Quezada SA, Larkin J, Swanton C.** 2015. Translational implications of tumor heterogeneity. Clin Cancer Res **21:**1258-1266.

305. **Mitra A, Mishra L, Li S.** 2013. Technologies for deriving primary tumor cells for use in personalized cancer therapy. Trends Biotechnol **31:**347-354.

306. **Paul MK, Bisht B, Darmawan DO, Chiou R, Ha VL, Wallace WD, Chon AT, Hegab AE, Grogan T, Elashoff DA, Alva-Ornelas JA, Gomperts BN.** 2014. Dynamic changes in intracellular ROS levels regulate airway basal stem cell homeostasis through Nrf2-dependent Notch signaling. Cell Stem Cell **15:**199-214.

307. **Ligaba SB, Khurana A, Graham G, Krawczyk E, Jablonski S, Petricoin EF, Glazer RI, Upadhyay G.** 2015. Multifactorial analysis of conditional reprogramming of human keratinocytes. PLoS One **10:**e0116755.

308. **Hiyama E, Hiyama K.** 2007. Telomere and telomerase in stem cells. Br J Cancer **96:**1020-1024.

309. **Ramunas J, Yakubov E, Brady JJ, Corbel SY, Holbrook C, Brandt M, Stein J, Santiago JG, Cooke JP, Blau HM.** 2015. Transient delivery of modified mRNA encoding TERT rapidly extends telomeres in human cells. FASEB J **29:**1930-1939.

310. **Butler CR, Hynds RE, Gowers KH, Lee DD, Brown JM, Crowley C, Teixeira VH, Smith CM, Urbani L, Hamilton NJ, Thakrar RM, Booth HL, Birchall MA, De Coppi P, Giangreco A, O'Callaghan C, Janes SM.** 2016. Rapid Expansion of Human Epithelial Stem Cells Suitable for Airway Tissue Engineering. Am J Respir Crit Care Med doi:10.1164/rccm.201507-1414OC.

311. **Banks-Schlegel SP, Quintero J.** 1986. Growth and differentiation of human esophageal carcinoma cell lines. Cancer Res **46:**250-258.

312. **Wang X, Yamamoto Y, Wilson LH, Zhang T, Howitt BE, Farrow MA, Kern F, Ning G, Hong Y, Khor CC, Chevalier B, Bertrand D, Wu L, Nagarajan N, Sylvester FA, Hyams JS, Devers T, Bronson R, Lacy DB, Ho KY, Crum CP, McKeon F, Xian W.** 2015. Cloning and variation of ground state intestinal stem cells. Nature **522:**173-178.

313. **Lechner JF, Haugen A, Autrup H, McClendon IA, Trump BF, Harris CC.** 1981. Clonal growth of epithelial cells from normal adult human bronchus. Cancer Res **41:**2294-2304.

314. **Yaeger PC, Stiles CD, Rollins BJ.** 1991. Human keratinocyte growth-promoting activity on the surface of fibroblasts. J Cell Physiol **149:**110-116.

315. **Horani A, Nath A, Wasserman MG, Huang T, Brody SL.** 2013. Rho-associated protein kinase inhibition enhances airway epithelial Basal-cell proliferation and lentivirus transduction. Am J Respir Cell Mol Biol **49:**341-347.

316. **Davies SP, Reddy H, Caivano M, Cohen P.** 2000. Specificity and mechanism of action of some commonly used protein kinase inhibitors. Biochem J **351:**95-105.

317. **Chapman S, McDermott DH, Shen K, Jang MK, McBride AA.** 2014. The effect of Rho kinase inhibition on long-term keratinocyte proliferation is rapid and conditional. Stem Cell Res Ther **5:**60.

318. **Watanabe K, Ueno M, Kamiya D, Nishiyama A, Matsumura M, Wataya T, Takahashi JB, Nishikawa S, Muguruma K, Sasai Y.** 2007. A ROCK inhibitor permits survival of dissociated human embryonic stem cells. Nat Biotechnol **25:**681-686.

319. **Coleman ML, Olson MF.** 2002. Rho GTPase signalling pathways in the morphological changes associated with apoptosis. Cell Death Differ **9:**493-504.

320. **Olson MF.** 2008. Applications for ROCK kinase inhibition. Curr Opin Cell Biol **20:**242-248.

321. **Bharadwaj S, Thanawala R, Bon G, Falcioni R, Prasad GL.** 2005. Resensitization of breast cancer cells to anoikis by tropomyosin-1: role of Rho kinase-dependent cytoskeleton and adhesion. Oncogene **24:**8291-8303.

322. **Minambres R, Guasch RM, Perez-Arago A, Guerri C.** 2006. The RhoA/ROCK-I/MLC pathway is involved in the ethanol-induced apoptosis by anoikis in astrocytes. J Cell Sci **119:**271-282.

323. **McMullan R, Lax S, Robertson VH, Radford DJ, Broad S, Watt FM, Rowles A, Croft DR, Olson MF, Hotchin NA.** 2003. Keratinocyte differentiation is regulated by the Rho and ROCK signaling pathway. Curr Biol **13:**2185-2189.

324. **Yugawa T, Narisawa-Saito M, Yoshimatsu Y, Haga K, Ohno S, Egawa N, Fujita M, Kiyono T.** 2010. DeltaNp63alpha repression of the Notch1 gene supports the proliferative capacity of normal human keratinocytes and cervical cancer cells. Cancer Res **70:**4034-4044.

325. **Yugawa T, Handa K, Narisawa-Saito M, Ohno S, Fujita M, Kiyono T.** 2007. Regulation of Notch1 gene expression by p53 in epithelial cells. Mol Cell Biol **27:**3732-3742.

326. **Yugawa T, Nishino K, Ohno S, Nakahara T, Fujita M, Goshima N, Umezawa A, Kiyono T.** 2013. Noncanonical NOTCH signaling limits self-renewal of human epithelial and induced pluripotent stem cells through ROCK activation. Mol Cell Biol **33:**4434-4447.

327. **Alitalo K, Kuismanen E, Myllyla R, Kiistala U, Asko-Seljavaara S, Vaheri A.** 1982. Extracellular matrix proteins of human epidermal keratinocytes and feeder 3T3 cells. J Cell Biol **94:**497-505.

328. **Smola H, Thiekotter G, Fusenig NE.** 1993. Mutual induction of growth factor gene expression by epidermal-dermal cell interaction. J Cell Biol **122:**417-429.

329. **Kaplan MH, Schindler U, Smiley ST, Grusby MJ.** 1996. Stat6 is required for mediating responses to IL-4 and for development of Th2 cells. Immunity **4:**313-319.

330. **Blease K, Schuh JM, Jakubzick C, Lukacs NW, Kunkel SL, Joshi BH, Puri RK, Kaplan MH, Hogaboam CM.** 2002. Stat6-deficient mice develop airway hyperresponsiveness and peribronchial fibrosis during chronic fungal asthma. Am J Pathol **160:**481-490.

331. **Ito Y, Correll K, Zemans RL, Leslie CC, Murphy RC, Mason RJ.** 2015. Influenza induces IL-8 and GM-CSF secretion by human alveolar epithelial cells through HGF/c-Met and TGF-alpha/EGFR signaling. Am J Physiol Lung Cell Mol Physiol **308:**L1178-1188.

332. **Daines MO, Andrews RP, Chen W, El-Zayaty SA, Hershey GK.** 2003. DNA binding activity of cytoplasmic phosphorylated Stat6 is masked by an interaction with a detergent-sensitive factor. J Biol Chem **278:**30971-30974.

333. **McBride KM, Banninger G, McDonald C, Reich NC.** 2002. Regulated nuclear import of the STAT1 transcription factor by direct binding of importin-alpha. EMBO J **21:**1754-1763.